1. Рад M21a

Plasma Sources Science and Technology

PAPER

A set of cross sections and transport coefficients for CF_3^+ ions in CF_4

To cite this article: J V Jovanović *et al* 2019 *Plasma Sources Sci. Technol.* **28** 045006

IOP Publishing Plasma Sources Science and Technology

Plasma Sources Sci. Technol. **28** (2019) 045006 (6pp) https://doi.org/10.1088/1361-6595/ab122f

A set of cross sections and transport coefficients for CF_3^+ ions in CF_4

J V Jovanović[1,2], V Stojanović[1], Z Raspopović[1], J de Urquijo[3] and Z Lj Petrović[1,4]

[1] Institute of Physics University of Belgrade, POB 68, 11080 Belgrade, Serbia
[2] Faculty of Mechanical Engineering, University of Belgrade, Kraljice Marije 16, 11000 Belgrade, Serbia
[3] Instituto de Ciencias Físicas, Universidad Nacional Autónoma de México, PO Box 48-3, 62251 Cuernavaca Mor., Mexico
[4] Serbian Academy of Sciences and Arts, Knez Mihajlova 35, 11000 Belgrade, Serbia

E-mail: jjovanovic@mas.bg.ac.rs

Received 29 October 2018, revised 26 February 2019
Accepted for publication 21 March 2019
Published 9 April 2019

Abstract

A cross section set for CF_3^+ ions in CF_4 gas has been assembled from the available experimental and theoretical data using a swarm method. Elastic cross section consistent with the available experimental mobility data has been derived and the set also includes the reactive cross sections. Reactive rates are deduced for collision energies of up to 500 eV. The transport properties of CF_3^+ ions in CF_4 gas in DC (direct current) electric field fields at a gas temperature of $T = 300$ K were calculated as a function of the reduced electric field E/N (E is electric field and N is gas number density) by using a Monte Carlo simulation. The non-conservative collisions are also taken into account in the definition of transport coefficients.

Supplementary material for this article is available online

Keywords: kinetic and transport theory of gases, atomic, molecular, ion and heavy-particle collisions, Monte Carlo methods

1. Introduction

A major effort has been undertaken worldwide to study ion transport processes and, in particular, dissociation of CF_4 molecules by means of several forms of excitation. Some representative examples are given in [1–10]. The most notable goal was to establish the kinetics of reactive plasmas in applications related to integrated circuit manufacturing. A significant reactivity of these plasmas is based on both neutral and ionic forms of the CF_4 radicals (F, F_2, C, CF, CF_2 and CF_3). Of all the reactive products of dissociation, ions are the most prominent constituents of either pure CF_4 plasmas or its mixtures with other processing gases (Ar, N_2, O_2, etc) [8–11] since their flux and energy may control the kinetics of surface processes, reactive ion etching in particular. The density and polarity of charge carriers make such plasmas more or less electronegative [8–10] depending on various plasma properties in the bulk and at the electrode boundaries. One must admit that in spite of numerous studies, the specific properties of either radicals or reactions necessary to model plasma applications are still poorly known. As a consequence, transport properties of radicals, either neutral or charged, are highly desirable in the regimes where plasmas are collisionally dominated, either as a test for plasma models or in any attempt to predict plasma properties for specific applications.

CF_3 radicals formed in plasma chemical processes [3] are present in plasma mixtures with high abundances of CF_4. The density of CF_3 radicals in processing plasmas at room temperature depends mainly on the electron density [12].

The CF_3^+ ion is the most abundant positive ion in pure CF_4 plasmas and also in most gas mixture plasmas containing CF_4 [8–10]. It is known that CF_3^+ ions in their electronic ground or excited states are mainly produced by dissociative ionization (in a low pressure plasma, mostly by electrons). It is also possible that CF_3^+ may be produced in different ion-molecule reactions. The main product of CF^+ and CF_2^+ collisions with CF_4 is the CF_3^+ ion [13]. Thus one definitely finds the need for a collision cross section set for CF_3^+ ions in CF_4 over a wide energy range. These data are indispensable for the modeling of technologically relevant plasmas.

Georgieva *et al* [14, 15] assembled cross section sets for charged radicals in low pressure Ar/ CF_4 mixtures mainly by using Denpoh–Nanbu theory (DNT) [16, 17], and taking into account the long-range effects of an ion-induced dipole interaction. Although based on a simple theory, a very wide range of possible reactions of radical ions with CF_4 targets were considered in a consistent way.

In this paper we present our compiled total cross section for CF_3^+ ions scattering from CF_4, transport and rate coefficients of these ions in pure CF_4 obtained for a gas temperature $T = 300$ K and gas pressure of 1 Torr (3.3×10^{16} cm^{-3}). This study presents a necessary effort to include the relatively recent mobility measurements [18] in the analysis of the cross sections. In this study we will select only the most important processes observed in the experiments and try to assemble, as precisely as possible, a cross section set that can be used directly in simulations of plasmas containing CF_3^+ ions.

We do not model plasmas here; we do a swarm study which is the model of an ionized gas in the limit of low ionization. We actually model the Drift tube-mass spectrometer experiment of de Urquijo and coworkers [18]. In doing so, we start from an initial set of cross sections. Swarm studies always suffer from non-uniqueness and of a limited energy range, so it is optimal to augment the initial data with some input that would not be subject to modification. In this case we use the measured inelastic/reactive cross section [4] extended towards the threshold by using the so called DNT. The theory in its original form has been included into a plasma modeling code whereby collision probabilities (rates) were transferred to the Monte Carlo collision section of the code. However, it is possible also to convert these rates into the cross sections and DNT data for CF_3^+ ions have been used through the use of cross sections in most cases when kinetic plasma modeling has been attempted [14, 15, 19, 20]. These sets of cross sections have not been normalized to any transport data. In other words, a swarm normalization has not been made, mainly because the transport data were not published at that time. We, on the other hand, take advantage of the recent measurements [18] and renormalize the data to fit the mobilities. All extrapolations to higher energies are the same as in previous studies except that we add the measured cross sections due to Peko *et al* [4] extrapolated to the threshold by using DNT. When calculated transport data agree well with measured transport data, then one can claim that over the energy range covered by swarms in the given *E/N* range, the balances of momentum, energy and number are met and thus the distribution functions are well calculated. Without such verification it is possible that some of these balances may not be calculated accurately. The DNT is used as an initial set to extrapolate the cross sections, and the final outcome should not depend on the initial set but the speed of achieving a good fit does.

A preliminary presentation of a subset of the present data has been made in conference proceedings published as a contributed conference paper [21].

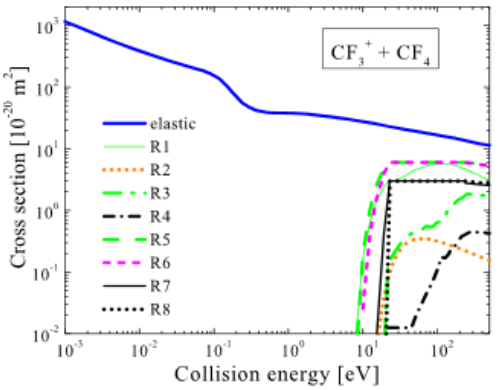

Figure 1. Cross section set for CF_3^+ ions in CF_4 as a function of collision energy in the centre of mass reference frame.

2. Cross section set

We have combined several techniques in order to obtain a cross section set (see figure 1) that would fit the available experimental data [18].

First, we have tried to fit the low energy part of the measured mobility data. The most recent value for the dipole polarizability of CF_4 of 3.86×10^{-30} m^3, was recommended in [22], rather than the value selected by Denpoh and Nanbu of 2.9×10^{-30} m^3, originally given by Smirnov [23, 24], and used in [14]. The former value decreases the zero-field mobility from 1.308 cm^2 V^{-1} s^{-1} to 1.13375 cm^2 V^{-1} s^{-1}, that is, closer to the measured low-field mobility of this ion of 0.96 ± 0.04 cm^2 V^{-1} s^{-1} [18]. The differences in the limit of mobility and in the low *E/N* behavior of the mobility are shown in figure 2. Arrows are calculated by using Langevin–Hasse formula [25] and two different published experimentaly determined polarizabilities. The zero-field mobilities were obtained from the cross sections by calculating the mobilities with a Monte Carlo code at low *E/N* and then extrapolating the values to zero field.

Our primary goal was to model the *E/N* dependence of the measured mobility data. To do repeated fits we have used very quick calculations by simple, semi-analytic momentum transfer theory (MTT) [26–28] to obtain the momentum transfer integral cross section. We did so bearing in mind the difference between the approximate MTT results and exact MC simulations.

MTT consists of a simplification of the energy distribution function that allows semi-analytic solutions of the Boltzmann equation [26–28], quickly and with rather limited accuracy (typically up to 10% but, when reactive processes are important, the discrepancy could be somewhat larger). Thus it is easy to make adjustments of the cross sections to improve the agreement with the measured transport data by using MTT and quickly converge close to the final set of cross sections. Typically, we adjust the value of the zero energy limit of the cross section to fit the zero-field mobility. It may

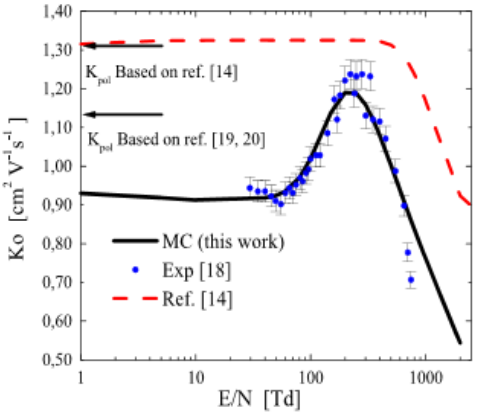

Figure 2. Reduced mobility of CF3+ ions in CF4 as a function of E/N. MC—data obtained by MCS in this work; exp—the measurements of [18] and predictions based on cross sections used in [14]. The arrows show the values of the zero-field mobility calculated by the Langevin–Hasse formula, using the polarizabilities from [14] and [22].

be expected that this limit is about 10% different from the data that can be obtained using what has been stated before, the polarizability of the molecule from the literature in the Langevin–Hasse theory. We try to maintain the standard energy dependence of the cross section up to a point where the peak in the mobility requires the cross section to drop down faster. We adjust the cross section point by point. Then, starting from the limit of the energy range where the measured mobility data are sensitive to the cross section towards higher energies, we use extrapolations that follow standard energy dependences and have the addition of the contribution of the reactive collisions as calculated by the DNT. Once our fitting procedure produces results sufficiently close to the experimental data, we make final adjustments of the cross sections and calculations by using a Monte Carlo code to provide more accurate values. For all practical purposes we may claim to have used the Monte Carlo code to calculate the transport data, to fit the available experimental data and to establish the cross section set.

The final values (see figure 2) were thus obtained by using MC simulations after further albeit minor adjustments of the cross section in the final stage of calculations.

Most importantly, the experimental data have a mobility peak which is the result of the descending part of the elastic momentum transfer cross section (having assumed isotropic scattering). As can be seen from the same figure, the predictions based on the cross sections of Georgieva *et al* [14] and Denpoh and Nanbu [16] cannot reproduce the dependence with the peak in the experimental mobility data and also in the low energy limit [18]. [14, 16] did not have the advantage of the new experimental data, so our primary motivation was to update the cross section set.

Regarding the high energy in which both inelastic and reactive collisions take place, we have combined the available experimental data of Peko *et al* [4] and DNT. The DNT values of the inelastic cross sections were scaled to the experimental values of the inelastic cross sections at the lowest experimental energy (30 eV) and then the theory was used to extrapolate the measured cross sections to the thresholds. A wide range of ion-molecule reactions were included in the cross section set presented in [14], covering endothermic reaction paths established in order to study single and dual radiofrequency capacitively coupled discharges in pure CF_4 and mixtures including CF_4 [14, 15]. The whole scheme for CF_3^+ scattering in CF_4 was represented by 42 reaction paths in [14], as suggested by [16]. Instead of using all processes listed in [14], we have selected only the processes experimentally established as the most probable [4]. The reactions considered in this paper include collision-induced dissociation (CID) and dissociative charge transfer collisions (DCT). All representative endothermic reaction paths based on existing thermochemical data [29] are listed in table 1, together with the corresponding thermodynamic threshold energies.

Finally, in order to calculate transport parameters at high *E/N*, all cross sections were extrapolated up to 500 eV, following judiciously the trends of the measurements.

The complete set of cross sections is shown in figure 1.

Table 1. Products and endothermic reaction paths for the $CF_3^+ + CF_4$ reaction as considered in the model used in this paper and specified by this table, and the corresponding thermodynamic threshold energies reported in [4]. Endothermicities, Δ, are given in eV; the underlined products have roughly the same laboratory velocity as the reactant ion.

Number	Reaction products	Δ (eV)
R1	$\mathbf{CF_3^+} + F + \underline{CF_3}$ (DCT)	−5.7
R2	$\mathbf{CF_2^+} + F_2 + \underline{CF_3}$ (DCT)	−10.3
R3	$\mathbf{CF^+} + F + F_2 + \underline{CF_3}$ (DCT)	−13.1
R4	$\mathbf{C^+} + 2F_2 + \underline{CF_3}$ (DCT)	−19.2
R5	$\underline{\mathbf{CF_2^+}} + F + CF_4$ (CID)	−6.2
R6	$\underline{\mathbf{CF^+}} + \underline{F_2} + CF_4$ (CID)	−7.4
R7	$\underline{\mathbf{F^+}} + \underline{CF_2} + CF_4$ (CID)	−12.3
R8	$\underline{\mathbf{C^+}} + \underline{F} + \underline{F_2} + CF_4$ (CID)	−15.1

3. Monte Carlo technique

Detailed explanations and tests of our MC technique have been covered in our earlier studies [30, 31], therefore we will give only a brief overview here.

The Monte Carlo simulation (MCS) code was applied to perform calculations of transport parameters as well as rate coefficients in DC electric fields. In this paper we have used a code that properly takes into account thermal collisions [30] which has also passed all benchmarks and provided new benchmark results to test other codes. The effect of the non-conservative collisions on the drift velocity and diffusion coefficients (see figures 4 and 5) can be seen through the difference between bulk (the real space) and flux (the velocity space) transport coefficients [32].

4. Transport properties. Results and discussion

MC calculations were made for a room temperature of $T = 300$ K, a pressure of 1 Torr and electric field-to-gas density ratios (E/N) ranging from 1 to 2000 Td.

In figure 2 we show the reduced mobility of CF_3^+ ions in CF_4 as a function of E/N. The reduced mobility data, related to the calculated drift velocity, W, by

$$K_0 = \frac{W}{N_0(E/N)}, \tag{1}$$

where $N_0 = 2.69 \times 10^{19}$ cm^{-3} is gas density at standard temperature and pressure, were obtained from a Monte Carlo simulation and are shown by a solid line, whereas the data obtained on the basis of the cross section set of Georgieva *et al* [14] are shown by a broken line. When transport coefficients based on the cross section data from [14] are compared to the experimental results of Basurto and de Urquijo [18], a significant discrepancy is found over the entire E/N region, both in the domain of the polarization limit (<40 Td) [25] and near the peak of the mobility at around 300 Td.

Note in figure 2 that even the experimental points around the peak overlap with the calculated curve within the error limits that may be estimated for that type of experiment (±3%–5%). The mobility curve (shown as a solid line in figure 2) of CF_3^+ in CF_4 shows a well defined maximum for $200 < E/N < 300$ Td, then followed by a decrease, due to the predominance of the repulsive part of the interaction potential. The predominance of the repulsive part of the interaction potential is taken to mean that, under this energy range, capture into orbiting trajectories cannot occur, although scattering occurs through deflection from the initial orbit into any angle, and yet it is still elastic. In the intermediate region, the cross section may be affected by both repulsive and attractive force and may change fast enough to produce a peak in the mobility curve [33]. One can thus see that the choice of the cross section in the intermediate energy range (around 1 eV) is critical in describing the maximum in the mobility curve, which, if observed experimentally needs to be represented by the cross section fit.

The calculated mean energy of CF_3^+ in CF_4 as a function of E/N is given in figure 3. At low energies the present results are in agreement with those using the cross section set in [14] since mean energies converge towards the thermal energy if collision frequencies and collisional energy losses are properly accounted for. As a matter of fact, the convergence of the mean energies at the lowest E/N may be regarded as a test of the quality of the Monte Carlo code [30]. At high E/N the differences are considerable, and the mean energies calculated from the cross sections in [14] are higher.

Bulk and flux values for the drift velocities and the longitudinal and transverse component of the density-normalized diffusion tensor, ND_L and ND_T, are shown as a function of E/N in figures 4 and 5, respectively. The drift velocities and diffusion coefficients are almost unaffected by the influence of reactive collisions. A similar behavior is observed when using the cross section set of Georgieva *et al* [14]. The first mention of non-conservative effects in ion transport was given in [34–36]. In both cases the threshold energies for reactive processes are high enough (starting from 5.7 eV) so that transport data up to 1000 Td are only slightly affected. Only for $E/N \geqslant 1000$ Td a significant number of reactive processes included in the calculation of the cross sections [14] split the drift velocity curve into two (figure 4), and also the flux and bulk components of the longitudinal diffusion coefficient (figure 5) in our calculations. The small difference between flux and bulk drift velocity and longitudinal diffusion tensor suggests a small effect of non-conservative processes of CF_3^+ transport in CF_4.

The calculated rate coefficients for the processes presented in table 1 and their corresponding cross sections in figure 1 are shown in figure 6, and may be used directly in fluid models. The rate coefficient for conversion of CF_4 to CF_3 radical is the largest with a similar production rate for

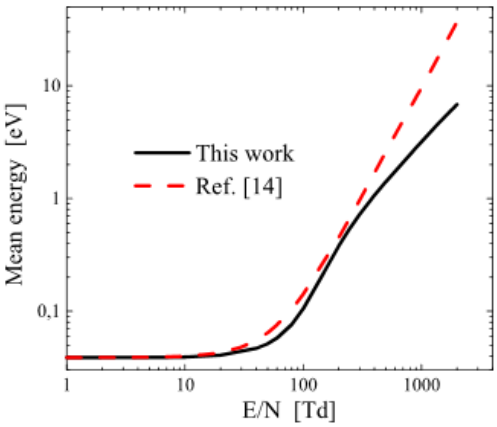

Figure 3. Calculated mean energy of CF_3^+ in CF_4 as a function of E/N. The data of Georgieva *et al* [14] are shown for comparison.

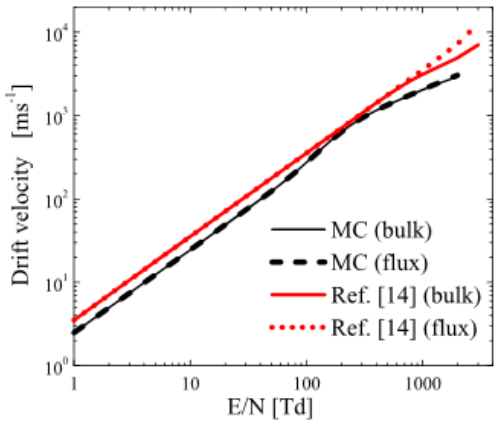

Figure 4. Bulk and flux values of drift velocity for CF_3^+ ions in CF_4 as a function of E/N.

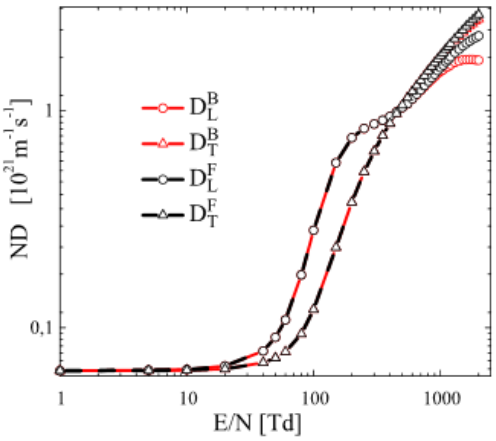

Figure 5. The longitudinal (D_L) and transverse (D_T) components of the diffusion tensor for CF_3^+ ions in CF_4 as a function of *E/N*, calculated for bulk (B) and flux (F) conditions.

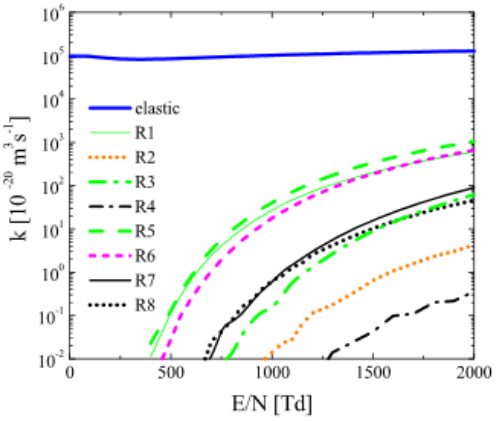

Figure 6. Calculated rate coefficients for CF_3^+ in CF_4 as a function of *E/N* at a temperature $T = 300$ K.

CF^+, CF_2^+ and CF_3^+ ions. The magnitudes of the reaction rates decrease substantially as the endothermicity of the reaction increases.

The rate coefficient for elastic scattering is about two orders of magnitude larger than the reactive rate coefficients even at the highest *E/N* covered here. This is a consequence of the latter having high endothermic thresholds, higher than the mean energy achieved at the highest *E/N*.

5. Conclusion

In this paper we have presented a cross section set for CF_3^+ in CF_4, originally assembled from experimental and theoretical data, and by fitting mobilities from a mass spectrometric swarm experiment. With this cross section set we have shown that there is a very good agreement with the experimental ion mobility data of CF_3^+ in CF_4 and have given predictions for other transport coefficients. The MTT was used only as the initial step to establish the cross section for elastic scattering up to 200 eV and also to make further adjustments, thereby saving significant amounts of computational time. All the final calculations were performed by Monte Carlo simulations. The transport parameters for DC electric fields were calculated for the CF_4 gas temperature of $T = 300$ K.

In the relevant *E/N* region the dominant process is that of elastic collisions that determines both the momentum and energy balances. Thus, as has been shown in the literature on charged particle swarms, one may expect unique results from a single set of transport data. Of course, the uncertainties depend on the experimental uncertainties.

Outside the energy range covered by experiment, we rely on extrapolation based on behavior of the mobility based on standard potentials, close to constant at the lowest *E/N* (below 30 Td) and decreasing according to the standard cross section dependencies determined by the repulsive potentials with the added experimental and DNT normalized cross sections for reactive collisions at the highest *E/N*. The extrapolation of cross sections at the higher energies is provided for completeness but it should be regarded an 'educated' compilation of the best available and recommended data and not as data with foundation in the present measured mobilities except perhaps for the normalization in the connecting energy range.

The fitting procedure proceeded by scaling cross sections with expected *E/N* dependences (in the low and in the high *E/N* limit) and patching them to results defined by fitting of the mobility curve that proceeded by adjusting points in a broad range around the mean energy of *E/N* where discrepancy was observed.

The quality of fit was verified by adhering to the expected experimental uncertainties that were somewhat relaxed at the points at the beginning and the end of the *E/N* range.

One can use mixture laws [32, 37] to predict properties in mixtures containing CF_4. For typical mixtures in plasma etching one would need mobilities of relevant ions in argon (or other rare gas buffers). Using either transport data or cross sections [38] for plasma modelling require a large amount of data. We have attempted to predict the best available cross section set for applications in plasma modelling. Further measurements, either of cross sections or swarm parameters at higher energies are needed in order to test the cross sections obtained in this paper as a whole and, in particular, at higher energies.

Acknowledgments

This project was carried out at the Laboratory of Gaseous Electronics Institute of Physics of the University of Belgrade, Serbia under the auspices of the Ministry of Education and Science, Projects No. 171037 and 410011. One of the authors Z Lj P is also grateful to the Serbian Academy of Sciences

and Arts project SANU 155 and J deU is grateful to Conacyt, Grant 240073, PAPIIT UNAM IN108417, and to A Bustos and G Bustos for their technical support.

ORCID iDs

J V Jovanović https://orcid.org/0000-0001-6606-5470

References

[1] Kurihara M, Petrović Z L and Makabe T 2000 *J. Phys. D: Appl. Phys.* **33** 2146
[2] Dujko S, White R D, Ness K F, Petrović Z L and Robson R E 2006 *J. Phys. D: Appl. Phys.* **39** 4788
[3] Rauf S and Kushner M J 1997 *J. Appl. Phys.* **82** 2805
[4] Peko B L, Dyakov I V, Champion R L, Rao M V V S and Olthoff J K 1999 *Phys. Rev.* E **60** 7449
[5] Yang X, Moravej M, Babayan S E, Nowling G R and Hicks R F 2005 *Plasma Sources Sci. Technol.* **14** 412
[6] Tachibana K 2002 *Plasma Sources Sci. Technol.* **11** A166
[7] Kim Y, Kim K-T, Cha M S, Song Y-H and Kim S J 2005 *IEEE Trans. Plasma Sci* **33** 1041
[8] Curley G A, Marić D, Booth J P, Corr C S, Chabert P and Guillon J 2007 *Plasma Sources Sci. Technol.* **16** S87
[9] Booth J P, Curley G A, Marić D and Chabert P 2010 *Plasma Sources Sci. Technol.* **19** 015005
[10] Takashi K and Masahisa N 2006 *J. Appl. Phys.* **100** 063303
[11] Tochikubo F, Petrović Z L, Kakuta S, Nakano N and Makabe T 1994 *Japan. J. Appl. Phys.* **33** 4271
[12] Hikosaka Y, Nakamura M and Sugai H 1994 *Japan. J. Appl. Phys.* **33** 2157
[13] Morris R A, Viggiano A A, Van Doren J M and Paulson J F 1992 *J. Phys. Chem.* **96** 2597
[14] Georgieva V, Bogaerts A and Gijbels R 2003 *J. Appl. Phys.* **93** 2369
[15] Georgieva V 2005 *PhD Thesis* Universiteit Antwerpen
[16] Denpoh K and Nanbu K 1998 *J. Vac. Sci. Technol.* A **16** 1201
[17] Petrović Z L *et al* 2007 *Appl. Surf. Sci.* **253** 6619
[18] Basurto E and de Urquijo J 2002 *J. Appl. Phys.* **91** 36
[19] Brandt S *et al* 2016 *Plasma Sources Sci. Technol.* **25** 045015
[20] Donkó Z and Lj P Z 2006 *Japan. J. Appl. Phys.* **45** 8151
[21] Stojanović V, Raspopović Z, Jovanović J V, de Urquijo J and Petrović Z L 2014 *J. Phys.: Conf. Ser.* **514** 012059
[22] McDaniel E W 1989 *Atomic Collisions-Electron and Photon Projectiles* (New York: Wiley)
[23] Smirnov B M 1982 *Negative Ions* (New York: Mc Graw-Hill)
[24] Radzig A A and Smirnov B M 1985 *Reference Data on Atoms, Molecules and Ions* (Berlin: Springer)
[25] Mason E A and McDaniel E W 1988 *Transport Properties of Ions in Gases* (New York: Wiley)
[26] Vrhovac S B and Lj P Z 1996 *Phys. Rev* E **53** 4012
[27] Robson R E 1986 *J. Chem. Phys.* **85** 4486
[28] Jovanović J V, Vrhovac S B and Petrović Z L 2002 *Eur. Phys. J.* D **21** 335
[29] Fisher E R, Weber M E and Armentrout P B 1990 *J. Chem. Phys.* **92** 2296
[30] Ristivojević Z and Petrović Z L 2012 *Plasma Sources Sci. Technol.* **21** 035001
[31] Petrović Z L and Stojanović V D 1998 *J. Vac. Sci. Technol.* A **16** 329
[32] Petrović Z L, Dujko S, Marić D, Malović G, Nikitović Ž, Šašić O, Jovanović J, Stojanović V and Radmilović-Rađenović M 2009 *J. Phys. D: Appl. Phys.* **42** 194002
[33] Robson R, White R and Hildebrandt M 2018 *Fundamentals of Charged Particle Transport in Gases and Condensed Matter* (Boca Raton: CRC, Taylor and Francis)
[34] Kumar K, Skullerud H R and Robson R E 1980 *Aust. J. Phys.* **33** 343
[35] Ness K and Robson R E 1986 *Phys. Rev.* A **34** 2185
[36] Robson R E, White R D and Petrović Z L 2005 *Rev. Mod. Phys.* **77** 1303
[37] Petrović Z L, Jovanović J V, Stojanović V, Raspopović Z M and Ristivojević Z 2008 *Eur. Phys. J.* D **48** 87
[38] Nakano N, Shimura N, Petrović Z L and Makabe T 1994 *Phys Rev.* E **49** 4455

2. Рад M21

PHYSICAL REVIEW E **108**, L053202 (2023)

Letter

Space-resolved average kinetic energy of ion swarms in a uniform electric field

Z. M. Raspopović

Institute of Physics Belgrade, University of Belgrade, Pregrevica 118, 11080 Belgrade, Serbia

(Received 30 March 2023; revised 1 September 2023; accepted 29 September 2023; published 13 November 2023)

A pulse of noninteracting charged particles in an unbounded gas, exposed to a low, constant, homogeneous electric field, was studied in both space and time using a Monte Carlo simulation technique. The difference in electrical potential between the leading and trailing edges of the swarm results in the space-resolved average ion kinetic energy becoming a linearly increasing function of space. This Letter analyzes whether the average ion kinetic energy at the leading edge reaches a stationary value during the spatiotemporal evolution of the swarm, as has been considered so far. When the swarm's mean kinetic energy reaches a steady-state value, indicating that an energy balance is established over time, the gains (from the field) and losses (due to collisions) are nonuniform across space. The local power balance is negative at the front of the swarm and positive at the tail. Cooling the ions at the front and heating the ions at the tail results in a decrease in the average ion kinetic energy at the front and an increase at the tail. Thus, it can be concluded that stationary values of average ion kinetic energy do not exist at the leading and trailing edges during the evolution. Instead, they tend to approach the swarm's mean kinetic energy as $t \to \infty$.

DOI: 10.1103/PhysRevE.108.L053202

Introduction. Today, many technologies use directional ions as one of the basic tools for etching [1] in microdischarges [2], nanotechnologies [3], and biomedical applications [4]. Tremendous resources are being invested in the advancement and development of these technologies to increase their accuracy [5]. Knowledge of the space-resolved density and average energy of charged particles during swarm evolution is in many cases crucial for understanding a great variety of basic mechanisms of physical and chemical processes between charged particles and background gas.

So far, transient and steady-state spatial profiles of the transport properties of electron swarms were investigated using a Monte Carlo simulation technique by Suvakov *et al.* [6], Raspopovic *et al.* [7], and Dujko *et al.* [8].

The physics of charged-particle swarms has always formed the foundation for the modeling of nonequilibrium plasmas. Swarm experiments and the associated transport theory of swarm particles are often used to determine the cross sections and/or interaction potentials. On the other hand, fluid models of plasma discharges require swarm transport coefficients as a function of the applied electric field.

In the work [8], it was found that full spatial relaxation is achieved under conditions when diffusion fluxes due to gradients in electron number density are much smaller than the corresponding drift due to the electric field force. Only under these conditions is the swarm fully relaxed in space, and local velocities at the leading and trailing edges of the swarm remain unchanged in time.

In the context of swarm studies, the spatial variation of the average ion kinetic energy along the swarm has played a central role in the explanation of many phenomena, including those associated with the implicit and explicit effects of nonconservative collisions and the anisotropic nature of the diffusion [9–11]. The duality of the transport coefficients, e.g., the existence of two families of transport coefficients, the flux and the bulk [12], is explained in terms of the anisotropic distribution of the average ion kinetic energy along the swarm and energy dependent collision frequencies for nonconservative collisions. The present Letter contributes to this body of research by calculating the evolution of the average kinetic energy along the swarm and exploring its properties.

The present study aims to (i) present the relaxation of the spatial profiles of transport properties of ions in the uniform electric field, and to determine their steady-state profiles. Special attention is paid to (ii) determining whether the average ion kinetic energy at the leading edge reaches some constant stationary value or decreases during swarm evolution and (iii) identifying the spatial locations where drifting ions gain and where they lose energy during swarm evolution.

This Letter is organized as follows: First, the model used is presented, and then a brief description of the Monte Carlo technique for simulating the spatiotemporal swarm evolution is given. Results and discussion, the initial conditions of the simulation are provided next. Along with a description of the temporal relaxation. Then the relaxation of the space-resolved properties along the field direction, including ion number density and average ion kinetic energy, are presented. Energy gains and losses of the drifting ions are then presented. Finally, the results are discussed and compared with the findings of prior studies, and based on that, the conclusion is reached. Additionally, Supplemental Material is provided to accompany the Letter.

Model approach. A swarm, i.e., a dilute gas of charged particles that collide with background gas particles at a temperature, T, moves under the influence of an external electric field ($\boldsymbol{E}$) in an infinite space (x, y, z). The ensemble of ions has sufficiently low density so that (i) mutual interactions between ions can be neglected; (ii) the background neutral gas remains essentially undisturbed, and (iii) space-charge fields are negligible in comparison with the applied field.

The duration of collisions is negligible compared to the mean time between two collisions. This means that all quantum-mechanical phenomena are exclusively described by collision cross sections, and the motion of a swarm of charged particles can be described by the laws of classical physics. Using the language of plasma physics, this physical system is usually referred to as the swarm of charged particles, or sometimes the so-called test particle limit.

A swarm of lithium ions ($^7Li^+$) in krypton gas (^{88}Kr) was studied. This is simply an artificial condition of basic research. We assume that the interaction between ions and atoms takes place under the influence of an induced dipole force, which corresponds to the momentum transfer cross section for elastic collisions:

$$\sigma_{\mathrm{MT}}(\mathrm{\AA}^2) = 29/\sqrt{E(\mathrm{eV})}.$$

The σ_{MT} includes anisotropic backward and forward scatterings, as well as the isotropic capture part.

Although the model describing the interaction of ions and background gas particles has a constant collision frequency of 55.6 MHz, i.e., the mean collision time of $t_c = 1.8 \times 10^{-8}$ s, which means that it is very simple, in this case, it is also completely realistic. In the range of reduced electric field strength $|\boldsymbol{E}|/N_g < 25$ Td (1 Td $= 10^{-21}$ V m^2, N_g is the gas number density), computed drift velocities by Koutselos *et al.* [13], Lozeille *et al.* [14], and Tan *et al.* [15], as well as in the presented simulations, agree well (<1%) with those experimentally measured by Ellis *et al.* [16] and Takebe *et al.* [17] at $T = 300$ K.

Monte Carlo simulation. The code used in these simulations was verified on benchmark tests [18]. It is based on tracking a large number of ions that gain the energy from the external electric field directed along the z axis and dissipate this energy through collisional transfer with neutral gas particles. Collisions are instantaneous and isotropic, and the instant of collision is determined by the null-collision method [19].

Swarm transport parameters (averaged on all of the swarm, such as the mean kinetic energy and drift velocity) and the space-resolved transport properties of ions (such as the average kinetic energy and number density) were observed through the temporal evolution for the sampling instants. When the swarm's mean energy $E(t_s)$ and drift velocity $v_d(t_s)$ reach their steady-state values they are denoted by E_s and v_d.

For sampling of the one-dimensional space-resolved transport properties of ions along the electric field direction, the space of the swarm is restricted in interval $z \in (z_{\mathrm{c.m.}} - 3\sigma_z,\ z_{\mathrm{c.m.}} + 3\sigma_z)$, where $z_{\mathrm{c.m.}}$ is the coordinate of the centers of mass (c.m.) of the swarm, and $\sigma_z = (\langle z^2\rangle - \langle z\rangle^2)^{0.5}$ is the standard deviation of the spatial distribution of ions along the electric field. The mean value of magnitude A is denoted as $\langle A\rangle$. The observed spatial interval is divided into N_b cells whose centers have z_p coordinates and these points are used to sample spatial profiles of the swarm. This study follows the development of the swarm in real space as well as in space normalized to six standard deviations ($6\sigma_z$). The width of the cell in real space increases with time as $\Delta z(t) = 6\sigma_z(t)/N_b \propto t^{0.5}$, while in normalized space it does not increase $\Delta\sigma(t) = 6/N_b = \mathrm{const}$.

In this Letter, we present the computation of one-dimensional spatial profiles of the transport properties of the ions along the direction of the field. These properties of the ions include the number density of the ions, $N(z,\ t)$; the average ion kinetic energy, $E(z,t)$; the average ion velocity, $v_z(z,t)$; the average electric power absorbed from the electric field by the ions, $P_E(z,t)$; and the average ion dissipated power losses due to collision processes, $P_C(z,t)$. The space-resolved number density of the ions, $N(z_p,t_s)$, represents the number of ions in the spatial cell p for the instants t_s per the width of the spatial cell, normalized to the total number of the ions, which is the same as the distribution function of the swarm along the z axis.

Results and discussion. In this section, the spatiotemporal evolution of drifting lithium ions in the background gas of krypton at a temperature of $T = 300$ K was considered in a reduced electric field strength of $|\boldsymbol{E}|/N_g = 20$ Td, where the gas number density was set to 3.54×10^{22}m^{-3}. At time $t = 0$, corresponding to a delta-function pulse in time, the ions are initially isotropically released from the origin according to the Maxwellian distribution, with a mean starting energy of $E_0 = 0.1$ eV. After approximately 50 collisions per ion or about 1 μs, the total balance of momentum and energy is established, i.e., drift velocity and swarm main kinetic energy have reached their steady-state values of $v_d = 188$ m/s and $E_s = 0.0555$ eV.

Spatiotemporal relaxation of the ion number density and average ion kinetic energy. At the beginning of the initial collision-free phase until the moment $t = 0.1$ ns, there were practically no collisions between the ions and the gas particles ($t/t_c = 0.0056$). In such a short time, the electric field has negligibly changed the individual ion energies in relation to their initial values at the origin. As a consequence, the ions generally occupy simple positions corresponding to their starting energy. For times sufficiently short after the instant of isotropic emission, the swarm will display spherical symmetry in three-dimensional space, with ions of the same initial energy assuming positions on a sphere whose radius is dependent on their energy [$r = (2E/m)^{0.5}t$].

The one-dimensional spatial profile of the $N(z)$ has a Gaussian shape while the profile of the $E(z)$ has the shape of a parabola (Fig. 1). Figure 1 shows that the $E(z)$ around the c.m. is less than the mean starting energy E_0. The c.m. neighborhood for that instant contains only ions that have a small velocity component along or opposite to the field, in order for ions to remain in the central spatial cell ($z < 0.5\Delta z$).

When the swarm accelerates, the maximum of the $N(\sigma)$ profile moves backwards relative to the c.m., shown in Fig. 2. Afterwards, when the total balance of momentum is established, the collisions shift the maximum back towards the c.m. Figure 2 also shows the Gaussian function (gray symbols), which represents the shape to which the profile of the $N(\sigma)$ approaches during its further evolution.

Figure 3 displays the $N(z)$ profiles as solid lines and the $E(z)$ profiles as symbols, for the instants of 0.5, 1, 1.5, and 2 μs. The swarm has not yet completely passed the origin (situated at $z = 0$), and the swarm transport parameters have already reached their steady-state values ($t > 1$ μs).

Between $t = 0.1$ ns and 2 μs there is a significant evolution of the $E(z)$, as shown in Figs. 1 and 3. It changes from a

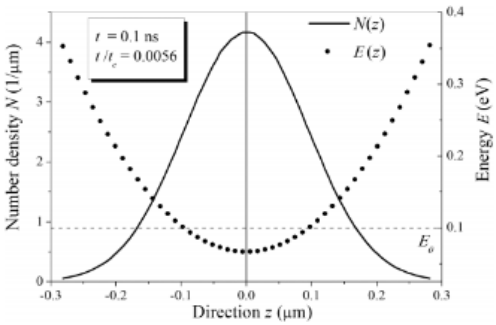

FIG. 1. Space-resolved ion number density and average ion kinetic energy, for the instant of $t = 0.1$ ns.

symmetric distribution to an asymmetric distribution with a much lower $E(z)$, and with the ions behind the c.m. having energy close to the thermal energy of the gas. The evolution of the shape of the $E(z)$ profile, from a parabolic to a linearly increasing function of space, is due solely to the field and the initial conditions. However, collisions can erase the local memory of the initial conditions.

Figure 4 shows that for the instant of $t = 100$ μs the profile of the $N(\sigma)$ coincided with the Gaussian shape. This coincidence does not mean that the $N(\sigma)$ is spatially relaxed, but only that the displacement of the maximum of the $N(\sigma)$ profile relative to the c.m. is less than half the width of the spatial cell $(0.5\Delta\sigma)$ for that instant.

After some point in the swarm evolution, the simulations used cannot determine the behavior of the slope of the $E(\sigma)$ line due to its small changes with time as shown in Fig. 4.

Although the slope of the steady-state profile of the $E(\sigma)$ cannot be determined by these simulations based on profile slope monitoring, it can be sought based on the spatial locations where the ions gain and lose energy during swarm relaxation.

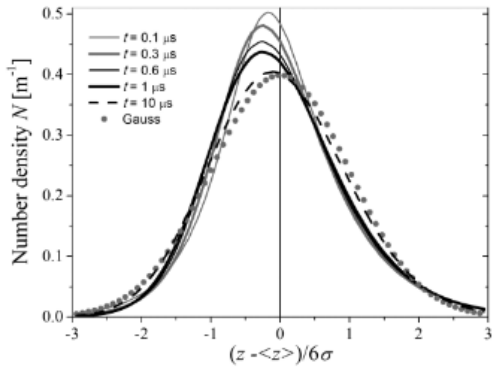

FIG. 2. Space-resolved ion number density in the normalized space for different instants.

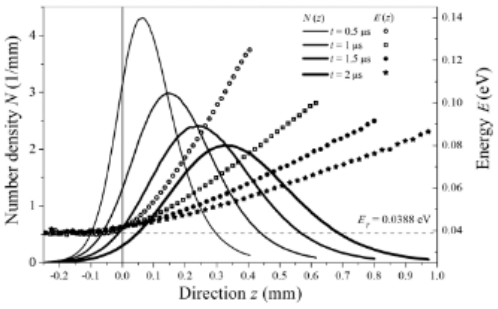

FIG. 3. Space-resolved ion number density (solid lines) and average ion kinetic energy (symbols), for the instants when the swarm did not leave the origin yet. E_T represents the thermal energy of the background gas.

Spatiotemporal relaxation of the energy gains and losses of the drifting ions. The nature of the spatial profile of the transport properties of ions is dependent on the interplay between the local electric and dissipated power. The work done by an ion while moving in a constant uniform electric field is proportional to the displacement of ions along the direction of the field. In the absence of nonconservative collisions [12], the local average electric energy absorbed by ions from the field is proportional to the local average ion velocity $[\Delta E(z) \propto v_z(z)\Delta t]$. The energy transmitted between an ion and a gas particle during an elastic collision is proportional to the ion kinetic energy. The local average dissipated energy by ions due to collision processes is proportional to the local average ion kinetic energy $[\Delta E(z) \propto E(z)\Delta t/t_c]$. Due to the different functional forms when total energy balance is established, local electric gains and dissipated losses of energy are generally not in balance. In this section, the spatiotemporal relaxation of the electric and dissipated power spatial profiles, and the associated phenomena induced by nonlocal effects are shown.

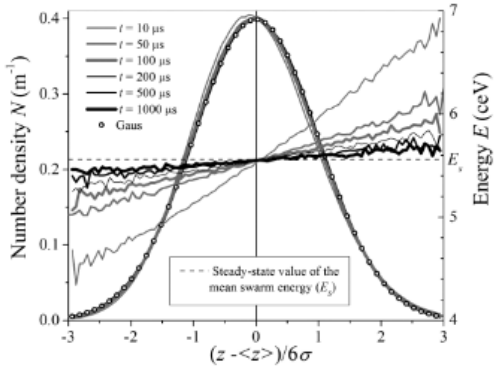

FIG. 4. Space-resolved ion number density (like Gaussian shape) and average ion kinetic energy (linearly increasing functions of space) for different instants in which they aspire to their steady-state forms.

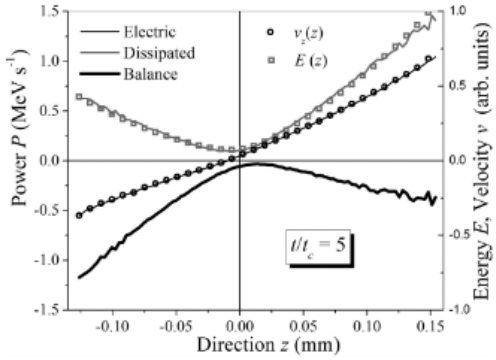

FIG. 5. Space-resolved average ion power including average ion electric power, average ion dissipative power losses, and average ion power balance for the instant of $t = 5t_c$. The units for $E(z)$ and $v_z(z)$ profiles were chosen for the curves to overlap the power profiles.

During the relaxation of the swarm's mean kinetic energy from its starting value of 0.1 eV to its steady-state value of 0.056 eV, for the instant of $t/t_c = 5$, the local average power balance, $P(z)$, is less than zero in the whole swarm space, as we can see in Fig. 5. The spatial profile of the average dissipated power due to collision processes, $P_C(z)$, for that instant, coincided with the shape of the $E(z)$ profile, while the profile of the average power deposited into ions by the electric field, $P_E(z)$, coincided with the shape of the $v_z(z)$ profile, according to their functional dependencies. The $E(z)$ and $v_z(z)$ profiles are shown as symbols in Fig. 5.

During the further swarm evolution, the $P_E(z)$ and $P_C(z)$ profiles are linearly increasing functions of space as shown in Fig. 6. The fact that the slope of the $P_C(z)$ profile is higher than

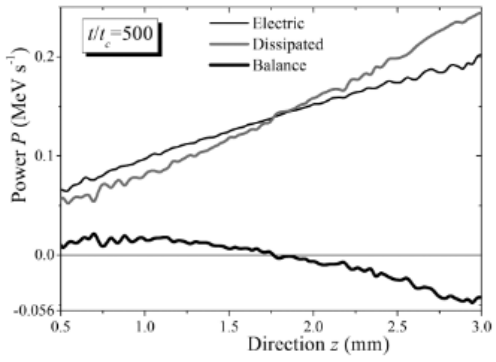

FIG. 6. Space-resolved average ion power including average ion electric power, average ion dissipative power losses, and average power balance of the ions for the instant of $t = 500t_c$.

that of the $P_E(z)$ profile, leads to a conclusion that $P(z) < 0$ at the swarm front, while $P(z) > 0$ is at the tail.

In real space, the slopes of the $E(z)$, $v_z(z)$, and $P(z)$ profiles decrease due to both the increase in swarm dimensions caused by diffusion and the shape of the $P(z)$ profile. However, in normalized space, their decrease is due to the shape of the $P(\sigma)$ profile. Furthermore, the behavior of local ion kinetic energies at the leading and tail edges of the swarm is more clearly observed in normalized space, as shown in Fig. 4. Cooling the front and heating the tail of the swarm results in a decrease in the slope of the $E(\sigma)$ and $v_z(\sigma)$ profiles, and less difference between $P_E(\sigma)$ and $P_C(\sigma)$. This self-consistent decrease in the slope of the $E(\sigma)$ and $v_z(\sigma)$ profiles on the one hand, and the decrease in the slope of the $P(\sigma)$ profile on the other, causes a slower change in the slope of the $E(\sigma)$, $v_z(\sigma)$, and $P(\sigma)$ profiles over time. When $t \to \infty$, the energy gain and loss mechanism becomes locally balanced and spatially independent, causing the $P(\sigma)$ profile to approach its steady-state form of zero slope and constant zero value.

The Supplemental Material [20] contains a comparison of the $P(z)$ and $P(x)$ profiles. Here, the x direction denotes any direction perpendicular to the field. The $P_C(x)$ profile follows the shape of the $E(x)$ profile, which, due to free diffusion, resembles spreading parabolas. In contrast, the $P_E(x)$ profiles are constant, independent of x. Different forms of the $P_C(x)$ and $P_E(x)$ result in $P(x) > 0$ near the c.m., and $P(x) < 0$ at the periphery of the swarm.

Conclusion. During the final phase of relaxation of a swarm of charged particles in a constant electric field, the interplay of electrical gains and losses in the elastic collisions of ions, leads to the shape of the $P(z)$ profile as a linearly decreasing function of space, with zero in the c.m. and with a slope approaching zero.

The $E(z)$ changes from the initial parabolic shape, due to the initial condition, to a linearly increasing function of space, due to the electric field. In the final phase of relaxation the local value of the $E(z)$ on the leading edge decreases, while on the trailing edge, it increases. This is a result of the shape of the $P(z)$ profile. When $t \to \infty$, the $E(z)$ profile tends to its steady-state shape, and becomes spatially independent and locally equal to the mean energy of the swarm, despite the significant difference in electrical potential between the leading and trailing edges of the swarm. This is not in accordance with the conclusion of the work [8], given in the Introduction.

The obtained steady-state spatial profiles of the transport properties of ions for very simple so-called "closed-shell" systems, such as $^7Li^+$ in ^{88}Kr, can also be generalized to systems, in which there are different ion-neutral interactions. These are primarily systems in which (1) the total collision frequency increases with energy or (2) the ion energy losses in the collision increase in relation to the losses in elastic collisions. Examples for the first group are the soft sphere scattering models, for which $\nu(E) \propto E^n$ is satisfied, where $n \in (0, \frac{1}{2})$, as well as the hard spheres scattering model [$\sigma_{MT} = \text{const} \to \nu(E) \propto E^{1/2}$]. The second group includes systems, in which inelastic collisions, neutral dissociation, ionization, or symmetric charge-exchange collisions exist between charged particles and background gas.

The presence of the mentioned ion-neutral interactions (1) and (2) in the plasma results in a greater energy exchange between ions and gas at higher ion kinetic energies compared to the considered elastic interaction. As a result, these interactions accelerate the relaxation process of the swarm and facilitate the formation of ion spatial profiles that correspond to those depicted in this study.

Acknowledgment. This work is supported by the Ministry of Science, Technological Development and Innovations of the Republic of Serbia and Institute of Physics Belgrade. This work is also supported by the Science Fund of the Republic of Serbia, Grant No. 7749560, Exploring ultra-low global warming potential gases for insulation in high-voltage technology: Experiments and modelling—EGWIn.

[1] M. A. Lieberman and A. J. Lichtenberg, *Principles of Plasma Discharge and Materials Processing* (Wiley, Hoboken, NJ, 2005).
[2] R. H. Stark and K. H. Schoenbach, J. Appl. Phys. **85**, 2075 (1999).
[3] K. Ostrikov, U. Cvelbar, and A. Murphy, J. Phys. D: Appl. Phys. **44**, 174001 (2011).
[4] R. E. J. Sladek and E. Stoffels, J. Phys. D: Appl. Phys. **38**, 1716 (2005).
[5] H. Sugawara, H. Tagashira, and Y. Sakai, J. Phys. D: Appl. Phys. **29**, 1168 (1996).
[6] M. Suvakov, Z. Ristivojevic, Z. Petrovic, S. Dujko, Z. Raspopovic, N. Dyatko, and A. Napartovich, IEEE Trans. Plasma Sci. **33**, 532 (2005).
[7] Z. Raspopovic, S. Dujko, R. White, and Z. Petrovic, IEEE Trans. Plasma Sci. **39**, 2566 (2011).
[8] S. Dujko, R. White, Z. Raspopovic, and Z. Petrović, Nucl. Instrum. Methods Phys. Res. Sect. B **279**, 84 (2012).
[9] I. Simonović, D. Bošnjaković, Z. Lj. Petrović, P. Stokes, R. D. White, and S. Dujko, Phys. Rev. E **101**, 023203 (2020).
[10] S. Dujko, R. D. White, Z. Lj. Petrović, and R. E. Robson, Phys. Rev. E **81**, 046403 (2010).
[11] I. Simonović, D. Bošnjaković, Z. L. Petrović, R. D.White, and S. Dujko, Plasma Sources Sci. Technol. **31**, 015003 (2022).
[12] R. E. Robson, Aust. J. Phys. **44**, 685 (1991).
[13] A. D. Koutselos, E. A. Mason, and L. A. Viehland, J. Chem. Phys. **93**, 7125 (1990).
[14] J. Lozeille, E. Winata, P. Soldán, P. F. Lee Edmond, L. A. Viehland, and T. G. Wright, Phys. Chem. Chem. Phys. **4**, 3601 (2002).
[15] T. L. Tan, P. P. Ong, and M. M. Li, Phys. Rev. E **52**, 4294 (1995).
[16] H. W. Ellis, M. G. Thackston, E. W. McDaniel, and E. A. Mason, At. Data Nucl. Data Tables **31**, 113 (1984).
[17] M. Takebe, Y. Satoh, K. Iinuma, and K. Seto, J. Chem. Phys. **76**, 5283 (1982).
[18] Z. Ristivojevic and Z. Lj. Petrović, Plasma Sources Sci. Technol. **21**, 035001 (2012).
[19] H. K. Skullerud, J. Phys. D: Appl. Phys. **1**, 1567 (1968).
[20] See Supplemental Material at http://link.aps.org/supplemental/10.1103/PhysRevE.108.L053202 for longitudinal and perpendicular spatially resolved profiles of average powers during the swarm evolution.

3. Рад М22

A Letters Journal Exploring the Frontiers of Physics

October 2019

EPL, **128** (2019) 15001
doi: 10.1209/0295-5075/128/15001

www.epljournal.org

Reduced mobility of Ar^+ in Ar/BF_3 mixtures

Ž. D. Nikitović, Z. M. Raspopović and V. D. Stojanović

Institute of Physics, University of Belgrade - Pregrevica 118, Belgrade, Serbia

received 7 August 2019; accepted in final form 1 October 2019
published online 15 November 2019

PACS 51.10.+y – Kinetic and transport theory of gases
PACS 52.20.Hv – Atomic, molecular, ion and heavy-particle collisions
PACS 52.65.Pp – Monte Carlo methods

Abstract – In this work we present a cross-section set and transport properties of Ar^+ in Ar/BF_3 mixtures. These data are needed for modeling in numerous applications of technological importance. A Monte Carlo simulation method is applied to accurately calculate transport parameters in the hydrodynamic regime. We discuss new data for Ar^+ ions in Ar/BF_3 mixtures where the mean energy the flux and bulk values of reduced mobility and other transport coefficients are given as a function of low and moderate reduced electric fields E/N (E-electric field, N-gas density).

Introduction. – Cold plasmas are frequently used in new technologies where they open up the possibilities of non-intrusive production or modification of various substances [1]. These plasmas have a high electron temperature and low gas temperature so the non-equilibrium behavior of a large number of species becomes important [2]. Current computer resources allow studies of complex global models [3] which describe the behavior of such plasmas by taking into account a very large number of particles. The knowledge of ion-neutral reactions is generally avaliable [4] although the effects of reactions on transport parameters of particular ions are much less studied due to non-detectability of rapidly vanishing ionic fluxes. This especially holds for ions whose transport is affected by fast reactions [5,6].

The transport of Ar^+ plays a significant role in various etching and deposition processes [7,8], in dark matter detection [9] and many more applications. It is known that the transport parameters of Ar^+ in Ar are affected by resonant charge transfer reactions [10] leaving slow ions as a result. Charge transfer reactions are the most important collisional events in BF_3 gas where they introduce neutralization of Ar^+ ions [11]. The large rate coefficient for exothermic reactions (recombination energy of the ion is higher than the ionization potential of the gas particles) limits the number of ions necessary to determine the ion mobility. Boron dopant penetration in silicon is technologically achieved by a DC pulsed-plasma system (PLAD) most widely applying BF_3 gas [12,13]. Uniform plasma and implantation with normal ion incidence are the main goals in this technological process. By using Monte Carlo simulations one may calculate transport parameters for the cases that are out of the reach of experimental efforts provided the complete cross-section set is known. Reduced mobility data of both flux and bulk values as a function of E/N, are expected to be significantly affected by the presence of endothermics and exothermic reactions in the case of Ar^+ transport in the Ar/BF_3 mixtures.

Cross-section sets. – Complete cross-section sets for ion transport are scarce in spite of a broad range of specific methods relevant for quantification of particular cross-sections. The main problem in heavy-particle scattering, easily and precisely selecting the state of the projectile and target before the collision, is still very complicated for a range of conditions, so databases for ion scattering [4,13] are still devoid of such data. Phelps established the first worldwide accessible database with cross-section sets [14] tested for each particular case either for swarm conditions of spatially resolved measurements of emission or ion mobility values. Another range of cross-section sets was established by measurements of ionic transport coefficients [4] and this work is ongoing. In all cases only the most important cross-sections may be established from the transport data. In the following section we will establish a complete cross-section set for Ar^+ scattering on Ar and BF_3 from 0.1 meV to 1000 eV which will be used to calculate transport properties. Generally one may distinguish three characteristic energy ranges: the low-energy regime where polarization scattering is dominant, the medium-energy regime where the polarization scattering is gradually replaced by the hard sphere repulsion, and the high-energy approximation regime.

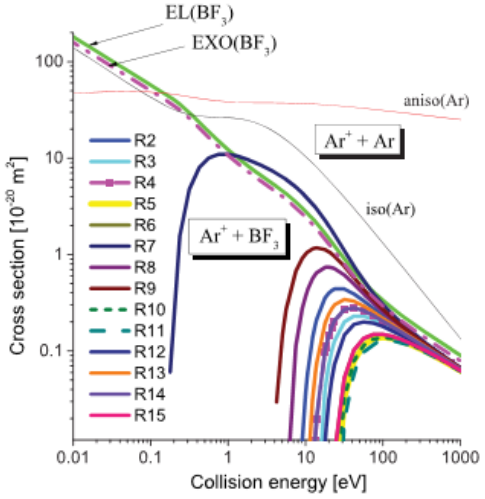

Fig. 1: Cross-sections for Ar^+ in BF_3 gas.

Table 1: Reaction products and thermodynamic thresholds for $Ar^+ + BF_3$.

1	EL	$Ar^+ + BF_3$ (el)	0.0000
2	R2	$Ar^+ + BF_2 + F$	7.4373
3	R3	$Ar^+ + BF + 2F$	12.2940
4	R4	$Ar^+ + BF + F2$	10.6461
5	R5	$Ar^+ + B + 3F$	20.1367
6	R6	$Ar^+ + B + F + F_2$	18.4889
7	R7	$BF_2^+ + Ar + F$	0.1544
8	R8	$BF^+ + 2F + Ar$	5.0115
9	R9	$BF^+ + F_2 + Ar$	3.3637
10	R10	$F^+ + B + F_2 + Ar$	20.1488
11	R11	$F^+ + B + 2F + Ar$	21.7966
12	R12	$F^+ + BF + F + Ar$	13.9539
13	R13	$F^+ + BF_2 + Ar$	9.0972
14	R14	$F_2^+ + BF + Ar$	10.5846
15	R15	$F_2^+ + B + F + Ar$	18.4273
16	EXO	$BF_3^+ + Ar$	−0.2125

Extensive discussion about transport properties of Ar^+ ions scattering in BF_3 gas applied to plasma physics problems was presented by Phelps [15] and Petrović and Stojanović [16]. Analytical expressions were given in [11] to express both isotropic and anisotropic components of the cross-section set (see fig. 1). In order to focus on effects of reactive processes introduced by BF_3 we neglected all but these two components of the $Ar^+ + Ar$ cross-section set. The complete cross-section sets used in this work are shown in fig. 1.

In table 1 we present the reaction products and thermodynamic thresholds for $Ar^+ + BF_3$.

Therefore we have assumed in this work that exothermic processes are non-resonant because the fast charge transfer reaction for $BF_3{}^+$ production proved that the internal states of the target, which are populated, are those closest to the recombination energy of the Ar^+ [10,17].

Transport parameters. – Monte Carlo Simulations (MCS) have many applications in the analysis of transport of charged particles in plasmas. MCS provide swarm data with the only uncertainty due to statistical fluctuations and uncertainties in the cross-sections. In addition, MCS is the basis of hybrid models of plasmas allowing easy and accurate representation of the end effects and of the non-local high-energy groups of particles which are essential in the production of plasmas and the treatment of surfaces. The MC code used in our analysis is based on the null collisions method. We assume that our intersections give the transport coefficients at low energies with 30% errors and at high energies they describe well the order of magnitude. Experimentally determined cross-sections or transport parameters significantly reduce the errors. Monte Carlo code errors are below 0.1%.

Transport properties of species in gas plasmas are of great importance in understanding the nature of molecular and ionic interactions in gas mixtures [18,19]. These properties include the mean energy, drift velocity, diffusion coefficients, ionization and chemical reaction coefficients, chemical reaction coefficients for ions and rarely gases. A Monte Carlo simulation code appropriate for the calculation of transport parameters [16,18] of Ar^+ ions in Ar/BF_3 mixtures at non-zero temperature [20] has been used. In Monte Carlo simulations exothermic reactive collisions are followed in a similar way as all non-conservative collisions, *i.e.*, the swarm particle dissappears from the ensemble after the exothermic collisions. This results in changes of the swarm particle number in the entire energy range introducing non-conservative effects in kinetic equations and thus division of transport parameters to flux and bulk values [18].

In fig. 2 we show the results for the mean energy as a function of E/N (E is the electric field and N the gas density). Significant reduction and uniform control of the mean energy of Ar^+ is obtained for argon content below 90%. For Ar content below 10% the largest variations of mean energy are obtained for $E/N > 100$ Td (1Td = 10^{-21} Vm^2). These variations are the consequence of a reduced momentum transfer cross-section for Ar^+ scattering with BF_3 (see fig. 1) as compared to the scattering with Ar. At a high content of Ar, charge transfer collisions dominate and make the variation of mean energy with Ar content more uniform. Note, that for the transport coefficients of Ar^+ in pure Ar one may find benchmark data presented in tabular form by Ristivojević and Petrović [20].

In fig. 3 we show the characteristic energies (diffusion coefficient normalized to mobility eD/K in units

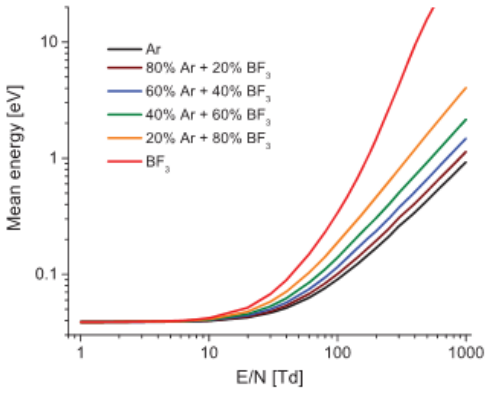

Fig. 2: Mean energy as a function E/N for Ar^+ in Ar/BF_3 gas.

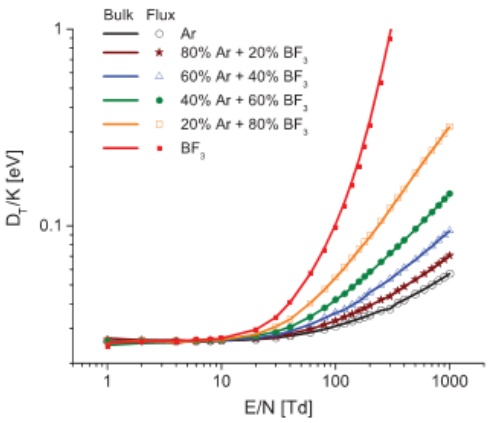

Fig. 3: Characteristic energy as a function E/N for Ar^+ in Ar/BF_3 gas.

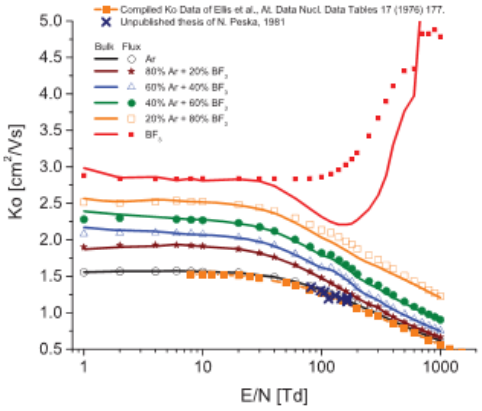

Fig. 4: Reduced mobility as a function E/N for Ar^+ in Ar/BF_3 gas.

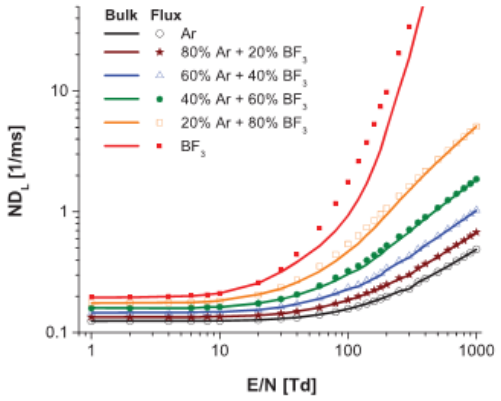

Fig. 5: Longitudinal diffusion coefficients as a function E/N for Ar^+ in Ar/BF_3 gas.

of eV) based on transversal (D_T) diffusion coefficients. The difference between bulk and flux values is small.

In fig. 4 the variations of reduced mobility as a function of E/N are shown. The mobility K of a ion is a quantity defined as the velocity attained by an ion moving through a gas under a unitary electric field. One often exploits the reduced or standard mobility defined as

$$K_0 = \frac{v_d}{N_0 E} N, \tag{1}$$

where v_d is the drift velocity of the ion, N is the gas density at elevated temperature T, $N_0 = 2.69 \cdot 10^{25}\,\mathrm{m}^{-3}$ and E is the electric field. The behavior of reduced mobility significantly changed with E/N with small additions of Ar, up to about 10%. Especially intriguing are variations of flux reduced mobility which points to the particle flux variations of Ar^+ ions as a function of their mean energy. On the one side, small additions of Ar cause significant variations of the particle flux at E/N close to 200 Td and, on the other, in that region we obtain a significant difference of the flux and bulk drift velocities due to the BF_3 reactive processes (see also [10]) which also significantly reduce the Ar^+ density in favour of fast Ar [11]. Control of the fast Ar flux at the surface thus can be easily achieved by small variations of the Ar content in the Ar/BF_3 mixture. Due to reactive collisions the bulk and flux values of reduced mobility are separated.

Longitudinal diffusion coefficients for Ar^+ ions in Ar/BF_3 mixtures as a function of E/N are shown in fig. 5. Note that the difference between the flux and bulk values of the diffusion coefficients, which have the same origin, have the same initial value as the drift velocities. Due to the large resonant charge transfer for $Ar^+ + Ar$ the value

of ND_L is small and is slowly changing with the increase of the electric field. Since there are no reactions in which Ar^+ ions disappear, flux and bulk values are equal for all transport parameters.

On the other side, for the scattering of Ar^+ on BF_3 due to the increase of collision frequency with energy, ions of large energy mostly disappear, decelerating the spread of swarm in the field direction. So bulk values of ND_L become smaller than the flux values. Another point is that the decrease of the elastic momentum transfer cross-section with energy causes the increase of flux values of drift velocity $V_F = \langle v \rangle$ as well as $D_L(F) = \langle xVx \rangle - \langle x \rangle \langle Vx \rangle$.

There are no published experimental data for the longitudinal and transverse diffusion coefficients of Ar^+ in Ar/BF_3.

Conclusion. – Data of swarm parameters for ions are needed for hybrid and fluid codes and the current focus on liquids or mixtures or liquids with rare gases dictates the need to produce data compatible with those models. In this paper we show transport parameters for Ar^+ in Ar/BF_3 mixtures which do not exist in the literature. In addition to presenting the data we show here the effects of non-conservative collisions to ion transport.

The Monte Carlo technique was applied to carry out calculations of the mean energy and characteristic energy, reduced mobility, longitudinal diffusion coefficients as a function of a reduced DC electric field. The results are believed to be a good base for modeling, which will be able to further improve when the measured values of transport coefficients become available and then we will be able to perform this analysis again.

* * *

Results obtained in the Institute of Physics University of Belgrade under the auspices of the Ministry of Education, Science and Technology, Projects OI 171037 and III 45016.

REFERENCES

[1] Makabe T. and Petrović Z., *Plasma Electronics: Applications in Microelectronic Device Fabrication* (Taylor and Francis, CRC Press, New York) 2006.

[2] Robson R. E., White R. D. and Petrović Z. Lj., *Rev. Mod. Phys.*, **77** (2005) 1303.

[3] Murakami T., Niemi K., Gans T., O'Connell D. and Graham W. G., *Plasma Sources Sci. Technol.*, **22** (2013) 015003.

[4] `https://nl.lxcat.net/data/set_type.php`.

[5] Stojanović V., Nikitović Ž., Raspopović Z. and Jovanović J., *Acta Phys. Pol. A*, **125** (2014) 46.

[6] Nikitović Ž., Gilić M., Raspopović Z. and Stojanović V., *EPL*, **116** (2016) 15002.

[7] Stojanović V., Raspopović Z., Jovanović J., Nikitović Ž. and Petrović Z. Lj., *EPL*, **101** (2013) 45003.

[8] Lieberman M. A. and Lichtenberg A. J., *Principles of Plasma Discharges and Materials Processing* (Wiley, New York) 1994.

[9] Kaboth A., Monroe J., Ahlen S., Dujmić D., Henderson S., Kohse G., Lanza R., Lewandowska M., Roccaro A., Sciolla G., Skvorodnev N., Tomita H., Vanderspek R., Wellenstein H., Yamamoto R. and Fisher P., *Nucl. Instrum. Methods Phys. Res. A*, **592** (2008) 63.

[10] Parker E. and El-Ashhab F. S. M., *Int. J. Mass Spectrom. Ion Phys.*, **47** (1983) 159.

[11] Phelps A. V., *J. Appl. Phys.*, **76** (1994) 747.

[12] Koo B.-W., Fang Z., Godet L., Radovanov S. B., Cardinaud C., Cartry G., Grouillet A. and Lenoble D., *IEEE Trans. Plasma Sci.*, **32** (2004) 456.

[13] Nikitović Ž., Radovanov S., Godet L., Raspopović Z., Šašić O., Stojanović V. and Petrović Z. Lj., *EPL*, **95** (2011) 45003; Petrović Z. Lj., Dujko S., Marić D., Malović G., Nikitović Ž., Šašić O., Jovanović J., Stojanović V. and Radmilović-Radenović M., *J. Phys. D: Appl. Phys.*, **42** (2009) 194002.

[14] Phelps database Ar^+/Ar, retrieved on June 27, 2018.

[15] Phelps database, `www.lxcat.net`, retrieved on February 4, 2019.

[16] Petrović Z. Lj. and Stojanović V. D., *J. Vac. Sci. Technol.*, **16** (1998) 329.

[17] Jarvis G. K., Kennedy R. A., Mayhew C. A. and Tuckett R. P., *Int. J. Mass Spectrom*, **202** (2000) 323.

[18] Robson R. E., *Aust. J. Phys.*, **44** (1991) 685.

[19] Raspopović Z., Sakadžić S., Petrović Z. Lj. and Makabe T., *J. Phys. D*, **33** (2000) 1298.

[20] Ristivojević Z. and Petrović Z. Lj., *Plasma Sources Sci. Technol.*, **21** (2012) 035001.

4. Рад М22

Science of Sintering, **54** (2022) 169-176

https://doi.org/10.2298/SOS2202169N

UDK: .001.572; 662.765.5

Rate Coefficients for H^+ Ions in n-Butanol Gas

Željka Nikitović[*)], **Zoran Raspopović**
Institute of Physics, University of Belgrade, Pregrevica 118, Belgrade, Serbia

Abstract:

In this work we show predictions for the low energy cross sections and transport properties for the H^+ ions in n-Butanol gas. These data are needed for modelling in numerous applications of technologically importance. Appropriate gas phase enthalpies of formation for the products were used to calculate scattering cross section as a function of kinetic energy. Calculated cross sections can be used to obtain rate coefficients as a function of E/N (E -electric field strength; N-gas density) for H^+ in n-Butanol gas.

Keywords*: Monte Carlo Simulations; Positive ions; n-Butanol gas.*

1. Introduction

n-Butanol (C_4H_9OH) also known as 1-butanol or bio-butanol has a 4 carbon straight-chain structure, with the –OH at the terminal carbon. It is an important chemical feedstock used to produce solvents (butyl acetate, butyl glycol ethers) [1,2], polymers (butyl acrylate, butyl methacrylate) [3] and plastics. But the recent interest in n-Butanol is mostly due to its application as a biofuel for use in engines, as an alternative to conventional gasoline and diesel fuels [4-7]. Biofuels are attracting great interest as transportation fuels because they are renewable, can be locally produced, less polluting, more biodegradable, and reduce net greenhouse gas emissions [8]. n-Butanol, like ethanol, can blend with gasoline very well and could be a future option for blending with diesel. Butanol consists more oxygen content compared with biodiesel, leading to further reduction of the soot. n-Butanol occurs naturally as a minor product of the fermentation of sugars and other carbohydrates and is present in many foods and beverages as well as in a wide range of consumer products. Although most volatile organic compounds can be detected by fast methods such as ion mobility spectroscopy, precise determination is possible only if reaction of specific ions with targeted compound is well known.

n-Butanol is produced by alcoholic fermentation of the biomass feedstock [9-12] which include sugar beet, sugar cane, corn, wheat, and other various plant crops containing cellulose that could not be used for food and would otherwise go waste. Recently, the use of generically enhanced bacteria has also increased the fermentation process productivity.

The goal of this work is to calculate transport parameters of fragment ions of n-Butanol. Mechanical properties can also be modeled, i.e. elastic modulus [13] and mechanical impedance [14]. We employ Denpoh-Nanbu's theory (DNT) [15] to calculate transport cross section sets for H^+ ions scattering on n-Butanol appropriate for low energies of H^+ ions. By using Monte Carlo technique that properly takes into account thermal collisions [16] we calculated transport parameters as a function of *E/N*.

[*)] **Corresponding author:** zeljka@ipb.ac.rs

2. Calculation on the cross sections set

The calculation of cross sections would include the determination of the potential energy surface of the ion-neutral interaction, followed by quantum-mechanical calculations of ion-neutral scattering processes [17]. All these tasks can be performed only if a certain level of approximation is introduced. There is another approach where it is possible to use some statistical theory [18] where the specific reaction rate for a single molecular reaction can be used to obtain the cross section for each particular process [15,19].

The scattering cross sections of H^+ on n-Butanol are calculated by using the DNT [15] separating elastic from reactive collisions. The induced dipole polarizability of 8.9×10^{-24} cm^3 [20] is used for the n-Butanol target. In resemblance with our recent work [21] DNT method is used to separate elastic from reactive endothermic collisions by accounting for the thermodynamic threshold energy and branching ratio according to the Rice-Rampsperger-Kassel (RRK) theory [22]. Within the RRK theory the internal energy is being distributed among an empirical number of ***s*** equivalent effective modes of the complex selected from the total number of atoms involved in the complex.

Appropriate gas phase enthalpies of formation for the products [23] (Table I) were used to calculate thermodynamic thresholds. The cross-section for the exothermic reaction (EXO) forming a molecular ion H^+ in n-Butanol is commonly represented by ion capture cross-section:

$$\sigma_{exo} = \beta\sigma_L, \qquad (1)$$

where σ_L is the orbiting cross-section [17] and β is the probability of a specific exothermic reaction.

In this calculation, in the absence of resonant exothermic reactions, we assumed that the probability of exothermic reactions is zero ($\beta = 0$). At the low energy limit, the cross sections are similar due to the dominant polarization of the target. At higher energies, reactive collisions, including non-conservative collisions, become efficient for various possible processes.

It is well known that the swarm method [24,25] can be used to modify the cross section for the transmission of an elastic impulse if the transport parameters are known. Thus, an elastic pulse transmission cross section can be obtained if some initial, approximate cross section is available. Transport parameters are not available for n-Butanol transport [19]. We have separated the endothermic and exothermic processes by using the enthalpies from Ref. [23].

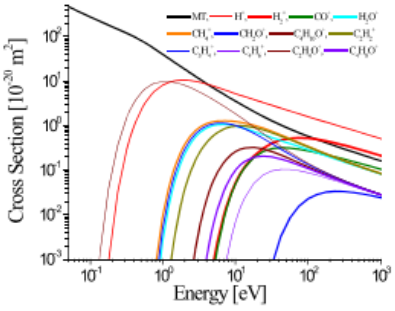

Fig. 1. Cross sections for H^+ ions in n-Butanol.

In this paper there are 20 exothermic processes. Exothermic process with lowest excess energy (H^+ + n-butanol→$C_3H_3OH^+$+C_3H_4 +H) has 0.118 eV excess energy while lowest endothermic threshold (H^++n-butanol→ $C_2H_4O^+$+C_2H_2+2H_2+H) is 0.061 eV. Therefore we have assumed in this work that exothermic processes are non-resonant, and neglected their effect on transport properties. With assumed product ions we have selected 47 endothermic processes with thermodynamic thresholds up to about 11 eV. In the reaction of H^+ in n-Butanol the product can be observed ion and the remaining particles in the collision are grouped in different ways. That number is indicated in parentheses next to the ion. If the number in parentheses is greater than 1 the cross sections are summed and shown as one in Fig. 1 next to the ion designation formed.

Tab. I Heats of formation $\Delta_f H^0$ at 298 K (kJ/mol).

Species	**ΔH_f^+ ion**	**ΔH_f^0 neutral**
H_2	1488.3	0
CO	1241.59	-393.51
CO_2	935.4	-393.51
CH_2O	940.5	-108.7
H_2O	975.0	-241.83
CH_4	1132	-74.5
C_2H_4	1066	52.2
C_2H_6	1028	-84.0
C_3H_6	959	20.2
C_3H_8	227.5	951.5
C_4H_8	924	-0.4
C_4H_{10}	889	-126.5
CH_4O	845.3	-201.6
C_2H_6O	775.4	-234.8
C_3H_8O	731	-254.8
C_2H_2	1327.9	228.0
C_3H_4	1186.2	186.6
C_4H_6	1033	162.3
C_2H_4O	821.1	-165.8
C_3H_6O	772.9	-187.4
C_4H_8O	742	-207.5

3. Results and Discussion

A precise treatment for obtaining ion transport parameters of higher accuracy in the E/N function would be to follow the solution of the generalization of the Boltzmann equation [26]. The non-equilibrium regime in discharges can be well represented under a broad range of conditions by using the Boltzmann kinetic equation or by following individual evolutions of all ions with Monte Carlo technique [27,28].

The transport properties of species in gas plasma are of great importance for understanding the nature of molecular and ionic interactions in gas mixtures [29,30]. These properties include mean energy, drift velocity, diffusion coefficients, ionization and chemical reaction coefficients, ion chemical reaction coefficients and rarely excitation coefficients, and are very useful in the chemical industry for the design of many types of transport and process equipment. Swarm parameters, which are functions of the reduced electric field E/N (E-electric field strength, N-gas density) in direct electric fields are usually used for plasma modeling and simulation.

In this work we have used a Monte Carlo code that properly takes into account the thermal collisions [16,19]. The code has passed all the tests and the benchmarks that were covered in our earlier studies [19,31]. Calculations are performed for the gas pressure 1 Torr and gas temperature of 300 K.

In Fig. 2 we show results for mean energy as a function of reduced electric field *E/N*. The mean energy cannot be directly measured in experiments but a map of mean energy versus *E/N* may be used directly to provide the data in fluid models especially when the local field approximation fails. The Monte Carlo code gives good results in which for all n-Butanol gas the mean energy converges to the thermal mean energy 3/2 kT = 0.0388 eV.

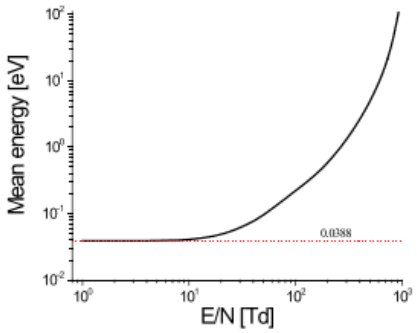

Fig. 2. Mean energy as a function *E/N* for H^+ ions in n-Butanol.

The flux and bulk drift velocities [28] for H^+ in n-Butanol gas as a function of *E/N* are given in Fig. 3. The drift velocities obtained by the Monte Carlo simulation are calculated in real space (bulk) and in velocity space (flux) values which are obtained as $\langle v \rangle$ and $d\langle x \rangle/dt$, respectively. As *E/N* increases, the high-energy ions from the distribution function increasingly have non-conservative collisions in which the H^+ ions disappear, shifting the center of mass of the swarm backward, resulting in a bulk velocity less than the flux.

In Fig. 4 we show the results of Monte Carlo simulation for reduced mobility as a function of *E/N*. The mobility *K* of an ion is a quantity defined as the velocity attained by an ion moving through a gas under the unit electric field strength. One often exploits the reduced or standard mobility defined as:

$$K_0 = \frac{v_d}{N_0 E} N \qquad (2)$$

where v_d is the drift velocity of the ion, N is the gas density at elevated temperature T, N_0= $2.69 \cdot 10^{25}$ m^{-3} and E is the electric field strength. Due to reactive collisions bulk and flux values of reduced mobility are separated.

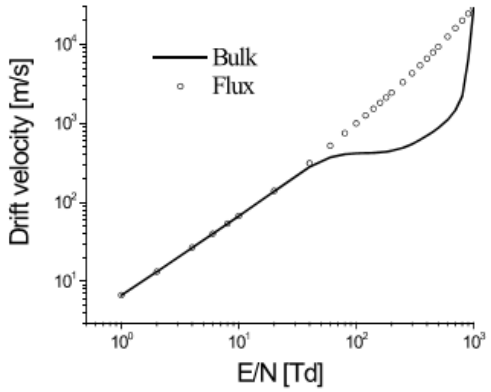

Fig. 3. Bulk and flux velocity as a function *E/N* for H^+ ions in n-Butanol.

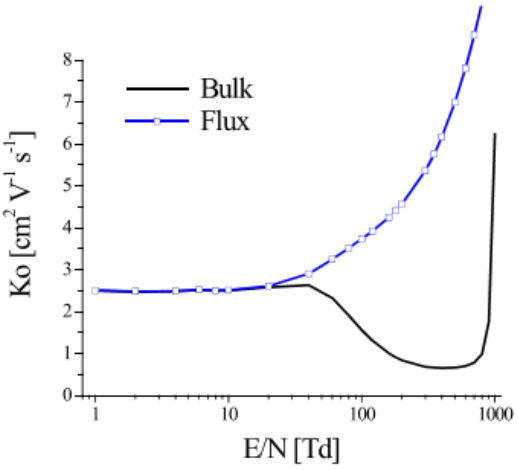

Fig. 4. Reduced mobility as a function *E/N* for H^+ ions in n-Butanol.

In Fig. 5 we show rate coefficients for reactions of H^+ ions with n-Butanol gas at T = 300 K. Rate coefficients are important for applications of the global model to n-Butanol gas. We present formation of H_2^+(8), CO^+(4), H_2O^+(3), CH_4^+(3), CH_2O^+(1), $C_4H_{10}^+$(1), $C_2H_2^+$(3),

$C_3H_4^+(1)$, $C_4H_6^+(1)$, $C_2H_4O^+(1)$, $C_4H_8O^+(1)$. The products of a) light ions, b) medium ions and c) heavy ions are also presented in Fig. 5.

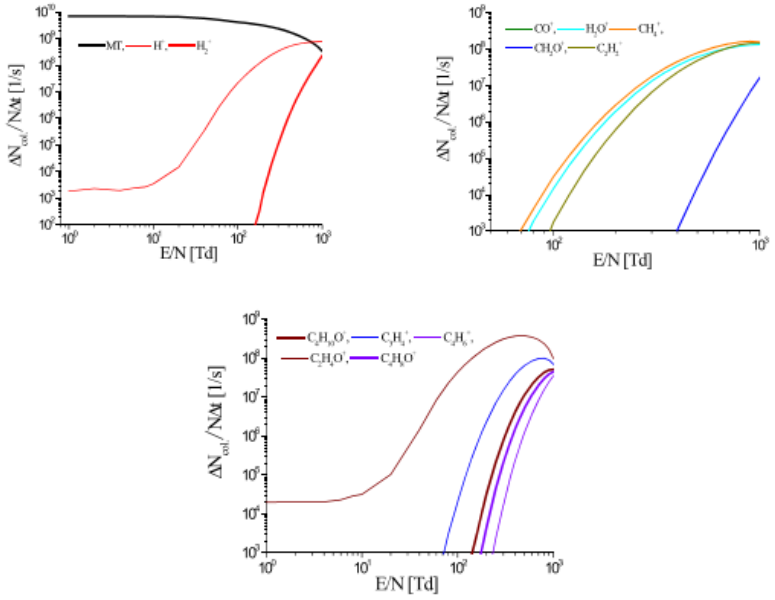

Fig. 5. Rate coefficients of a) light ions, b) medium ions and c) heavy ions as a function *E/N* in n-Butanol.

4. Conclusion

In this paper we show transport properties for the H^+ ions in n-Butanol gas. The cross section set has been determined by extending Denpoh-Nanbu's method.

The Monte Carlo technique was applied to carry out calculations of the mean energy, drift velocity, reduced mobility and specially rate coefficients as a function of reduced DC electric field. The results are believed to be a good base for modeling, which could be further improved when measured values of transport coefficients become available and then we could perform this analysis again.

Acknowledgments

The authors acknowledge funding provided by the Institute of Physics University Belgrade, through the grant by the Ministry of Education, Science and Technological Development of the Republic of Serbia No: 451-03-9/2021-14.
Authors are also grateful to Dr. Martina Gilić.

5. References

1. H. Xu, C. He, Sep. Purif. Technol. 56 (2007) 85-89.
2. M. Johnson, S. Barnes, R. Diasio, Anal. Biochem. 182 (1989) 360-365.
3. H. Jiang, S. Lu, X. Zhang, H. Peng, W. Dai, J. Qiao, Catal. Sci. Technol. 4 (2014) 2499-2503.
4. Z. Sahin, O. Aksu, Renew. Energy 77 (2015) 279-290.
5. N. Yilmaz, F. Vigil, K. Benali, S. Davis, A. Calva, Fuel 135 (2014) 46-50.
6. H. Liu, S. Li, Z. Zheng, J. Xu, M. Yao, Applied Energy 112 (2013) 246-256.
7. D. Rakopoulos, Fuel 105 (2013) 603-613.
8. A. Demirbas, Prog. Energy Combust. Sci. 33 (2007) 1-18.
9. A. C. Hansen, D. C. Kyritsis, C. F. Lee, Characteristics of biofuels and renewable fuel standards, Biomass to biofuels – strategies for global industries, John Wiley, New York (2009).
10. C. Togbe, G. Dayma, A. Mze-Ahmed, P. Dagaut, Energy Fuel 24 (2010) 3906-3916.
11. J. L. Fortman, S. Chhabra, A. Mukhopadhyay, H. Chou, T.S. Lee, E. Steen, J. Keasling, Trends Biotechnol. 26 (2008) 375-381.
12. T. C. Ezejia, N. Qureshib, H. P. Blascheka, J. Biotechnol. 115 (2005) 179-187.
13. A. T. Saleem,V. Petrović, A. Grbović, J. Lozanović Šajić, I. Balać, Sci. Sinter., 53 (2021) 127-136.
14. V. Ribić, A.Rečnik, G.Dražić, M. Podlogar, Z. Branković, G. Branković, Sci. Sinter., 53 (2021) 237-252.
15. K. Denpoh and K. Nanbu, J. Vac. Sci. Technol. A 16 (3) (1998) 1201-1207.
16. Z. Ristivojević and Z. Lj. Petrović, Plasma Sources Sci. Technol. 21 (2012) 035001.
17. E. W. McDaniel,V. Čermak., A. Dalgarno, E. E . Ferguson and L. Friedman, Ion-Molecule Reactions (Willey-Interscience) 1970.
18. P. B. Armentrout, K. M. Ervin and M. T. Rodgers, J. Phys. Chem. A 112, No. 41 (2008) 10071.
19. Z. Lj. Petrović, Z. M. Raspopović, V. D. Stojanović, J. V. Jovanović, G. Malović, T. Makabe and J. de Urquijo, J. Appl. Surf. Sci. 253 (2007) 6619-6640.
20. A. M. Ababneh, C. C. Large and S. Georghiou, Biophysical Journal, 85 (2003) 1111-1127.
21. V. Stojanović, Z. Raspopović, J. Jovanović, Ž. Nikitović and Z. Lj. Petrović, EPL, 101 (2013) 45003.
22. O. K. Rice, H. C. Ramsperger, J. Am. Chem. Soc. 50 (3) (1928) 617-620;L. S. Kassel, J. Phys. Chem. 32(2) (1928) 225-242.
23. S. Lias, J. Bartmess, J. Liebman, J. Holmes, R. Levin, W. Mallard, J Phys Chem Ref Data, 17 (1988) 1-861.
24. Ž. Nikitović, V. Stojanović, Z. Raspopović and J. Jovanović, Acta Physica Polonica A, 126 (2014) 724-726.
25. Ž. Nikitović, Z. Raspopović, V. Stojanović and J. Jovanović, EPL ,108 (2014) 35004.
26. K. Kumar, Aust. J. Phys. 33 (1980) 449-468; L. A. Viehland, S. L. Lin -and E. A. Mason., Chem. Phys. 54 (1981) 341-364; K. F. Ness and L. A Viehland, Chem. Phys. 148 (1990) 255-275; L. A. Viehland and Y. Chang Mol. Phys., 110 (2012) 259-266.
27. K. Kumar, H. R. Skullerud and R. E. Robson, Aust. J. Phys., 33 (1980) 343-448.

28. R. E. Robson, R. D. White, Z. Lj. Petrovic, Rev. Mod. Phys. 77 (2005) 1303-20; A. M. Nolan, M. J. Brennan, K. F. Ness and A. B. Wedding, J. Phys. D: Appl. Phys., 30 (1997) 2865-71; K. F. Ness and R. E. Robson., Phys. Rev. A 34 (1986) 2185-209.
29. B. Todd, J. B. Young J. Power Sources 110 (2002) 186-200.
30. E. Mason, J. Chem. Phys. 27 (1957) 782.
31. J. de Urquijo, J. V. Jovanović, A. Bekstein, V. Stojanović and Z. Lj. Petrović, Plasma Sources Sci. Technol. 22 (2013) 025004.

Сажетак: *У овом раду предлажемо сет пресека за јоне H^+ у гасу n-Бутанол на ниским енергијама и њима придружене транспортне параметре. Ови подаци су потребни за моделовање у бројним технолошки важним применама. За израчунавање пресека за судare у функцији кинетичке енергије коришћене су одговарајуће енталпије формирања гасне фазе за производе реакција. Израчунати попречни пресеци су коришћени за добијање коефицијената брзине у функцији E/N (E – јачина електричног поља; N– густина гаса) за јоне H^+ у гасу n-Бутанол.*
Кључне речи*: Монте Карло Симулације, позитивни јони, n-Бутанол гас.*

5. Рад М23

Eur. Phys. J. D (2018) 72: 168
https://doi.org/10.1140/epjd/e2018-90059-1

THE EUROPEAN PHYSICAL JOURNAL D

Regular Article

Cross sections set and transport coefficients for Ar^+ in Ar/CF_4 mixtures

Željka D. Nikitović[a], Zoran M. Raspopović, and Vladimir D. Stojanović

Institute of Physics, University of Belgrade, POB 68, 11080 Belgrade, Serbia

Received 9 February 2018 / Received in final form 30 April 2018
Published online 2 october 2018

Abstract. In this letter, we present a cross section set for Ar^+ in Ar/CF_4 mixtures where existing experimentally obtained data are selected and extrapolated. A Monte Carlo simulation method is applied to accurately calculate transport parameters in hydrodynamic regime. We discuss new data for Ar^+ ions in Ar/CF_4 mixtures where mean energy, flux and bulk values of reduced mobility and other transport coefficients are given as a function of low and moderate reduced electric fields E/N (E-electric field, N-gas density).

1 Introduction

Cold plasmas are frequently used in new technologies where they open up possibilities of non-intrusive production or modification of various substances [1,2]. These plasmas have high electron temperature and low gas temperature so non-equilibrium behavior of a large number of species becomes important [3]. Current computer resources allow studies of complex global models [4–6] which describe the behavior of such plasmas by taking into account a very large number of particles. The knowledge of ion-neutral reactions is generally accessible [7] although effects of reactions on transport parameters of particular ions is much less studied due to inability of instrumentation to detect rapidly vanishing ionic fluxes. This especially holds for ions whose transport is affected by fast reactions [8,9].

Transport of Ar^+ plays significant role in various etching and deposition processes [10], in dark matter detection [11] and many more applications. It is known that transport parameters of Ar^+ in Ar are affected by resonant charge transfer reactions [12] leaving slow ions as a result. Charge transfer reactions are also a main collisional events in CF_4 gas where they introduce neutralization of Ar^+ ions [13]. If they are exothermic (recombination energy of the ion is higher than the ionization potential of the gas particles, see Tab. 1), with large rate coefficient, they may limit number of Ar^+ ions necessary to determine ion mobility.

If one focuses on Ar^+ scattering on CF_4, the only exothermic charge transfer reaction is the one producing $CF_3{}^+$:

$$Ar^+ + CF_4 \rightarrow CF_3{}^+ + F + Ar. \quad (1)$$

By using technique of Monte Carlo simulations one may calculate transport parameters for the cases that are out of the reach of experimental efforts provided complete cross section set is known. Transport parameters of Ar^+ in CF_4 are shown [14] to be significantly affected by exothermic collisions. Thus, one may expect that in Ar/CF_4 the gas mixtures kinetics of Ar^+ ions significantly vary. Reduced mobility data of both flux and bulk values as a function of E/N, are expected to be significantly affected by the presence of exothermic reactions in the case of Ar^+ transport in the Ar/CF_4 mixtures.

2 Calculation of the cross-section set

A Complete cross section sets for ion transport are scarce in spite of a broad range of specific methods relevant for quantification of particular cross sections. The main problem in heavy particle scattering, is easily and precisely selecting the state of the projectile and target before the collision, and this remains very complicated for range of conditions, so databases for ion scattering [15,16] are devoid of such data. Phelps established the first worldwide accessible database with cross section sets [17] tested for each particular case either for swarm conditions of spatially resolved measurements of emission or ion mobility values. Another range of cross section sets was established by measurements of ionic transport coefficients [16]

[a] e-mail: zeljka@ipb.ac.rs

Table 1. Recombination/ionization energies [eV] based on data in reference [18].

Ar^+	CF_4	CF_3	CF_2	CF	C	F
15.824	15.755*	9.134	11.4	9.12	11.326	17.488

* Value represents the mean of the adiabatic and vertical values for X^2T_1 state of CF_4^+.

and this work is ongoing. In all cases the most important cross sections may be established from the transport data. In the following section, we will establish a complete cross section set for Ar^+ scattering on Ar and CF_4 from 0.1 meV to 1000 eV which will be used to calculate transport properties. Generally one may distinguish three characteristic energy ranges: the low energy regime where polarization scattering is dominant, the medium energy regime where polarization scattering is gradually replaced by hard sphere repulsion, and the high energy approximation regime.

At the lowest presented energies polarization scattering is dominant as also observed in guided beam experiments [18]. Thus one may use simple scattering models [10,19] if a reliable value of the average polarizability of CF_4 is provided [20,21]. Stojanović et al. [20] found excellent agreement for mobility of CF_3^+ ions in CF_4 by using value of 3.86 A [21] as an acceptable value for average polarizability of CF_4. A similar value was previously found appropriate by Jarvis et al. [22]. It is also generally accepted that dipole and quadruple moments are negligible (see for example [18]) in the analyses with CF_4. Fisher et al. [18] fast charge transfer reaction for CF_3^+ by measuring production proved that internal states of the target which are populated, are those closest to the recombination energy of the projectile [12,22]. Accounting for all details of Ar^+ scattering on CF_4 in reference [14] a complete cross section set is presented that is also used in this work.

Extensive discussion about transport properties of Ar^+ ions scattering in Ar gas applied to plasma physics problems was presented by Phelps [13] and Petrović and Stojanović [23]. Analytical expressions were offered in [13] to express apparently isotropic and anisotropic components of the cross section set (see Fig. 1). In order to focus on effects of reactive processes introduced by CF_4, we neglected all but these two components of the $Ar^+ + Ar$ cross section set. Complete cross section sets used in this work are shown in Figure 1.

3 Discussion and results

A Monte Carlo simulation code appropriate to calculate transport parameters [24,25] of Ar^+ ions in Ar/CF_4 mixtures at non-zero temperature [26] has been used. In Monte Carlo simulations exothermic reactive collisions are followed in a similar way as all non-conservative collisions i.e. the swarm particle disappears from the ensemble after exothermic collisions. This results in changes of the swarm particle number in the entire energy range introducing

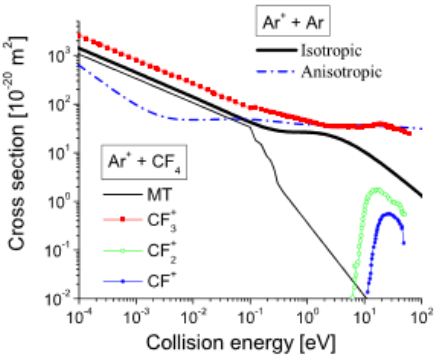

Fig. 1. Cross section sets for $Ar^+ + Ar$ [13] and $Ar^+ + CF_4$ [14,18] as a function of collision energy.

nonconserve effects in kinetic equations and thus division of transport parameters to flux and bulk ones [24].

In Figure 2, we show results for mean energy as a function of E/N (E-electric field and N-gas density). Significant reduction and uniform control of mean energy of Ar^+ is obtained for argon content below 90%. For Ar content below 10% largest variations of mean energy are obtained for $E/N > 100$ Td (1Td = 10^{-21} Vm^2). These variations are the consequence of a reduced momentum transfer cross section for Ar^+ scattering with CF_4 (see Fig. 1) as compared to the scattering with Ar. At a high content of Ar charge transfer collisions dominate and make variation of mean energy with Ar content more uniform. Note, that for transport coefficients of Ar^+ in pure Ar one may find benchmark data presented in tabular form by Ristivojević and Petrović [26].

The flux and bulk drift velocities [25,27] for Ar^+ in Ar/CF_4 as a function of E/N are given in Figure 3. The drift velocities obtained by the Monte Carlo simulation are calculated in real space (bulk) and in velocity space (flux) values which are obtained as $<v>$ and $d<x>/dt$, respectively. Up to 40% CF_4 has no difference between bulk and to flux values. Since the growth of the collision frequency with the energy of the reactive processes decreases the bulk drift velocity increases.

In Figure 4 variations of reduced mobility as a function of E/N are shown. Behaviour of reduced mobility significantly changed with E/N with small additions of Ar, up to about 10%. Especially intriguing are variations of flux reduced mobility which points to particle flux variations of Ar^+ ions as a function of their mean energy. On one side, small additions of Ar cause significant variations of particle flux at E/N close to 200 Td and on the other in that region we obtain significant difference of the flux and bulk drift velocities due to the CF_4 reactive processes (see also [12]) which also significantly reduce Ar^+ density in favour of fast Ar [13]. Control of fast Ar flux at the surface thus can be easily achieved by small variations of Ar contents in Ar/CF_4 mixture.

Longitudinal diffusion coefficients for Ar^+ ions in Ar/CF_4 as a function of E/N are shown in Figure 5.

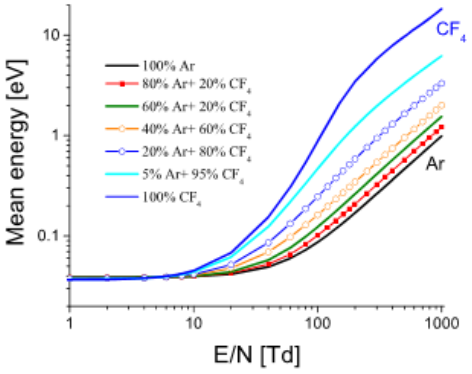

Fig. 2. Mean energy as a function of E/N for Ar^+ in Ar/CF_4 mixtures at 300 K.

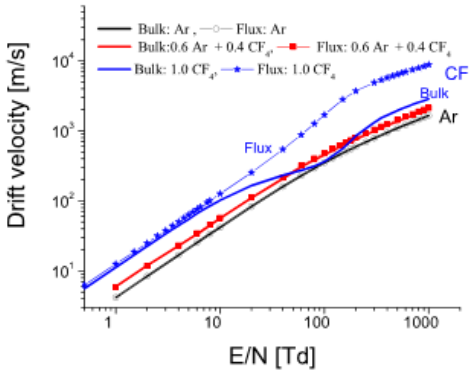

Fig. 3. Drift velocity as a function of E/N for Ar^+ in Ar/CF_4 mixtures at 300 K.

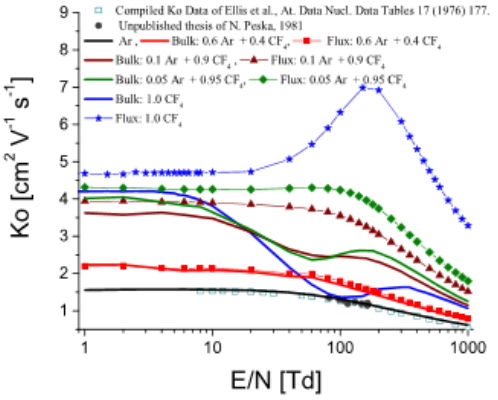

Fig. 4. Reduced mobility for Ar^+ in Ar/CF_4 at 300 K.

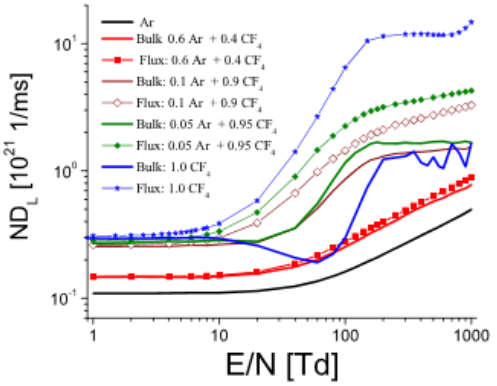

Fig. 5. Longitudinal diffusion coefficients for Ar^+ in Ar/CF_4 at 300 K.

Note that the differences between the flux and bulk values of diffusion coefficients have the same initial value as drift velocities. Due to the large resonant charge transfer for $Ar^+ + Ar$ ND_L is small and is slowly changing with increase of electric field. Since there are no reactions in which Ar^+ ions disappear, flux and bulk values are equal for all transport parameters.

From the other side, for scattering Ar^+ on CF_4 due to increase of collision frequency for reactions (loss of the ions) with energy, ions of large energy disappear mostly that are most abundant at swarm front, decelerating spread of swarm in the field direction, and so bulk values of NDL became smaller than flux values. Another point is that the decrease of elastic momentum transfer cross section with energy causes increase of flux values of drift velocity $V_F = < v >$ as well as $D_L(F) = <xVx> - <x><Vx>$. At energies over 5 eV ($E/N > 300$ Td) in case 100% CF_4 elastic cross sections became very small while reactions become noticeable, and ion swarm converts to ion beam that is accelerating in electric field and slowly disappearing, if there is no recovery in other reactions.

Consequence of that is if, we have fast ions in the field direction, that favors its spread in that direction, swarm is not spreading because fastest and furthers ions disappear. To this loss of fast ions that are at the swarm/beam front most sensitive transport coefficients are NDL bulk values which measures velocity <x2>-<x>2 so results for bulk NDL become non-stable.

There are no published experimental data for the longitudinal and transverse diffusion coefficients of Ar^+ in Ar/CF_4.

In Figure 6, we show rate coefficients for reactions of Ar^+ ions with Ar/CF_4 mixtures at $T = 300$ K. Rate coefficients are important for applications of the global model to Ar/CF_4 mixtures. We present formation of a) CF_3^+ ions and b) CF_2^+ ions resulting from collisions of Ar^+ with mixtures of Ar/CF_4 for different percentages of Ar and CF_4.

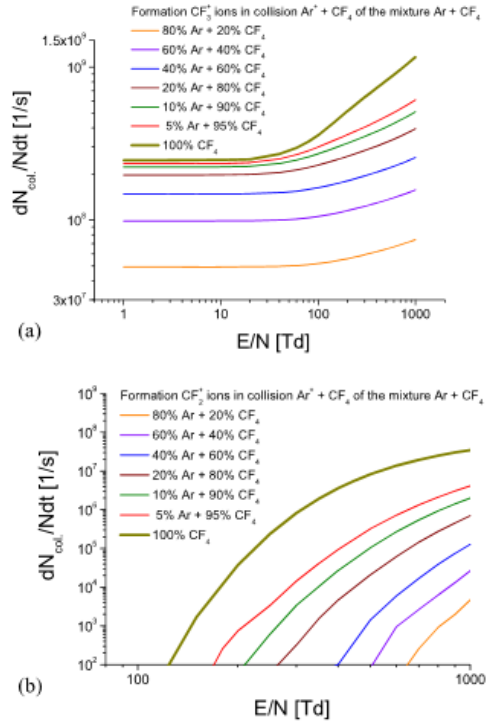

Fig. 6. Rate coefficients for reactions of Ar^+ ions with Ar/CF_4 mixtures.

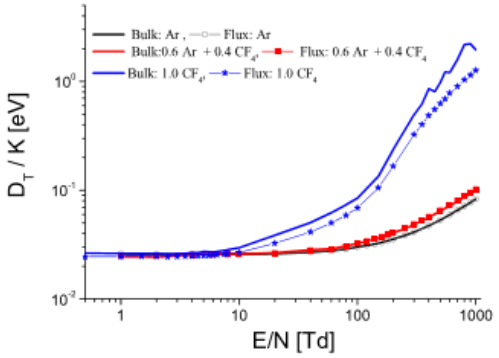

Fig. 7. Characteristic energy (eDT/K) for Ar^+ in Ar/CF_4 mixtures at 300 K.

At low E/N's (<10 Td), swarm mean energy is close to thermal, and so the energy distribution functions are similar. That also implies that collision frequency is almost constant, at these thermal energies, as well as its appropriate measurement – rate. In Figure 7, we show the characteristic energies (diffusion coefficient normalized to mobility eD/K in units of eV) based on transverse (D_T) diffusion coefficients. The difference between bulk and flux values is smaller.

4 Conclusion

Data for swarm parameters for ions are needed for hybrid and fluid codes and the current focus on liquids or liquids in the mixtures with rare gases dictates the need to produce data compatible with those models.

In addition, presented data clearly show the effects of non-conservative collisions on ion transport. Due to exothermic cross sections that are dominant at low energies, for small abundances of Ar (<10%) exothermic process may be larger than the elastic scattering cross section. Thus differences between flux and bulk transport coefficients are quite large as compared to the strongest cases of non-conservative transport observed for electrons [28] and even positrons [29].

Results obtained in the Institute of Physics, University of Belgrade, under the auspices of the Ministry of Education, Science and Technology, Projects Nos. 171037 and 410011.

Author contribution statement

Željka Nikitović – Thematic direction of research and work coordination. Organization and writing of the paper. Zoran Raspopović – Monte Carlo simulations for cases where endothermic and exothermic collisions are included. Vladimir Stojanović – Calculation of endothermic and exothermic cross sections, cross section set assesment, organization of input data and graphical presentation.

References

1. T. Makabe, Z. Petrović , *Plasma Electronics: Applications in Microelectronic Device Fabrication* (Taylor and Francis, CRC Press, New York, 2006)
2. Z.Lj. Petrović, P. Maguire, M. Radmilović-Radenović, M. Radetić, N. Puaé, D. Marić, C. Mahony, G. Malović, in *Nanotechnology for Electronics, Photonics and Renewable Energy* (2010), p. 85
3. R.E. Robson, R.D. White, Z.Lj. Petrović, Rev. Mod. Phys. **77**, 1303 (2005)
4. T. Murakami, K. Niemi, T. Gans, D. O'Connell, W.G. Graham, Plasma Sources Sci. Technol. **22**, 015003 (2013)
5. W. Van Gaens, A. Bogaerts, J. Phys. D: Appl. Phys. **46**, 275201 (2013)
6. S. Samukawa, M. Hori, S. Rauf, K. Tachibana, P. Bruggeman, G. Kroesen, J.C. Whitehead, A.B. Murphy, A.F. Gutsol, S. Starikovskaia, U. Kortshagen, J.-P. Boeuf, T. J. Sommerer, M.J. Kushner, U. Czarnetzki, N. Mason, J. Phys. D: Appl. Phys. **45**, 253001 (2012)
7. https://nl.lxcat.net/data/set_type.php
8. Ž. Nikitović, Z. Raspopović, V. Stojanović, J. Jovanović, EPL **108**, 35004 (2014)
9. Ž. Nikitović, M. Gilić, Z. Raspopović, V. Stojanović, EPL **116**, 15002 (2016)

10. M.A. Lieberman, A.J. Lichtenberg, *Principles of Plasma Discharges and Materials Processing* (Wiley, New York, 1994)
11. A. Kaboth, J. Monroe, S. Ahlen, D. Dujmic, S. Henderson, G. Kohse, R. Lanza, M. Lewandowska, A. Roccaro, G. Sciolla, N. Skvorodnev, H. Tomita, R. Vanderspek, H. Wellenstein, R. Yamamoto, P. Fisher, Nucl. Instrum. Meth. Phys. Res. A **592**, 63 (2008)
12. E. Parkerand, F.S.M. El-Ashhab, Int. J. Mass Spectrom. Ion. Phys. **47**, 159 (1983)
13. A.V. Phelps, J. Appl. Phys. **76**, 747 (1994)
14. Z. Raspopović, V. Stojanović, Ž. Nikitović, EPL **111**, 45001 (2015)
15. http://nl.lxcat.net/data/set_type.php
16. www.ruf.rice.edu/~atmol
17. https://nl.lxcat.net/cache/5b33772b61cf9/
18. E.R. Fisher, M.E. Weber, P.B. Armentrout, J. Chem. Phys. **92**, 2296 (1990)
19. G. Gioumousis, D.P. Stevenson, J. Chem. Phys. **29**, 294 (1958)
20. V. Stojanović, Z. Raspopović, J.V. Jovanović, J. de Urquijo, Z. Lj. Petrović, J. Phys.: Conf. Ser. **514**, 012059 (2014)
21. H. Martínez, F.B. Yousif, Phys. Rev. A **69**, 062701 (2004)
22. G.K. Jarvis, R.A. Kennedy, C.A. Mayhew, R.P. Tuckett, Int. J. Mass Spectrom. **202**, 323 (2000)
23. Z.Lj. Petrović, V.D. Stojanović, J. Vac. Sci. Technol. **16**, 329 (1998)
24. R.E. Robson, Aust. J. Phys. **44**, 685 (1991)
25. R.E. Robson, R.D. White, Z.Lj. Petrović, Rev. Mod. Phys. **77**, 1303 (2005)
26. Z. Ristivojević, Z.Lj. Petrović, Plasma Sources Sci. Technol. **21**, 035001 (2012)
27. Z. Raspopović, S. Sakadžić, Z.Lj. Petrović, T. Makabe, J. Phys. D **33**, 1298 (2000)
28. J. Mirić, D. Bošnjaković, I. Simonović, Z.Lj. Petrović, S. Dujko, Plasma Sources Sci. Technol. **25**, 065010 (2016)
29. A. Banković, S. Dujko, S. Marjanović, R.D. White, Z.Lj. Petrović, Eur. Phys. J. D **68**, 127 (2014)

6. Рад М23

Rate Coefficients of Ar^+ Ions in Ar/CF_4 Mixtures

Ž. Nikitović*, V. Stojanović and Z. Raspopović
Institute of Physics, University of Belgrade, POB 68, 11080 Belgrade, Serbia

(Received January 22, 2018; in final form October 5, 2018)

In this paper we present a cross-section set for Ar^+ in Ar/ CF_4 mixtures where existing experimentally obtained data are selected and extrapolated. The Monte Carlo simulation method is applied to accurately calculate transport coefficients in hydrodynamic regime. We discuss new data for Ar^+ ions in Ar/CF_4 mixtures where mean energy, flux and bulk velocity and rate coefficients are given as a function of E/N (E — electric field, N — gas density).

DOI: 10.12693/APhysPolA.134.1134
PACS/topics: 51.10.+y, 52.20.Hv, 52.65.Pp

1. Introduction

Transport of Ar^+ plays significant role in various etching and deposition processes [1], in dark matter detection [2] and many more applications. Transport parameters in the presence of exothermic reactions (recombination energy of the ion is higher than the ionization potential of the gas particles) are generally less studied than the other. In our selected case reason is a large rate coefficient for exothermic reactions (resonant [3]) that limits number of ions necessary for determination of mobility. By using Monte Carlo simulations one may calculate transport parameters for the cases that are out of the reach of experimental efforts provided complete cross-section set is known. Transport parameters of Ar^+ in Ar/CF_4 are shown [4] to be significantly affected by exothermic collisions. Mean energy as a function of E/N, both flux and bulk velocity are expected to be significantly affected by the presence of exothermic reactions in the case of Ar^+ transport in the Ar/CF_4 mixtures. These processes in the study of ion molecule reactions are of fundamental interest [5].

2. Monte Carlo simulation

Cross-section sets for ion transport are scarce in spite of a broad range of specific methods relevant for quantification of particular cross-sections. The main problem in heavy particle scattering, precisely selecting the state of the projectile and target before the collision, is still very complicated so databases for ion scattering [6, 7] are still devoid of such data. Phelps established the first worldwide accessible database with cross-section sets [6] tested for each particular case either for swarm conditions of spatially resolved measurements of emission or ion mobility values. Another range of cross-section sets was established by measurements of ionic transport coefficients [7] and this work is ongoing. In all cases only the most important cross-sections may be established from the transport data. In the following section we will establish a complete cross-section set for Ar^+ scattering on Ar and CF_4 from 0.1 meV to 1000 eV [8] which will be used to calculate transport properties. Generally one may distinguish three characteristic energy ranges: low energy regime where polarization scattering is dominant, medium energy regime where polarization scattering is gradually replaced by hard sphere repulsion, and high energy approximation regime.

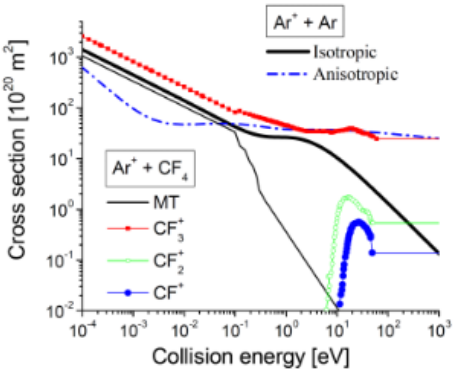

Fig. 1. Cross-section sets for Ar^++ Ar [14] and Ar^++ CF_4 [4, 9] as a function of collision energy.

At the lowest presented energies polarization scattering is dominant as also observed in guided beam experiment [9]. Thus one may use simple scattering models [1, 10] if a reliable value of the average polarizability of CF_4 is provided [11, 12]. Stojanović et al. [11] found excellent agreement for mobility of CF_3^+ ions in CF_4 by using value of 3.86 Å^3 [12] as an acceptable value for average polarizability of CF_4. A similar value was previously found appropriate by Jarvis et al. [13]. It is also generally accepted that dipole and quadruple moments are negligible (see for example [9]) in the analyses with CF_4. Fisher et al. [9] by measuring fast charge transfer reaction for CF_3^+ production proved that internal states of the target which are populated, are those closest to the recombina-

*corresponding author; e-mail: zeljka@ipb.ac.rs

tion energy of the projectile [3, 13]. Accounting for all details of Ar^+ scattering on CF_4 in Ref. [4] a complete cross-section set is presented that is also used in this work. Extensive discussion about transport properties of Ar^+ ions scattering in Ar gas applied to plasma physics problems was presented by Phelps [14] and Petrović and Stojanović [15]. Analytical expressions were offered in [14] to express apparently isotropic and anisotropic components of the cross-section set (see Fig. 1). In order to focus on effects of reactive processes introduced by CF_4 we neglected all but these two components of the Ar^++ Ar cross-section set. Complete cross-section sets used in this work are shown in Fig. 1.

3. Transport coefficients

The Monte Carlo simulations (MCS) have many applications for analysis of the transport of charged particles in plasmas. MCS provide swarm data with the only the uncertainty due to statistical fluctuations and uncertainties in the cross-sections. In addition, MCS is the basis of hybrid models of plasmas allowing easy and accurate representation of the end effects and of the non-local high energy groups of particles which are essential in production of plasmas and treatment of surfaces. The MC code used in our analysis is based on the null collisions method.

Monte Carlo simulation code appropriate to calculate transport parameters [16, 17] of Ar^+ ions in Ar/CF_4 mixtures at non-zero temperature [18] has been used. In the Monte Carlo simulations exothermic reactive collisions are followed in a similar way as all non-conservative collisions i.e. the swarm particle dissappears from the ensemble after exothermic collisions. This results in changes of the swarm particle number in the entire energy range introducing nonconserving effects in kinetic equations and thus division of transport parameters to flux and bulk ones [16].

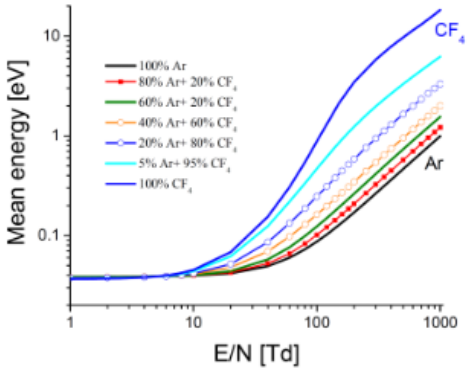

Fig. 2. Mean and characteristic energies of Ar^+ ions in Ar/CF_4 mixtures as a function of E/N.

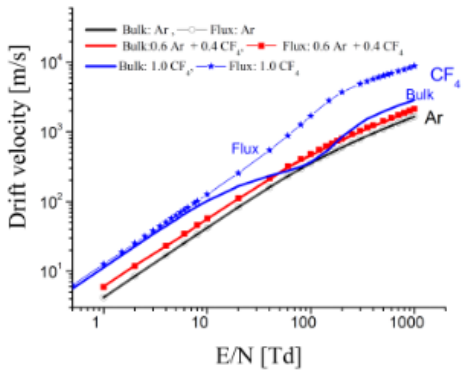

Fig. 3. Drift velocity as a function of E/N for Ar^+ in Ar/CF_4 mixtures at 300 K.

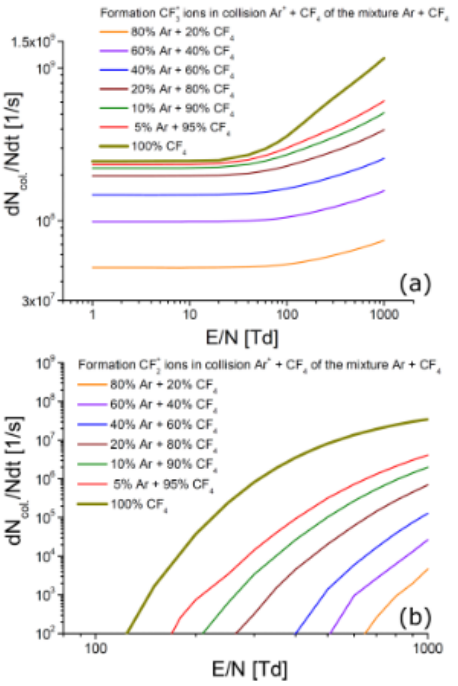

Fig. 4. Rate coefficients of Ar^+ in Ar/CF_4 mixtures.

In Fig. 2 we show results for mean energy as a function of E/N (E — electric field and N — gas density). Significant reduction and uniform control of mean energy of Ar^+ is obtained for argon content below 90%. For Ar content below 10% largest variations of mean energy are obtained for $E/N > 100$ Td (1 Td= 10^{-21} V m^2).

These variations are the consequence of a reduced momentum transfer cross-section for Ar^+ scattering with CF_4 (see Fig. 1) as compared to the scattering with Ar. At a high content of Ar charge transfer collisions dominate and make variation of mean energy with Ar content more uniform. Note that for transport coefficients of Ar^+ in pure Ar one may find benchmark data presented in tabular form by Ristivojević and Petrović [18].

The flux and bulk drift velocities [19] for Ar^+ in Ar/CF_4 as a function of E/N are given in Fig. 3. The drift velocities obtained by the Monte Carlo simulation are calculated in real space (bulk) and in velocity space (flux) values which are obtained as $\langle v \rangle$ and $\mathrm{d}\langle x \rangle/\mathrm{d}t$, respectively. Up to 40% CF_4 has no difference between bulk and flux values. Since the growth of the collision frequency with the energy of the reactive processes decreases the bulk drift velocity.

In Fig. 4 we show rate coefficients for reactions of Ar^+ ions with Ar/CF_4 mixtures at $T = 300$ K, calculated by the Monte Carlo simulations. Rate coefficients are important for applications of the global model to Ar/CF_4 mixtures. We are presenting formation (a) CF_3^+ ions in collision Ar^+ of the mixtures Ar/CF_4 and (b) CF_2^+ ions in collision Ar^+ of the mixtures Ar/CF_4 for different percent Ar and CF_4.

4. Conclusion

In this paper we show transport parameters for the Ar^+ in Ar/CF_4 mixtures which do not exist in the literature. In addition to presenting the data we show here the effects of non-conservative collisions to ion transport. Due to exothermic cross-sections that are dominant at low energies, for small abundances of Ar ($< 10\%$) exothermic process may be larger than the elastic scattering cross-section.

The Monte Carlo technique was applied to carry out calculations of the mean energy, drift velocity, and rate coefficients as a function of reduced DC electric field. Data for swarm parameters for ions are needed for hybrid and fluid codes and the current focus on liquids or liquids in the mixtures with rare gases dictates the need to produce data compatible with those models.

Acknowledgments

Results obtained in the Institute of Physics, University of Belgrade, under the auspices of the Ministry of Education, Science and Technology, Projects No. 171037, 41011 and 45016.

References

[1] M.A. Lieberman, A.J. Lichtenberg, *Principles of. Plasma Discharges and Materials Processing*, Wiley, New York 1994.

[2] A. Kaboth, J. Monroe, S. Ahlen, D. Dujmic, S. Henderson, G. Kohse, R. Lanza, M. Lewandowska, A. Roccaro, G. Sciolla, N. Skvorodnev, H. Tomita, R. Vanderspek, H. Wellenstein, R. Yamamoto, P. Fisher, *Nucl. Instrum. Methods Phys. Res. A* **592**, 63 (2008).

[3] E. Parker, F.S.M. El-Ashhab, *Int. J. Mass Spectrom. Ion. Phys.* **47**, 159 (1983).

[4] Z. Raspopović, V. Stojanović, Ž. Nikitović, *EPL* **111**, 45001 (2015).

[5] K. Bederski, *Acta Phys. Pol. A* **123**, 896 (2013).

[6] Plasma Data Exchange Project.

[7] Atomic and Molecular Collisions Group.

[8] Plasma Data Exchange Project, Cross section Phelps database Ar+ / Ar.

[9] E.R. Fisher, M.E. Weber, P.B. Armentrout, *J. Chem. Phys.* **92**, 2296 (1990).

[10] G. Gioumousis, D.P. Stevenson, *J. Chem. Phys.* **29**, 294 (1958).

[11] V. Stojanović, Z. Raspopović, J.V. Jovanović, J. de Urquijo, Z.Lj. Petrović, *J. Phys. Conf. Series* **514**, 012059 (2014).

[12] H. Martınez, F.B. Yousif, *Phys. Rev. A* **69**, 062701 (2004).

[13] G.K. Jarvis, R.A. Kennedy, C.A. Mayhew, R.P. Tuckett, *Int. J. Mass Spectrom.* **202**, 323 (2000).

[14] A.V. Phelps, *J. Appl. Phys.* **76**, 747 (1994).

[15] Z.Lj. Petrović, V.D. Stojanović, *J. Vac. Sci. Technol.* **16**, 329 (1998).

[16] R.E. Robson, *Aust. J. Phys.* **44**, 685 (1991).

[17] R.E. Robson, R.D. White, Z.Lj. Petrović, *Rev. Mod. Phys.* **77**, 1303 (2005).

[18] Z. Ristivojević, Z.Lj. Petrović, *Plasma Sources Sci. Technol.* **21**, 035001 (2012).

[19] V. Stojanović, Ž. Nikitović, Z. Raspopović, J. Jovanović, *Acta Phys. Pol. A* **125**, 46 (2014).

7. Рад М23

Eur. Phys. J. D (2021) 75:118
https://doi.org/10.1140/epjd/s10053-021-00061-3

THE EUROPEAN PHYSICAL JOURNAL D

Regular Article - Plasma Physics

Rate coefficients for Ar^+ in Ar/BF_3 mixtures

Ž. D. Nikitović[a] and Z. M. Raspopović

Institute of Physics, University of Belgrade, POB 68, 11080 Belgrade, Serbia

Received 13 October 2020 / Accepted 7 December 2020 / Published online 6 April 2021

Abstract. In this paper, we present most probable reactions of Ar^+ ion with Ar/BF_3 mixtures. Appropriate gas phase enthalpies of formation for the products were used to calculate scattering cross section as a function of kinetic energy. These data are needed for modeling in numerous applications of technologically important BF_3 discharges. Results for transport parameters, specially rate coefficients as a function of E/N (E-electric field; N-gas density) were obtained by using the Monte Carlo technique.

1 Introduction

Cold plasma is widely used in new technologies where they open the possibility of unobtrusive production or modification of various substances [1]. Due to the high temperature of the electrons and the low temperature of the gases, the unbalanced behavior of a large number of species becomes important in these plasmas [2]. Current computational resources allow the study of complex global models [3] that describe the behavior of such plasmas taking into account a very large number of particles. Information on ion neutral reactions is generally available [4], although the effects of reactions on the transport parameters of individual ions have been much less studied due to the detectability of rapidly disappearing ion fluxes. This is especially true for ions whose transport is affected by rapid reactions [5,6]. Ar^+ transport plays a significant role in numerous etching and deposition processes [7,8], dark matter detection [9] and many other applications. It is well-known that the transport parameters Ar^+ in Ar are affected by resonant charge transfer reactions [10], which results in a slow ion. Charging transfer reactions are mainly the most important collisions in BF_3 gas, where they introduce neutralization of Ar^+ ions [11]. The high velocity coefficient for exothermic reactions (ion neutralization energy is greater than the ionization potential of gas particles) limits the number of ions necessary to determine ion mobility. The penetration of boron addition into silicon is technologically achieved by means of a pulsed direct current plasma (PLAD) system, which most often uses BF_3 gas [12,13]. Uniform plasma and implantation with normal ion incidence are the main goals of this technological process. Using Monte Carlo simulations (MCSs), transport parameters can be calculated for cases that are beyond the reach of the experimental effort provided that the complete cross section is known. It is expected that the data on reduced mobility of flux values and volume in the E/N function will be significantly influenced by the presence of endothermic and exothermic reactions in the case of Ar^+ transport in Ar/BF_3 mixtures.

In this work, we select the most probable reactions of Ar^+ with BF_3 gases for thermodynamic threshold energies below about 15 eV.

2 Calculation of the cross-sections set

The cross-sections set for ion transport are rare despite the wide range of specific methods relevant to quantification of particular cross-sections. The main problem in the scattering of heavy particles, easy and precise selection of the state of the projectile and the target before the collision, is still very complex for a number of conditions, so the ion scattering databases [4,13] are still without such data. Phelps established the world's first available database with cross-sectional sets [14] tested on a case-by-case basis for either a swarm of spatially resolved measurements of ion emission values or ion mobility. The measurement of ionic transport coefficients has been determined by another series of cross-section sets [4] and this work is ongoing. In all cases, only the most important sections can be identified from the transport data. In the next section, we will establish a complete set of cross sections for Ar^+ scattering on Ar and BF_3 from 0.1 meV to 1000 eV that will be used to calculate the transport properties. In general, three characteristic energy ranges can be distinguished: a low-energy regime in which polarization scattering is dominant, a medium-energy regime where polarization scattering is gradually replaced by hard sphere rejection, and a high-energy approxima-

[a] e-mail: zeljka@ipb.ac.rs (corresponding author)

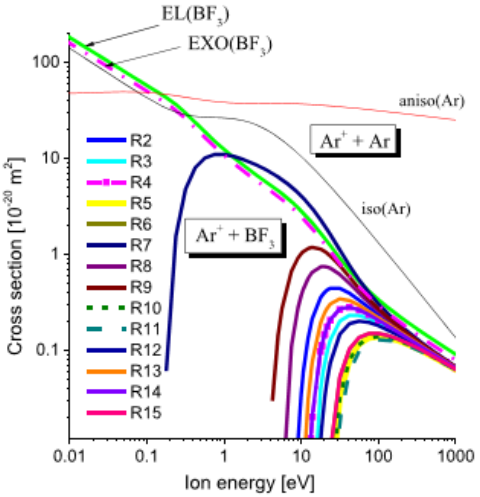

Fig. 1 Cross sections for Ar^+ in BF_3 gas

Table 1 Reaction products and thermodynamic thresholds for $Ar^+ + BF_3$

Reaction	Reaction type	Threshold [eV]
EL	$Ar^+ + BF_3$ (el)	.0000
R2	$Ar^+ + BF_2 + F$	7.4373
R3	$Ar^+ + BF + 2F$	12.2940
R4	$Ar^+ + BF + F2$	10.6461
R5	$Ar^+ + B + 3F$	20.1367
R6	$Ar^+ + B + F + F_2$	18.4889
R7	$BF_2 + +Ar + F$	.1544
R8	$BF^+ + 2F + Ar$	5.0115
R9	$BF^+ + F_2 + Ar$	3.3637
R10	$F^+ + B + F_2 + Ar$	20.1488
R11	$F^+ + B + 2F + Ar$	21.7966
R12	$F^+ + BF + F + Ar$	13.9539
R13	$F^+ + BF_2 + Ar$	9.0972
R14	$F_2^+ + BF + Ar$	10.5846
R15	$F_2^+ + B + F + Ar$	18.4273
EXO	$BF_3^+ + Ar$	−0.2125

tion regime. Phelps [15] and Petrović and Stojanović [16] presented an extensive discussion on the transport properties of Ar^+ ion scattering in BF_3 gas applied to problems in plasma physics. Analytical expressions are given in [11] to express both isotropic and anisotropic components of a set of cross sections (see Fig. 1). To focus on the effects of reactive processes introduced by BF_3, we neglected all but these two components of the set of cross sections Ar^++ Ar. The complete sets of cross sections used in this paper are shown in Fig. 1.

Table 1 presents the reaction products and thermodynamic thresholds for $Ar^+ + BF_3$.

Table 2 Heats of formation $\Delta_f H^0$at 298 K (kJ/mol)

Ion/neutral	ΔH_f(ion) kJ/mol	ΔH_f(neutral) kJ/mol
Ar^+/Ar	1520.57	0
Ar_2^+/Ar_2	1398.1	−1.01
B^+/B	1363.3	562.7
BF^+/BF	957	−115.8
BF_2^+/BF_2	314	−589.9
BF_3^+/BF_3	364.3	−1137.0
F^+/F	1760.2	79.4
F_2^+/F_2	1514.5	0

Therefore, in this paper, we assumed that exothermic processes are not resonant because the fast charge transfer reaction for BF_3^+ production proved that the internal states of the target inhabited are closest to the Ar^+ neutralization energy [10,17].

The cross section sets used in this work are shown in Fig. 1.

Appropriate gas phase enthalpies of formation for the products (Table 2) were used to calculate thermodynamic thresholds.

3 Results and discussion

In addition, MCS is the basis of hybrid models of plasmas allowing easy and accurate representation of the end effects and of the non-local high energy groups of particles which are essential in production of plasmas and treatment of surfaces. The MC code used in our analysis is based on the null collisions method. We assume that our intersections give the transport coefficients at low energies with 30% errors and at high energies they describe well the order of magnitude. Experimentally determined cross sections or transport parameters significantly reduce the errors. Monte Carlo code errors are below 0.1%.

The transport properties of species in gas plasma are of great importance for understanding the nature of molecular and ionic interactions in gas mixtures [18,19]. These properties include mean energy, drift rate, diffusion coefficients, ionization and chemical reaction coefficients, chemical reaction coefficients for ions, and rarely gases. A Monte Carlo simulation code suitable for calculating the transport parameters [16,18] of Ar^+ ions in Ar / BF_3 mixtures at a nonzero temperature was used [20]. In Monte Carlo simulations, exothermic reactive collisions are monitored in a similar way as all non-conservative collisions, i.e., the swarm particle disappears from the whole after exothermic collisions. This results in changes in the number of swarm particles in the entire energy range, introducing non-conserving effects into the kinetic equations, and thus the division of transport parameters into flux and bulk values[18,19].

The flux and bulk drift velocities [20,21] for Ar^+ in Ar/BF_3 as a function of E/N are given in Fig. 2. The

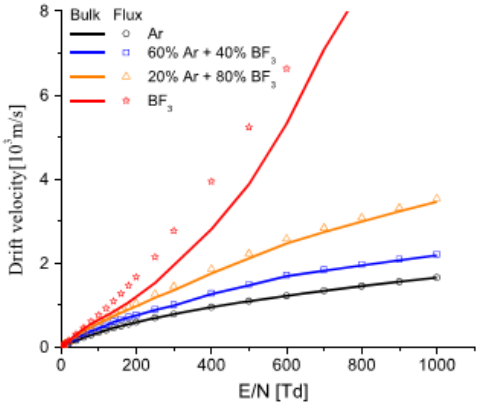

Fig. 2 Drift velocity as a function E/N for Ar^+ in Ar/BF_3 mixtures

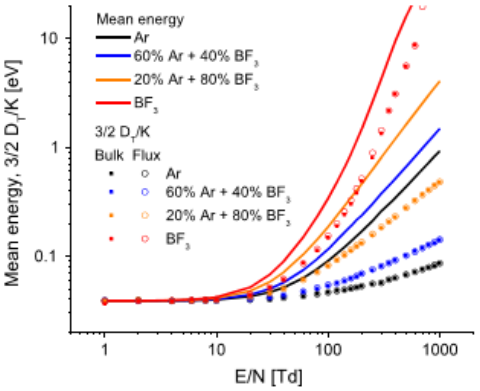

Fig. 3 Mean and characteristic energy as a function E/N for Ar^+ in Ar/BF_3 mixtures

drift velocities obtained by the Monte Carlo simulation are calculated in real space (bulk) and in velocity space (flux) values which are obtained as $< v >$ and $\mathrm{d} < x > /\mathrm{d}t$, respectively. Up to 60%, BF_3 has no difference between bulk and flux values. Bulk drift velocity is reaction corrected flux drift velocity: $\mathrm{W} = \mathrm{w} + \mathrm{S}$, where S is the term representing a measure of the effect of reactions on the drift velocity. Difference between bulk and flux drift velocity a consequence of energy-dependent reactions. Since the growth of the collision frequency with the energy of the reactive processes decreases the bulk drift velocity.

In Fig. 3, we show the characteristic energies (diffusion coefficient normalized to mobility eD/K in units of eV) based on transversal (D_T) diffusion coefficients. The difference between the bulk and flux values is smaller. We also show the mean energy, a parameter

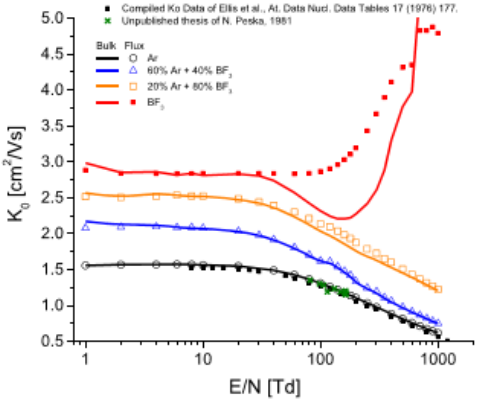

Fig. 4 Reduced mobility as a function E/N for Ar^+ in Ar/BF_3 mixtures

which cannot be directly measured in experiments but a map of mean energy versus E/N may be used directly to provide the data in fluid models especially when the local field approximation fails. At a high content of Ar, charge transfer collisions dominate and make variation of mean energy with Ar content more uniform. Note that for transport coefficients of Ar^+ in pure Ar, one may find benchmark data presented in tabular form by Ristivojević and Petrović [22].

Figure 4 shows the variations of reduced mobility in the E/N function. K ion mobility is a quantity defined as the speed achieved by an ion moving through a gas under a single electric field. Reduced or standard mobility is often used, defined as:

$$K_0 = \frac{v_d}{N_0 E} N, \tag{1}$$

where v_d is the drift velocity of the ion, N is the gas density at elevated temperature T, $N_0 = 2.69 \cdot 10^{25}\ \mathrm{m}^{-3}$ and E is the electric field. Behavior of reduced mobility significantly changed with E/N with small additions of Ar, up to about 10%. On one side, small additions of Ar cause significant variations of particle flux at E/N close to 250 Td, and on the other in that region, we obtain significant difference of the flux and bulk drift velocities due to the BF_3 reactive processes [10] which also significantly reduce Ar^+ density in favor of fast Ar [11]. Due to reactive collisions bulk and flux values of reduced mobility are separated.

In Fig. 5, we show the rate coefficients of Ar^+ ions with Ar/BF_3 mixtures at $T = 300$ K, calculated by Monte Carlo simulations. Rate coefficients are important for the applications of the global model to Ar / BF_3 mixtures. Introducing reaction products and thermodynamic thresholds for $Ar^+ + BF_3$ [8] formation a) total attachment and b) attachment to endothermic and exothermic reaction products.

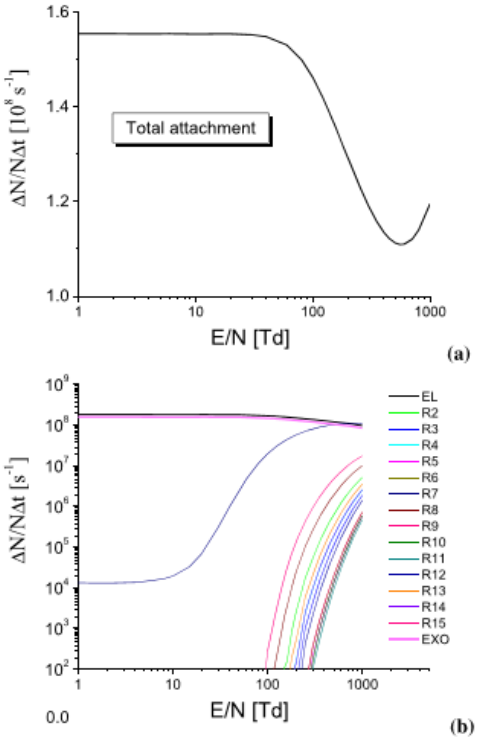

Fig. 5 Rate coefficients for Ar^+ in Ar/BF_3 mixtures at 300K

4 Conclusions

In this paper, we show transport parameters for the Ar^+ in Ar/BF_3 mixtures which do not exist in the literature. In addition to present the data, we show here the effects of non-conservative collisions to ion transport. Due to exothermic cross sections that are dominant at low energies, for small abundances of Ar ($< 10\%$) exothermic process may be larger than the elastic scattering cross section.

The Monte Carlo technique was applied for the calculation of drift velocity, mean and characteristic energy, reduced mobility, rate coefficients as a function of reduced direct electric field E/N [23]. The results are considered to be a good basis for modeling, which could be further improved when the measured values of the transport coefficients become available, and then we could perform this analysis again.

Acknowledgements The author acknowledge funding provided by the Institute of Physics University Belgrade, through the grant by the Ministry of Education, Science and Technological Development of the Republic of Serbia.

Author contributions

Željka Nikitović - Thematic direction of research and work coordination. Organization and writing of the paper, calculation of endothermic and exothermic collisions. Zoran Raspopović - Monte Carlo simulations for cases where endothermic and exothermic collisions are included, graphical presentation.

Data Availability Statement This manuscript has associated data in a data repository. [Authors' comment: All relevant data are in the paper.]

References

1. T. Makabe, Z. Petrović, *Plasma Electronics: Applications in Microelectronic Device Fabrication Taylor and Francis* (CRC Press, New York, 2006)
2. R.E. Robson, R.D. White, Z.Lj Petrović, Rev. Mod. Phys. **77**, 1303 (2005)
3. T. Murakami, K. Niemi, T. Gans, D. O'Connell, W.G. Graham, Plasma Sources Sci. Technol. **22**, 015003 (2013)
4. https://nl.lxcat.net/data/set_type.php
5. Ž. Nikitović, Z. Raspopović, V. Stojanović, Acta Phys. Pol. A **132**, 1420 (2017)
6. Ž. Nikitović, Z. Raspopović, V. Stojanović, Plasma Sources Sci. Technol. **26**, 044004 (2017)
7. V. Stojanović, Z. Raspopović, J. Jovanović, Ž. Nikitović, Z.Lj Petrović, EPL **101**, 45003 (2013)
8. M.A. Lieberman, A.J. Lichtenberg, *Principles of Plasma Discharges and Materials Processing* (Wiley, New York, 1994)
9. A. Kaboth, J. Monroe, S. Ahlen, D. Dujmić, S. Henderson, G. Kohse, R. Lanza, M. Lewandowska, A. Roccaro, G. Sciolla, N. Skvorodnev, H. Tomita, R. Vanderspek, H. Wellenstein, R. Yamamoto, P. Fisher, Nucl. Instrum. Methods Phys. Res. **592**, 63–72 (2008)
10. E. Parker, F.S.M. El-Ashhab, Int. J. Mass Spectrom. Ion Phys. **47**, 159 (1983)
11. A.V. Phelps, J. Appl. Phys. **76**, 747 (1994)
12. B.-W. Koo, Z. Fang, L. Godet, S.B. Radovanov, C. Cardinaud, G. Cartry, A. Grouillet, D. Lenoble, IEEE Trans. Plasma Sci. **32**, 456 (2004)
13. Ž. Nikitović, S. Radovanov, L. Godet, Z. Raspopović, O. Šašić, V. Stojanović, Z.Lj Petrović, EPL **95**, 45003 (2011)
14. https://nl.lxcat.net/cache/5b33772b61cf9/%20
15. Phelps A. database, private communication (2019) www.lxcat.net. Accessed 4 Feb 2019
16. Z. Lj Petrović, V.D. Stojanović, J. Vac. Sci. Technol. **16**, 329 (1998)
17. G.K. Jarvis, R.A. Kennedy, C.A. Mayhew, R.P. Tuckett, Int. J. Mass Spectrom. **202**, 323 (2000)
18. R.E. Robson, Aust. J. Phys. **44**, 685 (1991)
19. Z. Raspopović, S. Sakadžić, Z. Lj Petrović, T. Makabe, J. Phys. D **33**, 1298 (2000)
20. Ž. Nikitović, V. Stojanović, Z. Raspopović, Acta Phys. Pol. A **134**, 1134 (2018)
21. Ž. Nikitović, Z. Raspopović, V. Stojanović, Eur. Phys. J. D **72**, 168 (2018)

22. Z. Ristivojević, Z. Lj Petrović, Plasma Sources Sci. Technol. **21**, 035001 (2012)

23. Ž Nikitović, M. Gilić, J. Mitrić, Z. Raspopović, SPIG, Belgrade, Serbia **24–28**, 79 (2020)

8. Рад М23

Contrib. Astron. Obs. Skalnaté Pleso **52/3**, 78 – 89, (2022)
https://doi.org/10.31577/caosp.2022.52.3.78

Transport coefficients for He^+ ions in mixtures He/CF_4: modeling laboratory and astrophysical plasmas

Ž.D. Nikitović and Z.M. Raspopović

Institute of Physics Belgrade, University of Belgrade, Pregrevica 118, 11080 Belgrade, Serbia

Received: July 23, 2022; Accepted: October 1, 2022

Abstract. A complete set of cross sections for helium ions in a mixture of helium and carbon tetrafluoride is recommended. The transport properties for He^+ions in He/CF_4 mixtures required to model the discharge containing the mentioned ions were calculated by the Monte Carlo method at a temperature of T = 300 K. In this paper we give the drift velocity, characteristic energy, reduced mobility and specially rate coefficients for low and moderately reduced electric fields E /N (E-electric field, N-gas density) and accounting for non-conservative collisions. This paper is dedicated to the presentation of the set for He^+ions scattering cross-sections in CF_4 which is estimated using available experimental data for exothermic charge transfer cross-sections producing CF_3^+ and CF_2^+ions and endothermic charge transfer cross-section producing CF^+, C^+ and F^+ions. The aim of this paper is to determine how the addition of a percentage for He in He/CF_4 mixtures affects the separation of bulk and flux transport parameters for He^+ions.

Key words: He^+ – He/CF_4 mixtures – Monte Carlo simulations – cross sections – transport coefficients

1. Introduction

He-CF_4 mixtures are used in gaseous electronic multipliers for various imaging purposes (X-rays, charged particles, thermal neutrons and dark matter detection) (Fraga et al., 2003; Kaboth et al., 2008). After hydrogen, which makes up about 90% of the cosmos, helium is the second most abundant element (about 9%).

We notice the importance of obtained results as atomic and molecular data which are input parameters for modeling of various environments. Low temperature can change the state of metals, gases, liquids and solids, cause damage to organisms depending on length of exposure, and change the functionality of mechanized processes. Electron multiplication bursts affect the production of various ions that can affect the time distribution of detected particles (Bošnjaković, 2016). The experimental transport coefficients required as input data for He^+ion transport models in He are existing (Viehland et al., 2017;

Basurto et al., 2000; Helm, 1977; Stefansson et al., 1988; Viehland & Mason, 1995). Only bulk values in CF_4 of transport coefficients can be experimentally determined (Robson, 1991). Due to significant particle losses in He^+ in CF_4, the experimental transport coefficients were not measured. Although some experimental points for the cross sections of He^+ion scattering in CF_4 were obtained by (Fisher et al., 1990). A complete set of cross-sections for this system with more details is given in the paper (Nikitović et al., 2017). Quantum-mechanical calculation of a certain cross-section is a required task that requires knowledge of the surface potential energy of ions and molecules to be constructed from the structure of the reactants. Less intensive computational methods, such as the Denpoh-Nanbu theory (Denpoh & Nanbu, 1998; Nikitović et al., 2014; Petrović et al., 2007), require knowledge of thermodynamic formation data and are applicable to a range of molecules. Although thermodynamic formation data are known in this case, such an approach is difficult to apply, since the reaction does not take place via the excited ($HeCF_4^+$ *) complex but via the excited CF_4^+ (CF_4^+ *) states. It is also more appropriate to select the limit energies for the reaction products from the energy thresholds of the CF_4^+ state (Motohashi et al., 2005) than from the enthalpies of formation.

Ion charge transfer reactions with molecules are important elementary processes in modeling kinetics in all types of plasma. In many cases, it is known that the cross section for these reactions represents the most important part of the set of cross section. From the observation of the line spectra of excited F atoms obtained by spectrometric measurements (Motohashi et al., 2005) in CF_4, it can be concluded that the charge transfer reaction is the dominant process in collisions with inert gas ions. This argument seems to be enough to ignore other possible reactions. The aim of this paper is to report on a topic important for both basic studies and application. We estimated the set of cross sections for He^+ in He/CF_4 using existing experimental data (Viehland et al., 2017; Basurto et al., 2000; Helm, 1977; Stefansson et al., 1988; Viehland & Mason, 1995). In the next section, we will discuss the compilation of existing data and establish one possible set of cross-sections. We will then describe the calculation of transport parameters and finally discuss our results. The coefficients of velocity, flux and bulk reduced mobilities, calculated from flux and bulk drift velocities by Monte Carlo simulation are significantly different in the region of moderate E/N.

2. Cross section sets

Our goal in this section will be to establish a set of cross sections because only the set of cross sections contains relevant information for calculating the transport properties of the selected ion in a given gas. In our chosen case, the general knowledge of the total cross-section indicates that at low energies they

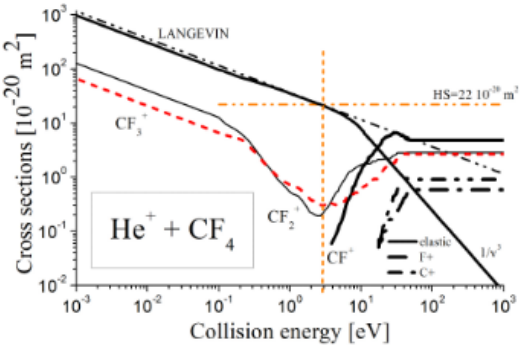

Figure 1.: Cross section set for $He^+ + CF_4$.

would be affected by attractive long-range forces, while at high energies they would be affected by repulsive forces.

For low energies, when the interaction potential is very close to the induced dipole potential, it can be assumed that the total cross section of the moment transfer is $\sigma_{mt} = 1.105\ \sigma_L$ where σ_L is the Langevin cross section (McDaniel et al., 1970). The Langevin cross section was determined using the average gas polarizability. The average polarizability of CF_4 is poorly determined (Fisher et al., 1990) and can lead to deviations in the calculated ion mobility in CF_4 (Stojanović et al., 2014; Georgieva et al., 2003). As a consequence, this would affect the prediction of plasma parameters in modeling. The value of 3.86 10-30 m3 used by Stojanović et al. (2014) who found an excellent agreement between the experimental and the calculated reduced mobility of CF_3^+ ions in CF_4.

From measurements of exothermic cross sections Fisher et al. (1990) for the production of CF_2^+ and CF_3^+ from $He^+ + CF_4$ it can be concluded that the scattering is appropriate to describe with induced polarization potential up to 0.2 eV. Thus, assuming that charge transfer reactions are the dominant interaction, a cross section of elastic moment transmission can be obtained by deduction of experimental reactive cross sections (Fisher et al., 1990) from the assumed total moment transfer.

Extrapolation of the behavior of the cross section of the transmission of elastic moment outside the Langevin point of intersection to the cross section of the soft sphere (Fisher et al., 1990) was done by smooth connection with the trend $1/v^3$ (Krstić & Schultz, 2009; Raspopović et al., 2015) where v is the center-velocity of mass (see Figure 1). Extrapolation is performed in the energy

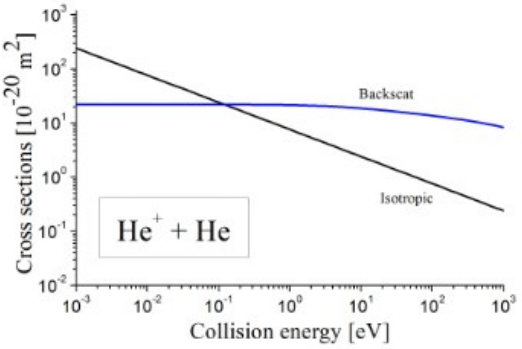

Figure 2.: Cross section set for He^+ + He.

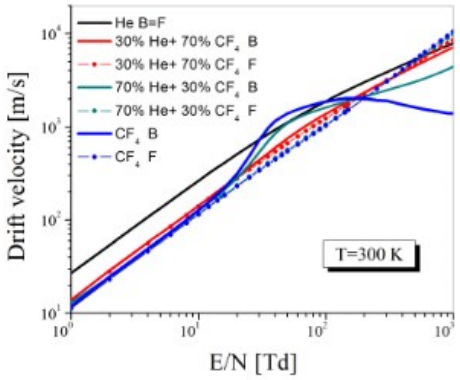

Figure 3.: Drift velocity for He^+ in He/CF_4 mixtures as a function of E/N.

region where a repulsive interaction is expected to occur, which is estimated to be above about 3 eV. Finally, all exothermic and endothermic cross-sections of Fisher et al. (1990). Reactive cross sections were approximated by constant values at all kinetic energies of ions above 50 eV using data for the production ratio between the observed ions as proposed in (Parker & El-Ashhab, 1983).

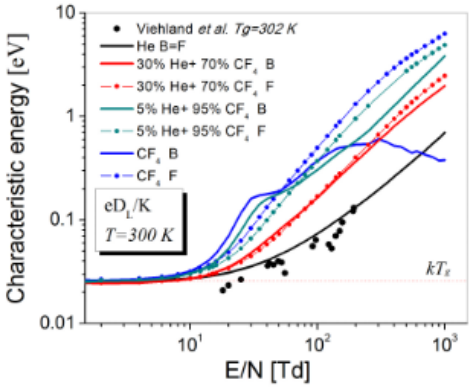

Figure 4.: Longitudinal characteristic energy for He^+ in He/CF_4 mixtures as a function of E/N.

It was found that different extrapolations (short dot-dashed or dashed line in Figure 1) of unusual low energy behavior observed by cross-sectional measurement led to CF_2^+ formation (where exothermic reaction behavior is expected regardless of, He^+ spin state) have negligible impact on mobility. In the case of the system, He^+ on He, the Phelps sections taken from the database were used for (Phelps, 2011). The section consists of two components: Isotropic and Backscat is given in Figure 2.

3. Transport parameters

Transport properties needed for modeling CF_4 discharges containing He^+ions are calculated by the Monte Carlo method. A code that properly takes into account thermal collisions was used (Ristivojevic & Petrović, 2012). It has passed all relevant benchmarks Fisher et al. (1990) and was tested in our work on several types of charged particles (Petrović et al., 2007; de Urquijo et al., 2013).

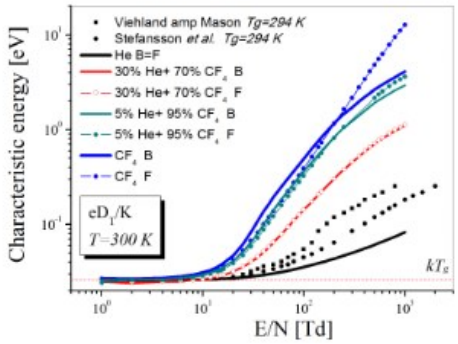

Figure 5.: Transversal characteristic energy for He^+ in He/CF_4 mixtures as a function of E/N.

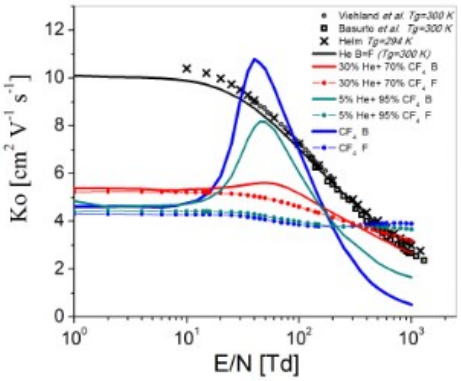

Figure 6.: The bulk and flux reduced mobility for He^+ in He/CF_4 mixtures as a function of E/N.

Swarm parameters of He^+ in He/CF_4 mixtures for a temperature of T=300 K are presented.

The calculated transport parameters are the mean energy, characteristic energy, drift velocity, diffusion coefficients, ionization and attachment coefficients and chemical reaction coefficients for ions (Petrović et al., 2009). The excitation coefficients are also measured but seldom used in modeling. Note that these transport parameters are the only information present in the literature up to now and there are no published experimental data for the transport coefficients of He^+ in He/CF_4 mixtures. The transport parameters of He^+ions swarm in neutral gases He and CF_4, as well as in mixtures were calculated: (1) 5% He + 95% CF_4 (2) 30% He + 70% CF_4 and (3) 70% He + 30% CF_4.

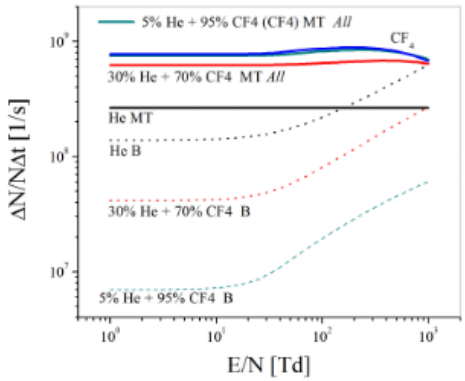

Figure 7.: Rate coefficients for He^+ in He/CF_4 mixtures as a function of E/N: momentum transfer.

The flux and bulk drift velocities (Robson et al., 2005; Ness & Robson, 1986; Nikitović et al., 2018; Nikitović & Raspopović, 2021) for He^+ in He/CF_4 mixtures as a function of E/N are given in Figure 3. The drift velocities obtained by the Monte Carlo simulation are calculated in real space (bulk) and in velocity space (flux) values which are obtained as $d < x > /dt$ and $< v >$, respectively. At low energies, at E/N<200 Td due to intense formation of CF_3^+ and CF_2^+ions in charge transfer reactions instead of He^+ions, the center of mass of the swarm moves forward, so that the bulk velocity is greater than the flux. With further increase E/N>200 Td when the high-energy ions from the distribution function increasingly have non-conservative collisions in which the CF^+, C^+ and F^+ be-

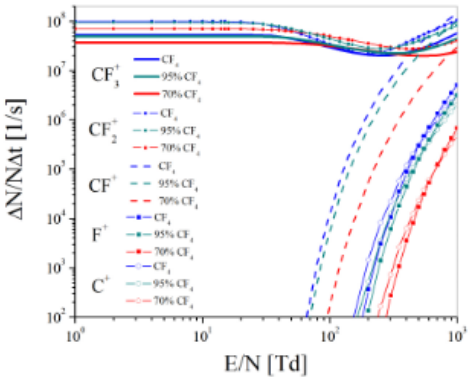

Figure 8.: Rate coefficients for He^+ in He/CF_4 mixtures as a function of E/N: production reactions.

coming He^+ions disappear, shifting the center of mass of the swarm backward, resulting in a bulk velocity less than the flux.

In Figure 4 we present the characteristic energies (diffusion coefficient normalized to mobility D/K in units of eV) determined in the direction of the electric field. Figure 4) are shown that with increasing percentage of CF_4 molecules in the mixture with He there is an increase in bulk and flux values of longitudinal characteristic energy, except in the case of balk values of eDL/K at CF_4 concentrations higher than 95% for E/N>40 Td. Already 5% He^+ions in a mixture with CF_4 significantly reduces the differences between balk and flux values of longitudinal characteristic energy, and in a mixture with 30% He these differences are still noticeable. Figure 4) also includes the experimentally measured values of eDL/K by Viehland et al. (2017) for the system He^+ + He (black symbols).

The transversal characteristic energy also increases with increasing percentage of He/CF_4 mixtures (Figure 5). Smaller differences between balk and flux values are in transversal compared to longitudinal characteristic energy. With 30% He in the mixture there is no difference between bulk and eDT/K flux. In Figure 5) the experimentally measured values of eDT/K by Stefansson et al. (1988) and Viehland & Mason (1995) for the system He^+ + He (black symbols).

Reduced mobility for He^+ions in CF_4 as a function of E/N (E-electric field strength, N-gas number density) compared with bulk and flux values is shown in Figure 6. Significant peak in the bulk reduced mobility is obtained as a

result of difference in energy dependence of elastic and exothermic cross sections (Nikitović et al., 2019) . Let us remind the reader that the bulk drift velocity ($W = d < x > /dt$) is reaction corrected flux drift velocity ($w =< v >$): $W = w + S$, where S is the term representing a measure of the effect of reactions on the drift velocity. Difference between bulk and flux reduced mobilities is a consequence of energy dependent reactions. We found that the cross section leading to formation of CF_2^+ (where irrespective of the He^+ spin state exothermic behavior of reaction is expected) are negligible on mobility.

Mobility of $He^+ + CF_4$ depending on E/N has a pronounced maximum at about 40 Td, while mobility of $He^+ + He$ does not; has a plateau at low E/N that immediately declines as a result of pronounced backs cat interaction. At low E/N higher values of Ko for the $He^+ + He$ system than those for $He^+ + CF_4$ are due to less the reduced mass of the ion neutral pair. At low E/N balk values for Ko are higher than flux values as a consequence of low-energy capture of He^+ions by CF_4 molecules in an exothermic reaction in which CF_3^+ion is formed. At large E/N flux values are higher than the balk values due to higher ion capture at high energies than at lower ones. With increasing He concentration in the mixture, the differences between bulk and flux values are significantly reduced. For a mixture of 30% He + 70% CF_4 these differences can be clearly seen only in the region of about 40 Td. In Figure 6 the experimentally measured values of Ko by Viehland et al. (2017), Basurto et al. (2000) and Helm (1977) for the system $He^+ + He$ (black symbols).

In Figures 7 and 8 we show rate coefficients for elastic momentum transfer and for all reactive processes as a function of E/N. The rate coefficients as final output of our calculations is needed as input in fluid equations for description of ion transport in He/CF_4 mixtures. The rate coefficients for all reactions presented in the cross-section sets are significantly different than one that should be obtained with cross sections obtained from statistical theories such are those obtained by Denpoh-Nanbu theory (Denpoh & Nanbu, 1998).

4. Conclusion

In this paper we have determined the cross section of elastic moment transport as a function of energy for He^+ scattering on CF_4 that can be used in modeling He^+ transport in He/CF_4 mixtures. We used the data for a simple theoretical cross-section of the transmission of the total moment and obtained the cross-section of the transmission of the elastic moment by deduction of all experimentally obtained cross-sections of the charge transfer. In doing so, we assumed that the measured cross-sections of the charge transfer were collisions with the highest probability. Thus, in this paper, we have estimated the set of cross sections for He^+ions in He/CF_4 that can be used as an independent input in modeling He^+ion transport. This estimation was performed using measured cross-sections of charge transfer.

Since, according to our knowledge, there is no direct information in the literature on how the mobility of high recombination energy ions, such as He^+ ions, behave in He/CF_4 mixtures, we calculated transport parameters using the Monte Carlo simulation method (Nikitović et al., 2014; Nikitović et al., 2016, 2019).

In this work, we obtained and considered data on longitudinal and transversal characteristic energy, bulk and flux reduced mobility and rate coefficients. Data on swarm coefficients for positive and negative ions are required for hybrid and fluid codes (White et al., 2014) and the current focus on liquids or liquids in rare gas mixtures dictates the need to produce data compatible with these models. Given the current interest in liquid and / or liquid models in mixtures with rare gases, data on swarm coefficients for positive and negative ions for hybrid and fluid codes are needed. Atmospheric and near-atmospheric pressure glow discharges generated in both pure helium and helium-air mixtures have been studied using a plasma chemistry code originally developed for simulations of electron-beam-produced air plasmas.

Acknowledgements. The authors acknowledge funding provided by the Institute of Physics University of Belgrade, through the grant by the Ministry of Education, Science and Technological Development of the Republic of Serbia.

References

Basurto, E., de Urquijo, J., Alvarez, I., & Cisneros, C., Mobility of He^+, Ne^+, Ar^+, N^+_2, O^+_2, and CO^+_2 in their parent gas. 2000, *Phys. Rev. E*, **61**, 3053, DOI: 10.1103/PhysRevE.61.3053

Bošnjaković, D., Ph Dissertation. 2016, *Faculty of Electrical Engineering, University of Belgrade, Belgrade, Serbia*

de Urquijo, J., Jovanović, J. V., Bekstein, A., Stojanović, V., & Petrović, Z. L., Ion mobilities and transport cross sections of daughter negative ions in N_2O and N_2O-N_2 mixtures. 2013, *Plasma Sources Sci. Technol.*, **22**, 025004, DOI: 10.1088/0963-0252/22/2/025004

Denpoh, K. & Nanbu, K., Self-consistent particle simulation of radio-frequency CF_4 discharge with implementation of all ion-neutral reactive collisions. 1998, *J. Vac. Sci. Technol. A*, **16**, 1201, DOI: 10.1116/1.581259

Fisher, E. R., Weber, M. E., & Armentrout, P. B., Dissociative charge transfer reactions of Ar^+, Ne^+, and He^+ with CF_4 from thermal to 50 eV. 1990, *J. Chem. Phys.*, **92**, 2296, DOI: 10.1063/1.457969

Fraga, M. M. F. R., Fraga, F. A. F., Fetal, S. T. G., et al., The GEM scintillation in He-CF_4, Ar-CF_4, Ar-TEA and Xe-TEA mixtures. 2003, *Nucl. Instrum. Meth. in Phys. Res. A*, **504**, 88, DOI: 10.1016/S0168-9002(03)00758-7

Georgieva, V., Bogaerts, A., & Gijbels, R., Particle-in-cell/Monte Carlo simulation of a capacitively coupled radio frequency Ar/CF_4 discharge: Effect of gas composition. 2003, *J. Appl. Phys.*, **93**, 2369, DOI: 10.1063/1.1542920

Helm, H., The cross section for symmetric charge exchange of He^+ in He at energies between 0.3 and 8 eV. 1977, *J. Phys. B*, **10**, 3683, DOI: 10.1088/0022-3700/10/18/025

Kaboth, A., Monroe, J., Ahlen, S., et al., A measurement of photon production in electron avalanches in CF $_4$. 2008, *Nucl. Instrum. Meth. in Phys. Res. A*, **592**, 63, DOI: 10.1016/j.nima.2008.03.120

Krstić, P. S. & Schultz, D. R., Elastic and related transport cross sections for singly charged ion-atom scattering of light metals (Li, Be, B) and hydrogen. 2009, *J. Phys. B: At. Mol. Opt. Phys.*, **42**, 065207, DOI: 10.1088/0953-4075/42/6/065207

McDaniel, E. W., Cermak, V., & Ferguson, E. E. 1970, *Ion-molecule reactions*

Motohashi, K., Takahashi, T., Takahashi, N., & Tsurubuchi, S., Emission cross sections in low-energy collisions between He^+, Ne^+ ions and CF_4 molecule. 2005, *J. Phys. B: At. Mol. Opt. Phys.*, **38**, 3339, DOI: 10.1088/0953-4075/38/18/005

Ness, K. F. & Robson, R. E., Velocity distribution function and transport coefficients of electron swarms in gases. II. Moment equations and applications. 1986, *Phys. Rev. A*, **34**, 2185, DOI: 10.1103/PhysRevA.34.2185

Nikitović, Ž., Raspopović, Z., Stojanović, V., & Jovanović, J., Transport parameters of F- ions in Ar/BF3 mixtures. 2014, *EPL*, **108**, 35004, DOI: 10.1209/0295-5075/108/35004

Nikitović, Ž. D. & Raspopović, Z. M., Rate coefficients for Ar^+ in Ar/BF_3 mixtures. 2021, *Eur. Phys. J. D*, **75**, 118, DOI: 10.1140/epjd/s10053-021-00061-3

Nikitović, Ž. D., Raspopović, Z. M., & Stojanović, V. D., Reduced mobility of He^+ in CF_4. 2017, *Plasma Sources Sci. Technol.*, **26**, 044004, DOI: 10.1088/1361-6595/aa61db

Nikitović, Ž. D., Raspopović, Z. M., & Stojanović, V. D., Cross sections set and transport coefficients for Ar^+ in Ar/CF_4 mixtures. 2018, *Eur. Phys. J. D*, **72**, 168, DOI: 10.1140/epjd/e2018-90059-1

Nikitović, Ž. D., Raspopović, Z. M., & Stojanović, V. D., Reduced mobility of Ar^+ in Ar/BF_3mixtures. 2019, *EPL*, **128**, 15001, DOI: 10.1209/0295-5075/128/15001

Nikitović, Ž. D., Stojanović, V. D., & Raspopović, Z. M., Modeling elastic momentum transfer cross-sections from mobility data. 2016, *EPL*, **114**, 25001, DOI: 10.1209/0295-5075/114/25001

Parker, J. E. & El-Ashhab, F. S. M., Charge-transfer reactions of carbon tetrafluoride. 1983, *Int.J. Mass Spectrom. Ion. Phys.*, **47**, 159, DOI: 10.1016/0020-7381(83)87160-5

Petrović, Z. L., Dujko, S., Marić, D., & Malović, G., ž Nikitović, O Šašić, J Jovanović, V Stojanović, and M Radmilović-Radjenović. Measurement and interpretation of swarm parameters and their application in plasma modelling. 2009, *J. Phys. D: Appl. Phys.*, **42**, 194002, DOI: 10.1088/0022-3727/42/19/194002

Petrović, Z. L., Raspopović, Z. M., Stojanović, V. D., et al., Data and modeling of negative ion transport in gases of interest for production of integrated circuits and nanotechnologies. 2007, *J. Appl. Surf. Sci.*, **253**, 6619, DOI: 10.1016/j.apsusc.2007.02.005

9. Рад M23, On Line

Submitted: 26.06.2023.

Accepted for publication: 25.07.2023.

CROSS SECTION SETS AND TRANSPORT PARAMETERS FOR Ar^+ IONS IN CF_4 GAS

Željka Nikitović* and Zoran Raspopović

Institute of Physics, University of Belgrade, Pregrevica 118, Belgrade, Serbia

https://doi.org/10.2298/SOS230326038N

Abstract

Understanding plasma distribution, characteristics and phenomena is important for the development and optimization of semiconductor device manufacturing plasma equipment, such as etching and deposition tools. For this reason, plasma simulation is currently being utilized at every stage of equipment design, development and improvement. The cross section sets obtained by applying Denpoh-Nanbu theory to Ar^+ on CF_4 collisions were found to be in general qualitative and in part quantitative agreement with data from the literature. The Monte Carlo technique was applied to perform calculations of transport parameters. Calculated cross sections can be used to obtain transport coefficients, specially drift velocity, characteristic energy, reduced mobility, longitudinal diffusion and rate coefficients for low and moderate reduced electric fields *E/N* (E-electric field strength; N-gas density) and accounting for the non-conservative collisions.

Keywords: *Monte Carlo Simulations, Ar^+ ions, CF_4 gas.*

Email: **zeljka@ipb.ac.rs**

1. Introduction

Transport of Ar^+ plays a significant role in various etching and deposition processes [1], in dark matter detection [2] and in many other scientific and technological applications. In this letter, the objective will be to study transport of Ar^+ in CF_4. Since quantitative information about ion-molecule reactions is essential for understanding the production and transport of ions in electrical discharges it is necessary to have the cross section set. Although for this particular case some experimental cross sections exist, neither complete cross section set [3] was established nor transport parameters were known. These data, although closely related, are both needed in plasma modeling.

In certain cases, charge transfer reactions are known to represent the most significant part of a cross section sets. Line spectra of excited atoms obtained in spectrometric measurements in CF_4 [4] indicate that the charge transfer reaction is dominant process in collisions with inert gas ions. Thus, in this work we assessed cross section set for Ar^+ in CF_4 by using existing experimental data [5] for charge transfer collisions producing radical ions of CF_4.

Since no direct information is found in the literature on how the mobility of inert ions, such as Ar^+ ions, behaves in CF_4, we have also calculated transport parameters using the Monte Carlo simulation technique and complete cross sections. Ions are tracked in infinite space, receive energy from a constant DC electric field, and dissipate it in collisions with neutral gas particles. Collisions are instantaneous and isotropic, and the collision trajectory is determined by the null-collision method [6]. The elastic properties of a solid were studied using a multiphase unit cell numerical model [7] and using computer simulations, it showed a relationship between the lattice parameter and the inversion parameter [8]. An initial set of cross-sections for this system with more details is given in our paper [9].

2. Calculation on the cross section sets

The cross sections presented by Fisher *et al.* [5] were used to determine the elastic momentum transfer cross section assuming the total momentum transfer cross section σ_{mt} is known. At low energies we assumed that σ_{mt} is Langevin's cross section and elastic momentum transfer cross section is determined by deducing all nonelastic and reactive cross sections.

Average polarizability of CF_4 is not well established [5] and may produce discrepancy for calculated mobility of ions in CF_4 [10] and thus affect plasma parameters prediction in modelling. We adopted value of 3.86 A^3 used by Stojanović *et al.* [10] who found excellent agreement between experimental and calculated mobility of CF_3^+ ions in CF_4. Note that usage of this polarizability increases Langevin's cross section above reaction cross sections of Fisher *et al.* (1990) at least in the region of validity of polarization potential approximation.

The elastic momentum transfer cross-section (indicated by the red line in Figure 1 and labeled as Elastic MT) extends as the Langevin cross-section at low energies and transitions to the hard sphere cross-section at higher energies [5]. The cross-section, denoted in the legend of Figure 1 as "Elastic MT (e < 1eV)," represents the transition from Langevin behavior to the hard sphere model, achieved by smoothly connecting it to the 1/v^3 trend [11], where v is the center-of-mass velocity (see Figure 1). For elastic collisions with energy greater than 1 eV, the collisions are described by the hard sphere model (HS), as depicted in the work of Denpoh-Nanbu [12], with an isotropic cross-section for momentum transfer (indicated by HS black dots in Figure 1).

Further, extrapolation of elastic momentum transfers cross section trend approximately beyond the crossing point of Langevin's and hard sphere (HS) cross section [5] is done by smoothly connecting to $1/v^3$ trend [11] where v is the center-of-mass velocity (see Figure 1).

At all ion kinetic energies above 50 eV, experimental reactive cross sections are extrapolated to constant values for experimental cross sections by Fisher et al. (CF_3^+, CF_2^+, and CF^+). This is done with the mind of considering measurements of emission cross section by Motohashi et al. [4], where slow oscillatory behavior of the emission cross sections was found at high projectile energies, and an almost constant reaction probability was found over a wide energy range.

When the collision energy increases, Langevin disappears and collisions are described as brittle or soft sever. For this reason, we assumed for this paper that the Langevin vanishes at about 1 eV when the Fisher rigid sphere is formed.

We added Fischer's experiment and all the others from the Denpoh-Nanbu's work to the new momentum transfer (with a hole), excluding those that make CF_3^+, CF_2^+ and CF^+ ions. With the added production of CF_3^+, CF_2^+ and CF^+ ions and the remaining reactions F^+ and C^+ inelastic process [12] the set of sections looks like Figure 3.

The cross-section image has too many lines, so we merged related cross-sections for a clearer view of the cross-section.

Fig. 1

Fig. 2

Fig. 3

3. Results and discussion

The cross section sets for ion transport are rare due to a broad range of specific methods reported in the literature relevant for quantification of particular cross sections. We have used a Monte Carlo code that properly takes into account thermal collisions [13]. The code has passed all the relevant benchmarks [14] and has been tested in our work on several types of charged particles [14, 15].

Results of Monte Carlo simulations are shown in Figs. 4-8. Note that these transport parameters are the only information present in the literature up to now there are no published experimental data for the transport coefficients of Ar^+ in CF_4 with complete cross section sets in best of our knowledge. Flux and bulk drift velocities [16, 17 and 18] as a function of *E/N* are given in Figure 4. Since the total collision frequency for endothermic reactions increases with energy at high *E/N*, the dominant loss of the fast ions happens at the front of the swarm. This shifts the swarm's centre of mass towards the lower values. The drift velocities obtained by Monte Carlo simulation calculated in real space (bulk) and in velocity space (flux) values which are obtained as dx/dt and $\langle v \rangle$, respectively.

Fig. 4

Reduced mobility for Ar^+ ions as a function of *E/N* (*E*-electric field, *N*-gas density) is shown in Figure 5. Values of the reduced mobility as a function of *E/N* [19-22] shown are obtained by using bulk drift velocities, as those are measured in most experiments, though proper quantities should be applied according to the source of experimental data [14, 15]. Significant increase of mobility at low *E/N* is a result of non-conservative process at low energy. At about 300 Td another mobility peak appears, representing significant increase of reactive collisions.

Fig. 5

In Figure 6 we show rate coefficients for reactions of Ar^+ ions with CF_4 gas at T=300K. Rate coefficients are important for applications of the global model to CF_4 gas. The largest production is CF_3^+, CF_2^+, CF^+, F^+ and C^+ are reduced. At E/N >300 Td, inelastic collisions are larger than elastic ones. For E/N> 800 Td Ar^+ can ionize CF_3^+.

The products a) total rate coefficients and b) all reactions are also presented in Figure 6.

Fig. 6

In the Figure 7 we show mean and characteristic (longitudinal L and transverse T) energy for Ar^+ in CF_4 gas. Transversal eD/K cuts off non-conservative processes more weakly than longitudinal eD/K. The decrease in eD_L/K from 180 to 300 Td when Ar^+ ions reach the energy threshold for the production of CF_2^+ ions, which increases sharply with increasing energy.

Fig.7

Diffusion coefficients ND_L are given in Figure 8 and one should notice the very large non-conservative effects almost a reminder of the positron transport [23]. Similar to the results for drift velocity, flux diffusion coefficients are significantly larger than bulk values.

Fig. 8

The bulk values of longitudinal diffusion decrease with an increase in the reduced electric field strength from 1 Td to 60 Td because the exothermic reaction decays more slowly

than the Langevin reaction, which occurs at a constant collision frequency. The decrease in the bulk values is attributed to the more rapid disappearance of fast Ar^+ ions under increasing electric field conditions, resulting in a compression of the swarm along the direction of the field. When the mean energy of Ar^+ ions is 0.2 eV (E/N = 60 Td), ions can reach energies up to 2 eV. In this energy range, the number of vibrations that increase the bulk and flux values of ND_L also increases (see Fig. 7). At these energies, a small number of Ar^+ ions reach the threshold energies for CF_2^+ and CF^+ reactions.

At 150- to 200 Td (energy is 1 eV to 1.5 eV, respectively) the flux and bulk values of ND_L reach their maximum values. However, as the electric field continues to increase, the bulk value of ND_L starts to decrease again. The reduction in the bulk and flux values of ND_L is attributed to the ions reaching the energy thresholds for the CF_2^+ and CF^+ reactions (8 and 10 eV respectively), which leads to the disappearance of high-energy ions and slows down the overall effect.

4. Conclusions

In addition to presenting the data, we show here the effects of non-conservative collisions on ion transport. Due to non-conservative cross sections that are larger than the elastic scattering cross section, the differences between the bulk flux and transport coefficients are quite large comparable to the strongest cases observed for electrons, even positrons. Data for ion swarm parameters [24, 25] are required for hybrid and fluid codes, and the current focus on liquids or liquids in rare gas mixtures dictates the need to produce data compatible with those models.

ACKNOWLEDGMENTS

The authors acknowledge funding provided by the Institute of Physics University Belgrade, through the grant by the Ministry of Education, Science and Technological Development of the Republic of Serbia No. 451-03-68/2022-14 and 451-03-47/2023-01.

Authors are also grateful to Dr Kazuki Denpoh.

References

[1] M. A. Lieberman and A. J. Lichtenberg, Principles of Plasma Discharges and Materials Processing. Wiley, New York (1994).

[2] A. Kabothc, J. Monroec, S. Ahlena, D. Dujmic, S. Hendersonc, G. Kohsec, R. Lanzac, M. Lewandowskaa, A. Roccaroa, G. Sciollac, N. Skvorodnevb, H. Tomitaa, R. Vanderspekc, H. Wellensteinb, R. Yamamotoc, P. Fisher, Nuclear Instruments and Methods in Physics Research **A 592** (2008) 63 -72.

[3] S. Pancheshnyi, S. Biagi, M. C. Bordage, G. J. M. Hagelaar, W. L. Morgan, A.V. Phelps, L. C. Pitchford, Chem. Phys. **398** (2012) 148-153.

[4] K. Motohashi, T. Takahashi, N. Takahashi S. Tsurubuchi, J. Phys. B: At. Mol. Opt. Phys. **38** (2005) 3339-3348.

[5] E. R. Fisher, M. E. Weber and P. B. Armentrout, J. Chem. Phys. **92 (4)** (1990) 2296-2302.

[6] Z. Lj. Petrović, M. Šuvakov, Ž. Nikitović, S. Dujko, O. Šašić, J. Jovanović, G. Malović and V. Stojanović, Plasma Sources Sci. Technol. **16** (2007) S1–S12.

[7]A. T. Saleem,V. Petrović, A. Grbović, J. Lozanović Šajić, I. Balać, Sci Sinter **53** (2021) 127-136.

[8] N. Obradović, S. Filipović, W. G. Fahrenholtz, B. A. Marinković, J. Rogan, S. Lević, A. Đorđević, V. B. Pavlović, Sci Sinter **55** (2023) 1-10.

[9] Z. Raspopović, V. Stojanović and Ž. Nikitović, EPL **111** (2015) 45001.

[10] V. Stojanović, Z. Raspopović, J. V. Jovanović, J. de Urquijo and Z. Lj. Petrović, J. Phys.: Conf. Series **514** (2014) 012059.

[11] P. S. Krstić and D. R. Schultz, J. Phys. B: At. Mol. Opt. Phys. **42** (2009) 065207.

[12] K. Denpoh and K. Nanbu, Journal of Vacuum Science & Technology A **40** (2022) 063007.

[13] Z. Ristivojević and Z. Lj. Petrović, Plasma Sources Sci. Technol. **21** (2012) 035001.

[14] Z. Lj. Petrović, Z. M. Raspopović, V. D. Stojanović, J. V. Jovanović, G. Malović, T. Makabe, J. De Urquijo, Appl. Surf. Sci. **253** (2007) 6619.

[15] J. de Urquijo, J. V. Jovanović, A. Bekstein, V. Stojanović and Z. Lj. Petrović, Plasma Sources Sci. Technol. **22** (2013) 025004.

[16] R. E. Robson, Aust. J. Phys. **44** (1991) 685-692.

[17] Z. Raspopović, S. Sakadžić, Z. Lj. Petrović and T. Makabe, J. Phys. **D 33** (2000) 1298-1302.

[18] Ž. Nikitović, M. Gilić, M. Petrović, N. Romčević, Z. Raspopović and V. Stojanović, Sci Sinter **48** (2016) 379-386.

[19] Ž. Nikitović, Z. Raspopović, V. Stojanović and J. Jovanović, Europhys. Lett. **108** (2014) 35004.

[20] Ž. Nikitović, V. Stojanović, Z. Raspopović and J. Jovanović, Acta Physica Polonica A **126** (2014) 724-726.

[21] Ž. Nikitović, Z. Raspopović and V. Stojanović, EPL **128** (2019) 15001.

[22] Ž. Nikitović and Z. Raspopović, Sci Sinter **54** (2022) 169-176.

[23] S. Dujko, A. H. Markosyan, R. D. White and U. Ebert, J. Phys.D: Appl. Phys. **46** (2013) 475202.

[24] R. D. White, W. Tattersall, G. Boyle, R. E. Robson, S. Dujko, Z. Lj. Petrović, A. Banković, M. J. Brunger, J. P. Sullivan, S. J. Buckman and G. Garcia, Applied Radiation and Isotopes **83** (2014) 77-85.

[25] S. Marjanović, A. Banković, D. Cassidy, B. Cooper, A. Deller, S. Dujko and Z. Lj. Petrović, J. Phys. B: At. Mol. Opt. Phys. **49** (2016) 215001.

Figure captions:

Figure 1. Cross section set for $Ar^+ + CF_4$ without Langevin.

Figure 2. Cross section set for $Ar^+ + CF_4$ with Denpoh-Nanbu reactions.

Figure 3. Complete cross section sets for $Ar^+ + CF_4$.

Figure 4. Bulk and flux drift velocity for Ar^+ in CF_4 at 300 K.

Figure 5. Reduced mobility for Ar^+ in CF_4 a function of *E/N*.

Figure 6. Rate coefficients for Ar^+ in CF_4 a function of *E/N* at 300 K.

Figure 7. Mean and characteristic energy for Ar^+ in CF_4 a function of *E/N*.

Figure 8. Longitudinal diffusion coefficients for Ar^+ in CF_4 a function of *E/N*.

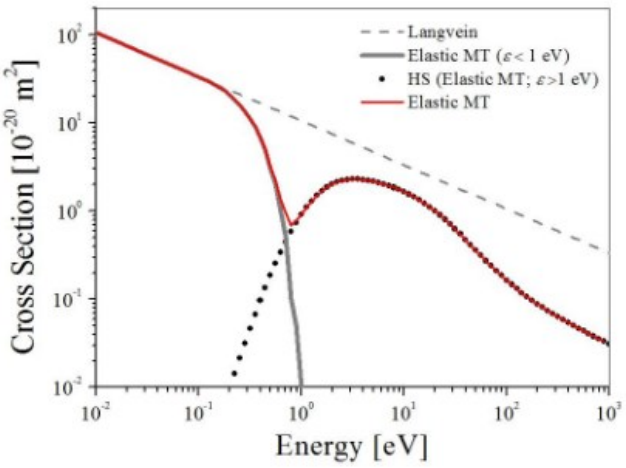
Langvein
Elastic MT (ε < 1 eV)
HS (Elastic MT; ε >1 eV)
Elastic MT
Cross Section [10^-20 m^2]
Energy [eV]

FIGURE 1

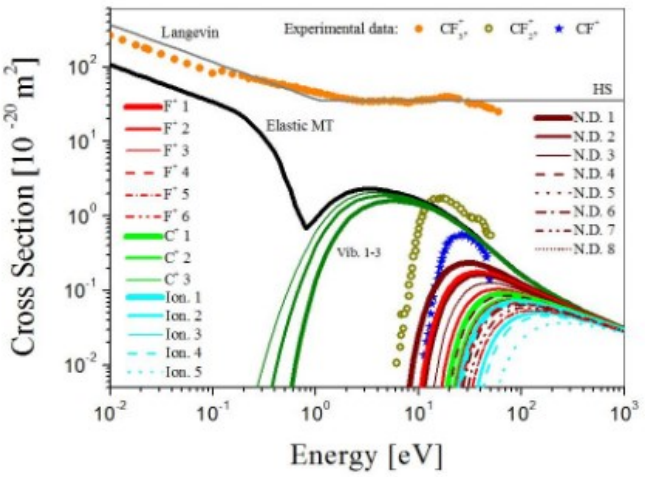
Langevin
Experimental data: CF_3^+, CF_2^+, CF^+
HS
Elastic MT
Vib. 1-3
F^+ 1
F^+ 2
F^+ 3
F^+ 4
F^+ 5
F^+ 6
C^+ 1
C^+ 2
C^+ 3
Ion. 1
Ion. 2
Ion. 3
Ion. 4
Ion. 5
N.D. 1
N.D. 2
N.D. 3
N.D. 4
N.D. 5
N.D. 6
N.D. 7
N.D. 8
Cross Section [10^{-20} m^2]
Energy [eV]

FIGURE 2

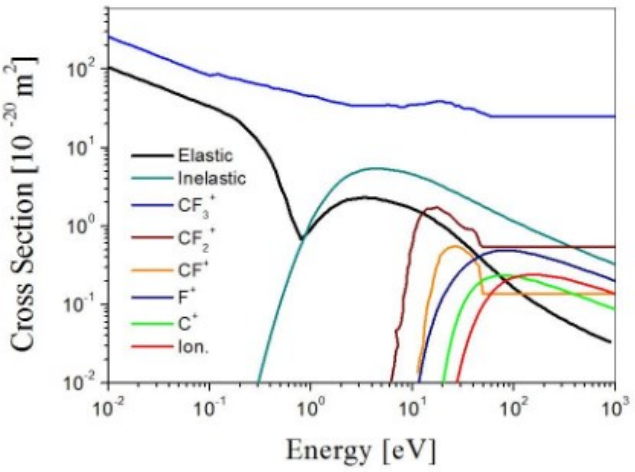
Cross Section [10 -20 m2]
Energy [eV]
Elastic
Inelastic
CF3+
CF2+
CF+
F+
C+
Ion.

FIGURE 3

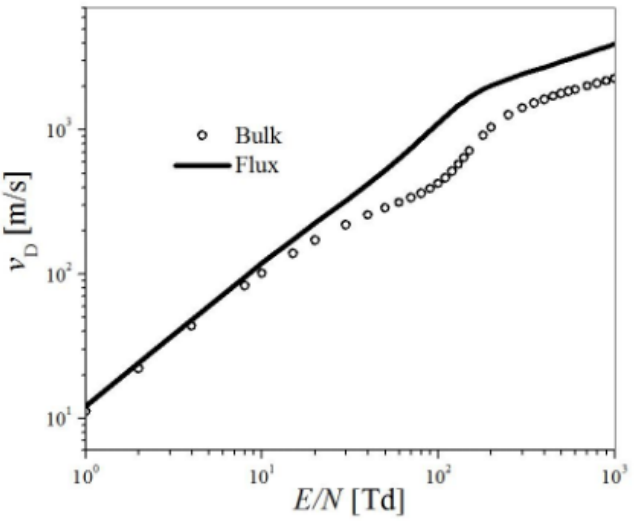

FIGURE 4

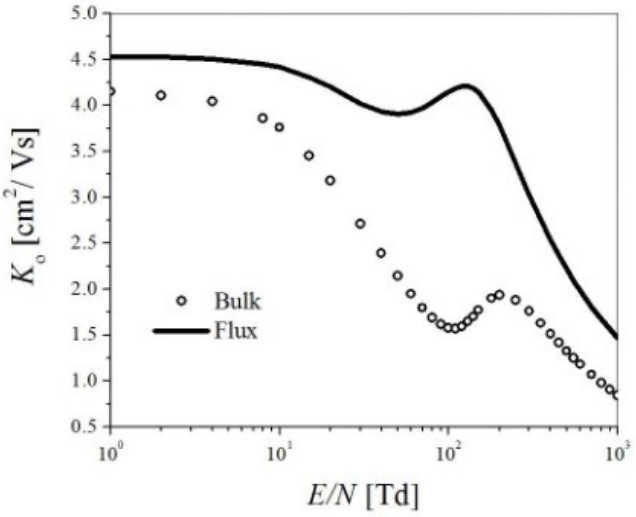
5.0
4.5
4.0
3.5
3.0
2.5
2.0
1.5
1.0
0.5
K_o [cm^2/ Vs]
Bulk
Flux
10^0
10^1
10^2
10^3
E/N [Td]

FIGURE 5

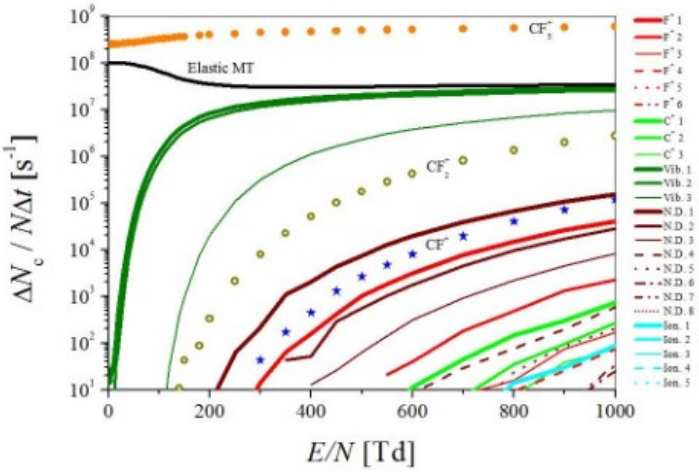
Elastic MT
CF_3^-
CF_2^-
CF^-
$\Delta N_c / N\Delta t$ [s^{-1}]
E/N [Td]
0
200
400
600
800
1000
10^9
10^8
10^7
10^6
10^5
10^4
10^3
10^2
10^1
F^- 1
F^- 2
F^- 3
F^- 4
F^- 5
F^- 6
C^- 1
C^- 2
C^- 3
Vib. 1
Vib. 2
Vib. 3
N.D. 1
N.D. 2
N.D. 3
N.D. 4
N.D. 5
N.D. 6
N.D. 7
N.D. 8
Ion. 1
Ion. 2
Ion. 3
Ion. 4
Ion. 5

a)

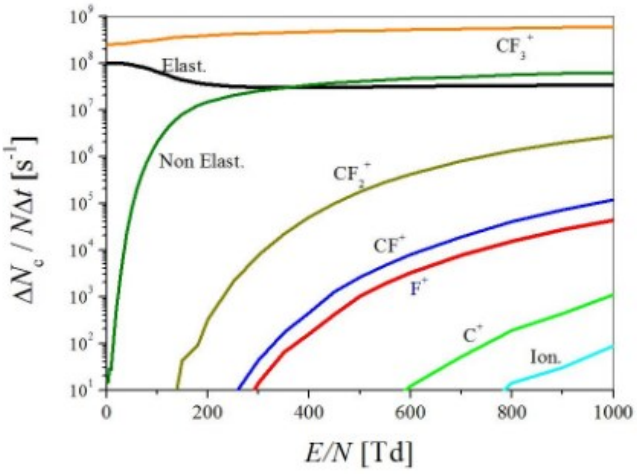
10^9
10^8
10^7
10^6
10^5
10^4
10^3
10^2
10^1
$\Delta N_c / N\Delta t$ [s^{-1}]
Elast.
Non Elast.
CF_3^+
CF_2^+
CF^+
F^+
C^+
Ion.
0
200
400
600
800
1000
E/N [Td]

b)

FIGURE 6

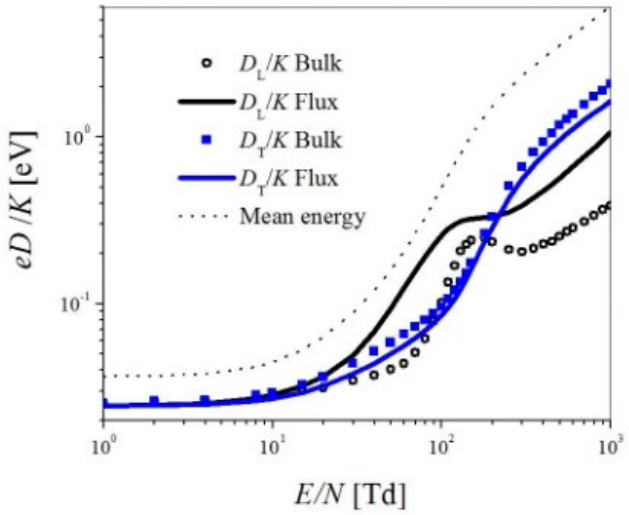
D_L/K Bulk
D_L/K Flux
D_T/K Bulk
D_T/K Flux
Mean energy
eD/K [eV]
10^0
10^{-1}
10^0
10^1
10^2
10^3
E/N [Td]

FIGURE 7

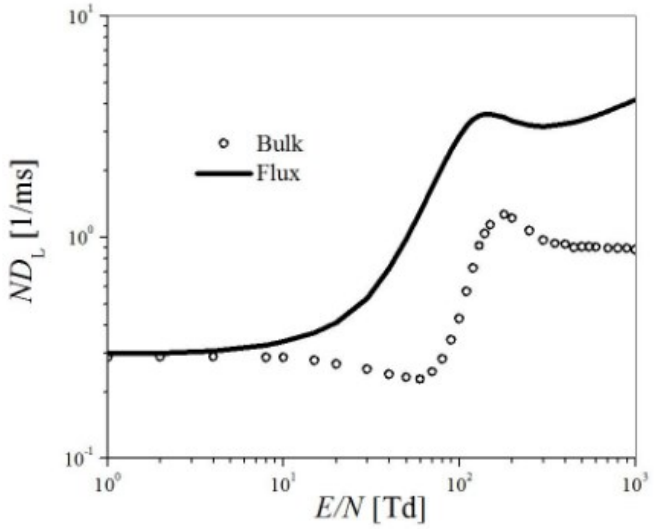

FIGURE 8

Садржај: Разумевање дистрибуције плазме, карактеристика и феномена је важно за развој и оптимизацију плазма опреме за производњу полупроводничких уређаја, као што су алати за гравирање и таложење. Из тог разлога, симулација плазме се тренутно користи у свакој фази дизајна, развоја и побољшања опреме. Утврђено је да су скупови попречних пресека добијени применом Denpoh-Nanbu теорије на Ar^+ код судара CF_4 у општем квалитативном и делимично квантитативном слагању са подацима из литературе. За прорачуне транспортних параметара примењена је Монте Карло техника. Израчунати попречни пресеци се могу користити за добијање коефицијената транспорта, посебно брзине дрифта, карактеристичне енергије, редуковане мобилности, лонгитудиналне дифузије и коефицијената брзине за ниска и умерено редукована електрична поља *E/N* (E-јачина електричног поља; N-густина гаса) и за израчунавање неконзервативних судара.

Кључне речи: *Монте Карло Симулације, Ar^+ јони, CF_4 гас.*

10. Рад M23, On Line

https://doi.org/10.2298/SOS220620021N

Submitted: 20.06.2022.
Accepted for publication: 22.08.2022.

UDK: 675.92.027; 519.872

CHARACTERISTIC ENERGY AND REDUCED MOBILITY FOR Ne^+ IONS IN CF_4 GAS

Željka Nikitović* and Zoran Raspopović

Institute of Physics, University of Belgrade, Pregrevica 118, Belgrade, Serbia
*corresponding author: zeljka@ipb.ac.rs

Abstract

A cross section set for scattering Ne^+ ions in CF_4 gas is assessed by using available experimental data for charge transfer cross sections. Calculated cross sections can be used to obtain transport parameters, specially characteristic energy and reduced mobilty for low and moderate reduced electric fields *E/N* (E-electric field strength; N-gas density) and accounting for the non-conservative collisions. These data are needed for modelling in numerous applications of technologically importance.

Keywords: *Monte Carlo Simulations, positive ions, CF_4 gas.*

1. Introduction

Ion charge transfer reactions with molecules are unavoidable elementary processes in modeling kinetics in terrestrial, industrial and astrophysical plasma in the detection of dark matter [1]. Motivational factors for this study have been identified and this paper reports on a topic important for both basic studies and application. Tetrafluoromethane or CF_4 molecule, which is widely used in the production of aluminum and the semiconductor industry, has an extremely long lifespan (~50,000 years) and the highest atmospheric content of all perfluorocarbons [2]. Therefore, it is very important to develop replacement materials or methods for efficient decomposition of CF_4 molecules in order to reduce man-made greenhouse gases (GHG).

In selected cases, it is known that charge transfer reactions represent the most significant part of the cross-sectional set. The linear spectra of the excited atoms obtained by spectrometric measurements in CF_4 indicate that the charge transfer reaction is the dominant process in collisions with inert gas ions. Cross-sectional data for CF_4 dissociative excitation [3] are essential to assess the degree of importance of many related processes. In this paper, we have estimated the set of cross sections for Ne^+ in CF_4 using existing experimental data [4] for charge transfer collisions producing CF_4 radical ions. Since no direct information has been found in the literature on how the mobility of high energy recombination ions moves, such as the behavior of Ne^+ ions in CF_4, we also calculated transport parameters using the Monte Carlo simulation technique [5]. Mechanical properties can also be modeled, i. e. modulus on the elastic properties was studied using multi-phase unit cell (MPUC) numerical model [6] and functional theory (DFT) calculations [7].

2. Calculation on the cross sections set

Cross-sections presented by Fisher et al. [4] were used to determine the elastic cross section of the torque transmission ("elastic" in Figure 1) under the assumption that the total

cross section of the torque transmission is known. At low energies, we assumed that σ_{mt} is the Langevin cross section, and the elastic cross section of the moment transmission is determined by the deduction of all reactive cross sections. The average polarizability of CF_4 is not well established [4] and may produce a discrepancy for the calculated ion mobility in CF_4 [8, 9] and thus affect the prediction of plasma parameters in modeling. We adopted value of 3.86 10^{-30} m^3 used by Stojanović et al. [8] who found excellent agreement between experimental and calculated mobility of CF_3^+ ions in CF_4. Extrapolation of the trend of the cross section of the transmission of elastic moment outside the point of intersection of the Langevin and the cross section of the hard sphere (HS) [1] is performed by smooth connection with the trend $1/v^3$ [10] where v is the velocity of the center of mass (see Figure 1).

At all kinetic energies of ions above 50 eV, the reactive cross sections are extrapolated to constant values. The effects of different extrapolations (short dot-dashed or dashed line in Figure 1) of unusual low energy behavior, observed by cross-sectional measurements leading to CF_2^+ formation (where exothermic reaction behavior is expected regardless of Ne^+ spin state) are considered negligible in terms of mobility.

Fig. 1

3. Results and discussion

The Monte Carlo technique was used to calculate the transport parameters. We used Monte Carlo code that correctly takes into account thermal collisions [11]. The code passed all relevant criteria [12] and was tested in our work on several types of charged particles [12, 13]. The results of Monte Carlo simulations are shown in Figures 2-5. Note that these transport parameters are the only information present in the literature so far, there are no published experimental data for Ne^+ transport coefficients in CF_4.

The flux and volume drift velocities [14] for Ne^+ in CF_4 gas as a function of *E/N* are given in Figure 2. The drift velocities obtained by the Monte Carlo simulation are

calculated in real space (bulk) and in velocity space (flux) values which are obtained as $\langle v \rangle$ and $d\langle x \rangle/dt$, respectively. As *E/N* increases, the high-energy ions from the distribution function increasingly have non-conservative collisions in which the Ne^+ ions disappear, shifting the center of mass of the swarm backward, resulting in a bulk velocity less than the flux.

Fig. 2

In Figure 3 we show the mean and characteristic energies (diffusion coefficient normalized to mobility eD/K in units of eV) based on transversal (D_T) diffusion coefficients. The mean energy, which cannot be directly measured in experiments but a map of mean energy versus *E/N* may be used directly to provide the data in fluid models especially when local field approximation fails. The difference between bulk and flux values of characteristic energy is smaller.

Fig. 3

Reduced mobility for Ne^+ ions as a function of *E/N* (*E*-electric field strength, *N*-gas density) compared with Langevin's value is shown in Figure 4. Generally, the presence of non-conservative collisions causes the drift velocity to be more complex i.e. one may define bulk drift velocity as a measure of center of mass displacement in time ($W=d\langle x \rangle/dt$) [15] and flux drift velocity $w=\langle v \rangle$ that describes ion flux. Bulk drift velocity is reaction corrected flux drift velocity: $w = W + S$, where *S* is the term representing a measure of the effect of reactions on the drift velocity.

For $E/N < 50$ Td, exothermic collision frequency is approximately corresponding to the energies below 0.1 eV. This causes the equality of the bulk and flux reduced mobilities [17-20] since the ions from the front and the tail are removed with equal rate [16]. For higher *E/N* the bulk reduced mobility is decreasing with *E/N* because of an increasing number of ions

removed from the regions of higher energy (from swarm front). That results in a shift in the centre-of-mass position. At the same time, flux reduced mobilities increase with *E/N* since number of elastic collisions decrease.

Due to exotermal collisions mobility is 10% higher than the polarisation limit predicted by Langevin's theory.

Fig. 4

In Figure 5 we show rate coefficients for reactions of Ne^+ ions with CF_4 gas at *T*=300K. Rate coefficients are important for applications of the global model to CF_4 gas. The products a) CF_3^+, CF_2^+ and CF^+ ions b) momentum transfer and all reactions are also presented in Figure 5.

Fig. 5a)

Fig. 5b)

4. Conclusions

Using the measured cross-sections of charge transfer, we estimated the complete set of cross-sections for Ne^+ ions in CF_4 used as input to Monte Carlo simulations in order to calculate the transport parameters. Focusing on the calculated data on characteristic energy and reduced mobility as a function of *E/N*, in this paper we found that it is necessary to discuss both data on reduced mobility and flux. Data on swarm coefficients for positive and negative ions [21] are required for hybrid and fluid codes and the current focus on liquids or liquids in rare gas mixtures dictates the need to produce data compatible with these models.

ACKNOWLEDGMENTS

The authors acknowledge funding provided by the Institute of Physics University Belgrade, through the grant by the Ministry of Education, Science and Technological Development of the Republic of Serbia.

5. References

[1] A. Kabothc, J. Monroec, S. Ahlena, D. Dujmic, S. Hendersonc, G. Kohsec, R. Lanzac, M. Lewandowskaa, A. Roccaroa, G. Sciollac, N. Skvorodnevb, H. Tomitaa, R. Vanderspekc, H. Wellensteinb, R. Yamamotoc, P. Fisher, Nuclear Instruments and Methods in Physics Research **A 592** (2008) 63 – 72.

[2] M. Aslam, K. Khalil, R. A. Rasmussen, J. A. Culbertson, J. M. Prins, E. P. Grimsrud and M. J. Shearer, Environ. Sci. Tecnol. **37** (2003) 4358 -4361.

[3] K. Motohashi, T. Takahashi, N. Takahashi S. Tsurubuchi, J. Phys. B: At. Mol. Opt. Phys. **38** (2005) 3339-3348.

[4] E. R. Fisher, M. E. Weber and P. B. Armentrout, J. Chem. Phys. **92 (4)** (1990) 2296-2302.

[5] Z. Lj. Petrović, S. Dujko, D. Marić, G. Malović, Ž. Nikitović, O. Šašić, J. Jovanović, V. Stojanović and M. Radmilović-Radjenović, J. Phys. D: Appl. Phys. **42** (2009) 194002.

[6]A. T. Saleem,V. Petrović, A. Grbović, J. Lozanović Šajić, I. Balać, Sci Sinter **53** (2021) 127-136.

[7]V. Ribić, A.Rečnik, G.Dražić, M.Podlogar, Z. Branković, G. Branković, Sci Sinter **53** (2021) 237-252.

[8] V. Stojanović, Z. Raspopović, J. V. Jovanović, J. de Urquijo and Z. Lj. Petrović, J. Phys.: Conf. Series **514** (2014) 012059.

[9] V. Georgieva, A. Bogaerts and R. Gijbels, J. Appl. Phys. **93 (5)** (2003) 2369-2379.

[10] P. S. Krstić and D. R. Schultz, J. Phys. B: At. Mol. Opt. Phys. **42** (2009) 065207.

[11] Z. Ristivojević and Z. Lj. Petrović, Plasma Sources Sci. Technol. **21,** 035001(2012).

[12] Z. Lj. Petrović, Z. M. Raspopović, V. D. Stojanović, J. V. Jovanović, G. Malović, T. Makabe, J. De Urquijo, Appl. Surf. Sci. **253** (2007) 6619.

[13] J. de Urquijo, J. V. Jovanović, A. Bekstein, V. Stojanović and Z. Lj. Petrović, Plasma Sources Sci. Technol. **22** (2013) 025004.

[14] R. E. Robson, R. D. White, Z. Lj. Petrovic, Rev. Mod. Phys. **77** (2005) 1303-20; A. M. Nolan, M. J. Brennan, K. F. Ness and A. B. Wedding, J. Phys. **D**: Appl. Phys., **30** (1997) 2865-71.

[15] K. F. Ness and R. E. Robson, Phys. Rev. **A 34 (**1986) 2185-2209.

[16] R. E. Robson, Aust. J. Phys. **44** (1991) 685-692.

[17] Ž. Nikitović, Z. Raspopović, V. Stojanović and J. Jovanović, Europhys. Lett. **108** (2014) 35004.

[18] Ž. Nikitović, V. Stojanović, Z. Raspopović and J. Jovanović, Acta Physica Polonica A **126** (2014) 724-726.

[19] Ž. Nikitović, Z. Raspopović and V. Stojanović, EPL **128** (2019) 15001.

[20] Ž. Nikitović and Z. Raspopović, Sci Sinter **54** (2022) 169-176.

[21] R. D. White, W. Tattersall, G. Boyle, R. E. Robson, S. Dujko, Z. Lj. Petrović, A. Banković, M. J. Brunger, J. P. Sullivan, S. J. Buckman and G. Garcia, Applied Radiation and Isotopes **83** (2014) 77-85.

Figure captions:

Fig.1. Cross sections for Ne^+ ions in CF_4 gas.

Fig.2. Bulk and flux velocity as a function *E/N* for Ne^+ ions in CF_4 gas.

Fig. 3. Mean and characteristic energy as a function *E/N* for Ne^+ ions in CF_4 gas.

Fig. 4. Reduced mobility as a function *E/N* for Ne^+ ions in CF_4 gas.

Fig. 5. Rate coefficients of a) CF_3^+, CF_2^+ and CF^+ ions b) momentum transfer and all reactions as a function *E/N* for Ne^+ ions in CF_4 gas.

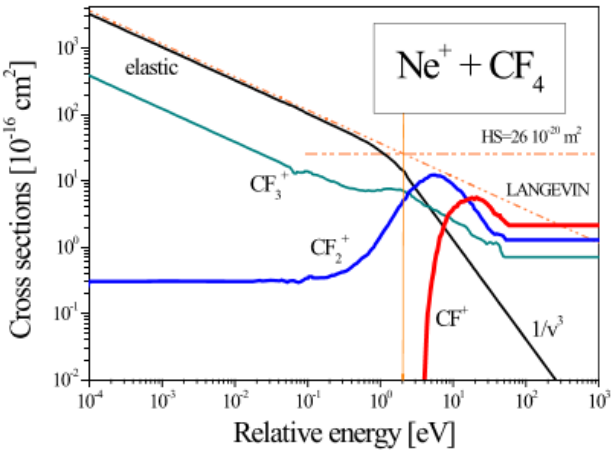

FIGURE 1

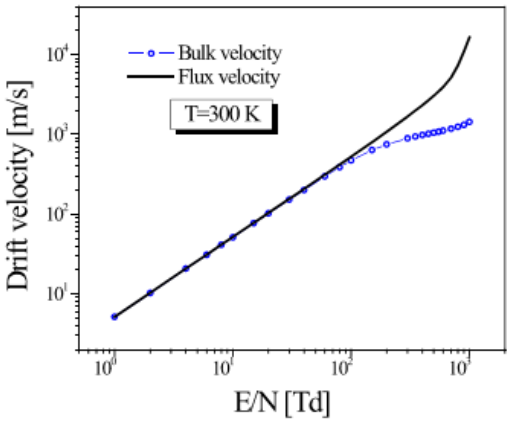

FIGURE 2

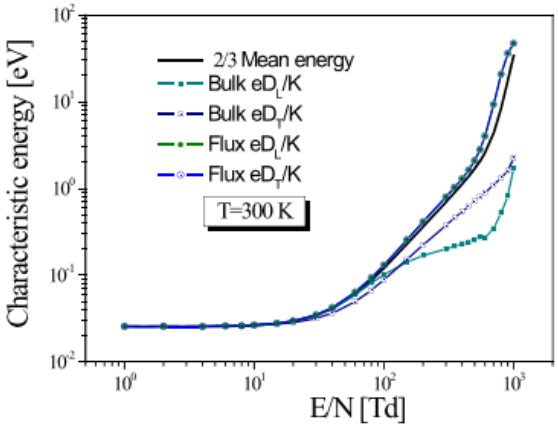
Characteristic energy [eV]
E/N [Td]
2/3 Mean energy
Bulk eD_L/K
Bulk eD_T/K
Flux eD_L/K
Flux eD_T/K
T=300 K

FIGURE 3

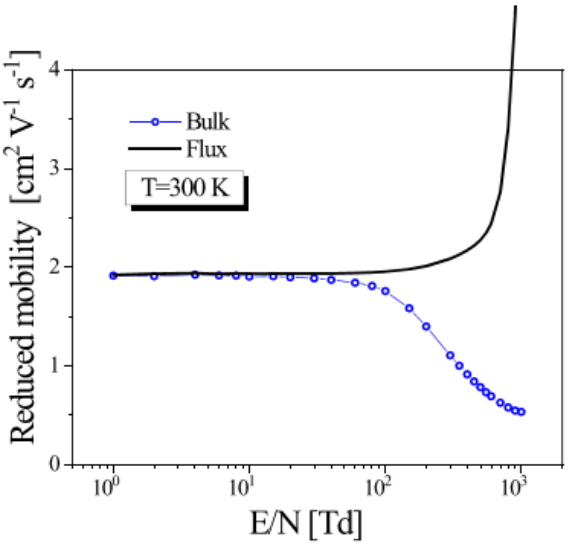
Reduced mobility [cm^2 V^{-1} s^{-1}]
E/N [Td]
Bulk
Flux
T=300 K
0
1
2
3
4
10^0
10^1
10^2
10^3

FIGURE 4

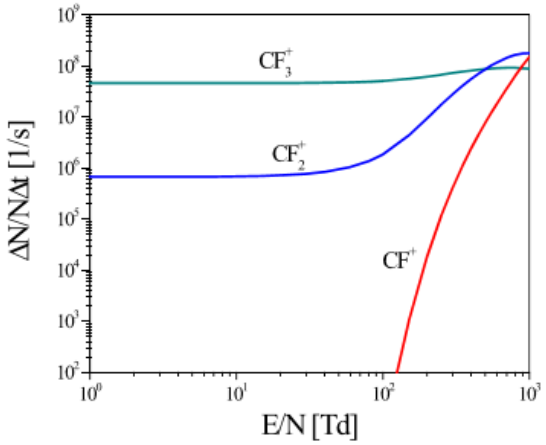
CF_3^+
CF_2^+
CF^+
ΔN/NΔt [1/s]
E/N [Td]

a)

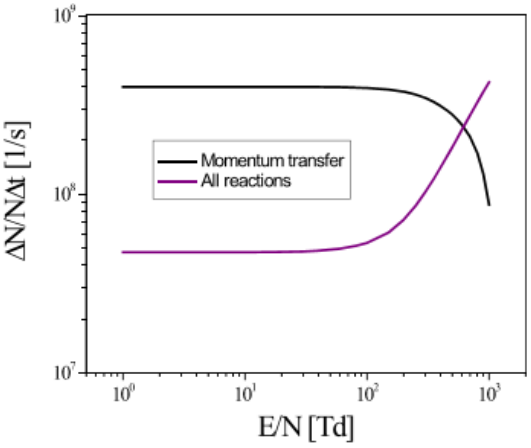
Momentum transfer
All reactions
ΔN/NΔt [1/s]
E/N [Td]

b)

FIGURE 5

Садржај: *У овом раду предлажемо сет пресека за јоне* Ne^+ *у гасу* CF_4 *на ниским енергијама и њима придружене транспортне параметре. Израчунати попречни пресеци су коришћени за добијање података специјално за карактеристичну енергију и редуковану мобилност у функцији E/N (E – јачина електричног поља; N– густина гаса) за јоне* Ne^+ *у гасу* CF_4*. Ови подаци су потребни за моделовање у бројним технолошки важним применама.*

Кључне речи: *Монте Карло Симулације, позитивни јони,* CF_4 *гас.*

11. Рад M32

http://www.serbianceramicsociety.rs/doc/aca01-10/aca10/ACA-X-Programme-and-Book-of-Abstracts.pdf

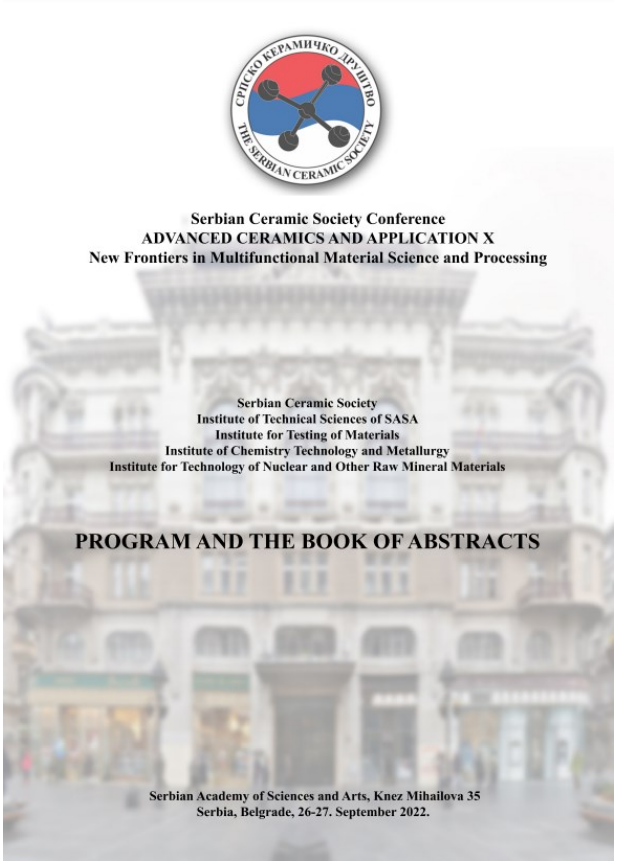

Serbian Ceramic Society Conference
ADVANCED CERAMICS AND APPLICATION X
New Frontiers in Multifunctional Material Science and Processing

Serbian Ceramic Society
Institute of Technical Sciences of SASA
Institute for Testing of Materials
Institute of Chemistry Technology and Metallurgy
Institute for Technology of Nuclear and Other Raw Mineral Materials

PROGRAM AND THE BOOK OF ABSTRACTS

Serbian Academy of Sciences and Arts, Knez Mihailova 35
Serbia, Belgrade, 26-27. September 2022.

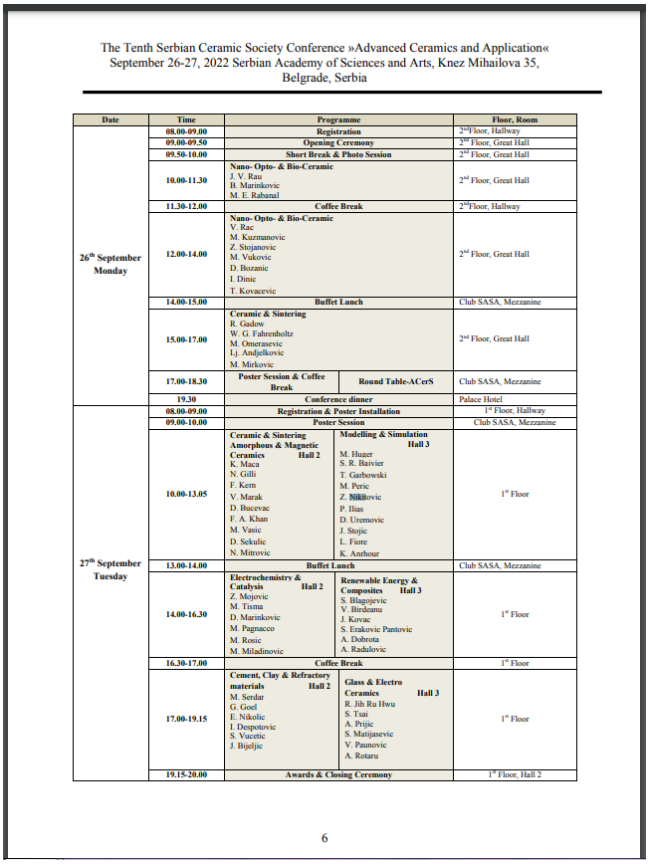

The Tenth Serbian Ceramic Society Conference »Advanced Ceramics and Application«
September 26-27, 2022 Serbian Academy of Sciences and Arts, Knez Mihailova 35,
Belgrade, Serbia

Date	Time	Programme		Floor, Room
26th September Monday	08.00-09.00	Registration		2nd Floor, Hallway
	09.00-09.50	Opening Ceremony		2nd Floor, Great Hall
	09.50-10.00	Short Break & Photo Session		2nd Floor, Great Hall
	10.00-11.30	Nano- Opto- & Bio-Ceramic J. V. Rau B. Marinkovic M. E. Rabanal		2nd Floor, Great Hall
	11.30-12.00	Coffee Break		2nd Floor, Hallway
	12.00-14.00	Nano- Opto- & Bio-Ceramic V. Rac M. Kuzmanovic Z. Stojanovic M. Vukovic D. Bozanic I. Dinic T. Kovacevic		2nd Floor, Great Hall
	14.00-15.00	Buffet Lunch		Club SASA, Mezzanine
	15.00-17.00	Ceramic & Sintering R. Gadow W. G. Fahrenholtz M. Omerasevic Lj. Andjelkovic M. Mirkovic		2nd Floor, Great Hall
	17.00-18.30	Poster Session & Coffee Break	Round Table-ACerS	Club SASA, Mezzanine
	19.30	Conference dinner		Palace Hotel
27th September Tuesday	08.00-09.00	Registration & Poster Installation		1st Floor, Hallway
	09.00-10.00	Poster Session		Club SASA, Mezzanine
	10.00-13.05	Ceramic & Sintering Amorphous & Magnetic Ceramics Hall 2 K. Maca N. Gilli F. Kern V. Marak D. Bucevac F. A. Khan M. Vasic D. Sekulic N. Mitrovic	Modelling & Simulation Hall 3 M. Huger S. R. Baivier T. Garbowski M. Peric Z. Nikitovic P. Ilias D. Uremovic J. Stojic L. Fiore K. Anthour	1st Floor
	13.00-14.00	Buffet Lunch		Club SASA, Mezzanine
	14.00-16.30	Electrochemistry & Catalysis Hall 2 Z. Mojovic M. Tisma D. Marinkovic M. Pagnacco M. Rosic M. Miladinovic	Renewable Energy & Composites Hall 3 S. Blagojevic V. Birdeanu J. Kovac S. Erakovic Pantovic A. Dobrota A. Radulovic	1st Floor
	16.30-17.00	Coffee Break		1st Floor
	17.00-19.15	Cement, Clay & Refractory materials Hall 2 M. Serdar G. Goel E. Nikolic I. Despotovic S. Vucetic J. Bijeljic	Glass & Electro Ceramics Hall 3 R. Jih Ru Hwu S. Tsai A. Prijic S. Matijasevic V. Paunovic A. Rotaru	1st Floor
	19.15-20.00	Awards & Closing Ceremony		1st Floor, Hall 2

6

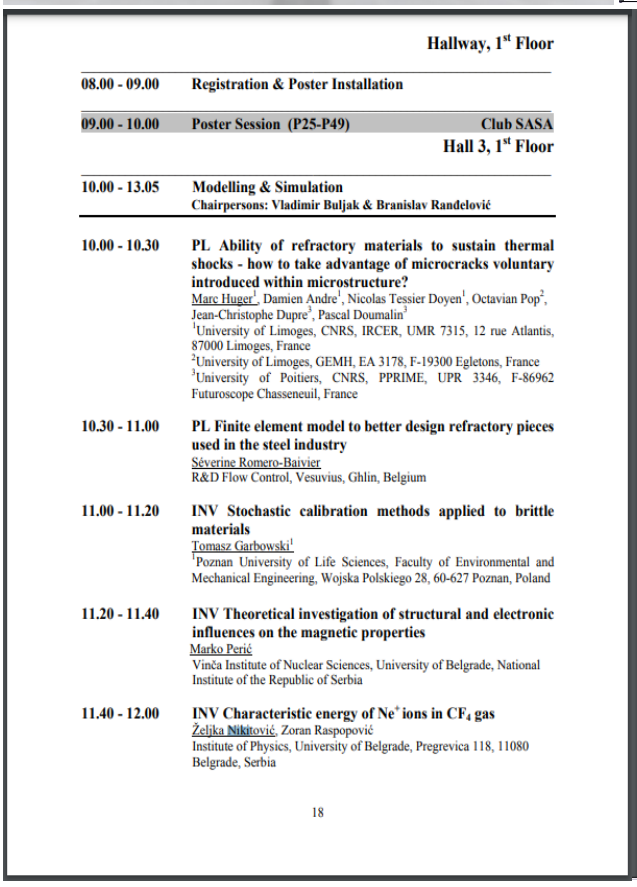

Hallway, 1st Floor

08.00 - 09.00 **Registration & Poster Installation**

09.00 - 10.00 **Poster Session (P25-P49)** **Club SASA**

Hall 3, 1st Floor

10.00 - 13.05 **Modelling & Simulation**
Chairpersons: Vladimir Buljak & Branislav Randelović

10.00 - 10.30 **PL Ability of refractory materials to sustain thermal shocks - how to take advantage of microcracks voluntary introduced within microstructure?**
Marc Huger[1], Damien Andre[1], Nicolas Tessier Doyen[1], Octavian Pop[2], Jean-Christophe Dupre[3], Pascal Doumalin[3]
[1]University of Limoges, CNRS, IRCER, UMR 7315, 12 rue Atlantis, 87000 Limoges, France
[2]University of Limoges, GEMH, EA 3178, F-19300 Egletons, France
[3]University of Poitiers, CNRS, PPRIME, UPR 3346, F-86962 Futuroscope Chasseneuil, France

10.30 - 11.00 **PL Finite element model to better design refractory pieces used in the steel industry**
Séverine Romero-Baivier
R&D Flow Control, Vesuvius, Ghlin, Belgium

11.00 - 11.20 **INV Stochastic calibration methods applied to brittle materials**
Tomasz Garbowski[1]
[1]Poznan University of Life Sciences, Faculty of Environmental and Mechanical Engineering, Wojska Polskiego 28, 60-627 Poznan, Poland

11.20 - 11.40 **INV Theoretical investigation of structural and electronic influences on the magnetic properties**
Marko Perić
Vinča Institute of Nuclear Sciences, University of Belgrade, National Institute of the Republic of Serbia

11.40 - 12.00 **INV Characteristic energy of Ne^+ ions in CF_4 gas**
Željka Nikitović, Zoran Raspopović
Institute of Physics, University of Belgrade, Pregrevica 118, 11080 Belgrade, Serbia

18

The Tenth Serbian Ceramic Society Conference »Advanced Ceramics and Application«
September 26-27, 2022 Serbian Academy of Sciences and Arts, Knez Mihailova 35,
Belgrade, Serbia

INV8
The ashes obtained from the combustion of agro-industrial waste as catalysts for biodiesel production

Marija Miladinović

University of Niš, Faculty of Agriculture, Kosančićeva 4, Kruševac, Srbija

The growing trend of biomass utilization for energy production generates a large amount of ash that needs to be managed in a way to reduce its disposal at landfills. Finding a new way of biomass ash utilization in addition to its applications as building materials or fertilizer would be a step forward. The ashes obtained by the combustion of agro-industrial solid waste have stood out as an alternative to conventional catalysts for biodiesel production due to their favorable elemental composition. Replacing the pure chemical compounds used as conventional catalysts with ashes could reduce biodiesel production costs and contribute to sustainability. The studies on several ashes produced by the combustion of walnut and hazelnut shells, and plum and cherry stones aimed to provide information on their characteristics and catalytic properties. The results revealed the similarity and difference in the elemental and phase composition, morphology, and textural parameters. The dominant elements such as potassium and calcium had a significant effect on the catalytic performance of ashes. Considering that ash-based catalysts can be recovered and reused, there is great potential for their application in the catalytic process of biodiesel production.

INV9
Characteristic energy of Ne^+ ions in CF_4 gas

Željka Nikitović, Zoran Raspopović

Institute of Physics, University of Belgrade, Pregrevica 118, 11080 Belgrade, Serbia

Charge transfer reactions of ions with molecules are unavoidable elementary processes in modeling kinetics in terrestrial, industrial and astrophysical plasmas in dark matter detection. Motivational factors for this study are identified and this paper reports on a topic important both for fundamental studies and for applications. A cross section set for scattering Ne^+ ions in CF_4 gas is assessed by using available experimental data for charge transfer cross sections. The Monte Carlo technique was applied to perform calculations of transport parameters. Calculated cross sections can be used to obtain transport coefficients, specially characteristic energy and rate coefficients for low and moderate reduced electric fields *E/N* (E-electric field strength; N-gas density) and accounting for the non-conservative collisions.

41

12.Рад M33

http://spig2018.ipb.ac.rs/SPIG2018-book-online.pdf

29th Summer School and International Symposium on the Physics of Ionized Gases
29. Летња школа и међународни симпозијум физике јонизованих гасова (SPIG 2018)

Belgrade, Serbia (28.08. - 1.09. 2018.)
Београд, Србија (28.08. - 1.09. 2018.)

Programme SPIG 2018
Програм SPIG 2018

ORGANIZERS
ОРГАНИЗАТОРИ

Serbian Academy of Sciences and Arts

Vinča Institute of Nuclear Sciences

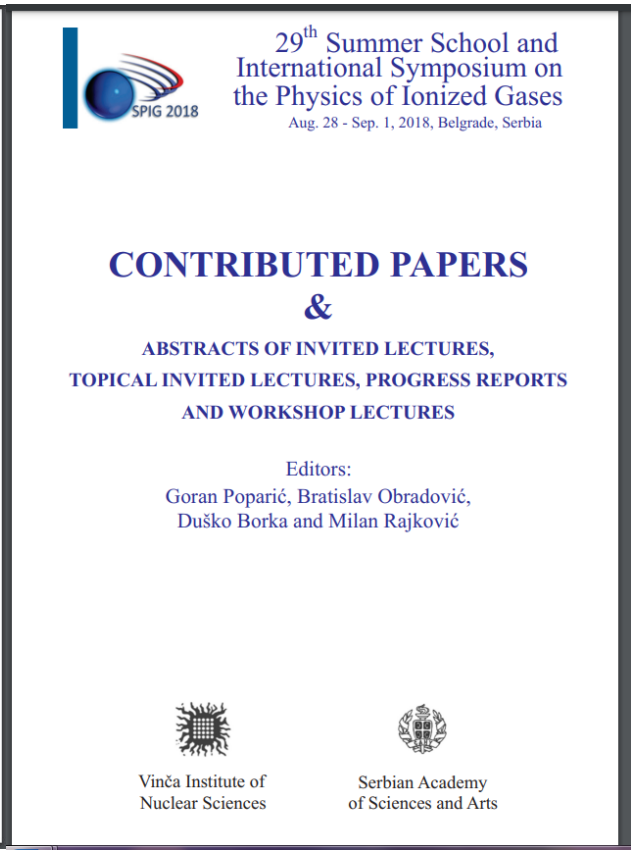

29th Summer School and International Symposium on the Physics of Ionized Gases
Aug. 28 - Sep. 1, 2018, Belgrade, Serbia

CONTRIBUTED PAPERS
&
ABSTRACTS OF INVITED LECTURES,
TOPICAL INVITED LECTURES, PROGRESS REPORTS
AND WORKSHOP LECTURES

Editors:
Goran Poparić, Bratislav Obradović,
Duško Borka and Milan Rajković

Vinča Institute of Nuclear Sciences

Serbian Academy of Sciences and Arts

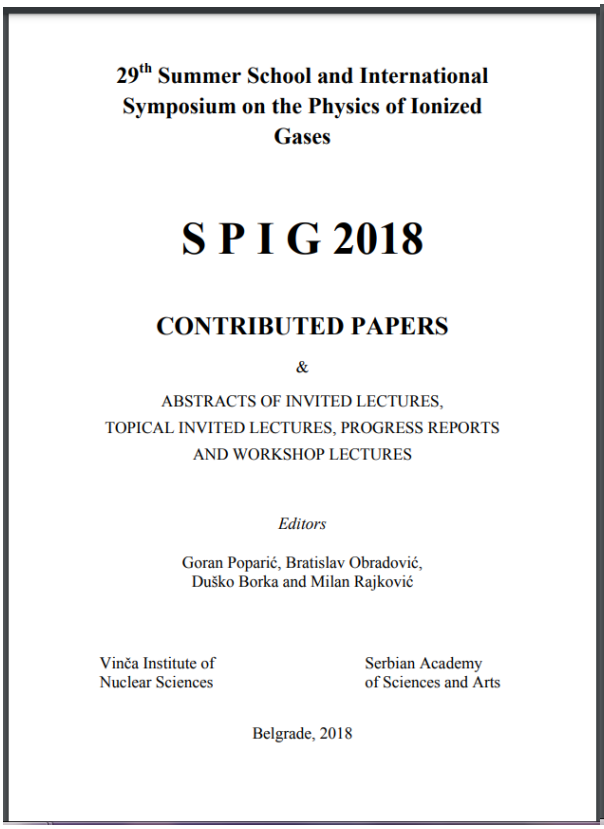

29th Summer School and International Symposium on the Physics of Ionized Gases

S P I G 2018

CONTRIBUTED PAPERS
&
ABSTRACTS OF INVITED LECTURES,
TOPICAL INVITED LECTURES, PROGRESS REPORTS
AND WORKSHOP LECTURES

Editors

Goran Poparić, Bratislav Obradović,
Duško Borka and Milan Rajković

Vinča Institute of Nuclear Sciences

Serbian Academy of Sciences and Arts

Belgrade, 2018

TRANSPORT COEFFICIENTS FOR Li^+ IN DIMETHOXYETHANE

Ž. Nikitović[1], M. Gilić[1], Z. Raspopović[1], M. Ćurčić[1] and V. Stojanović[1]

[1] *Institute of Physics, University of Belgrade, Pregrevica 118, 11080 Belgrade, Serbia*

Abstract. In this paper we present most probable reactions of alkali metal ion Li^+ with dimethoxyethane (DXE) molecule. Appropriate gas phase enthalpies of formation for the products were used to calculate scattering cross section as a function of kinetic energy. These data are needed for modeling in numerous applications of technologically important DXE discharges. Results for transport coefficients as a function of E/N (E -electric field; N-gas density) were obtained by using the Monte Carlo technique.

1. INTRODUCTION

Cold plasmas are often used in new technologies where they offer methods for nonintrusive production or modification of specific substances. Main characteristics of these plasmas are their high electron temperature and low gas temperature. Dimethoxy-containing compounds, such as dimethoxy ethane (DXE), can be produced from dimethyl ether by using dielectric barrier discharge (DBD) plasmas containing water vapor at atmospheric pressure [1]. As clear and colorless liquid at room temperature and atmospheric pressure, DXE is used as a precursor in production of ceramics or as a sole compound to make other chemicals such as those used in lithium batteries production, superconductor production and nanoparticles synthesis.

In this paper we firstly selected the most probable reactions of alkali metal ion Li^+ with DXE molecule (and its most probable products) for thermodynamic threshold energies below about 15 eV. Appropriate gas phase enthalpies of formation [2] for the products were used to calculate thermodynamic thresholds.

2. CROSS SECTION SETS

The scattering cross section of alkali ion Li^+ on DXE are calculated by using the Denpoh-Nanbu (DN) theory [3] separating elastic from reactive

collisions. DXE is known not to have dipole moment in its ground state. The dipole polarizability of 9.94×10^{-30} m^3 [4] is used for the DXE target. Similar to our recent papers [5] DN method is used to separate elastic from reactive endothermic collisions by accounting the thermodynamic threshold energy and branching ratio according to the Rice-Rampsperger-Kassel (RRK) theory [3]. Within the RRK theory the internal energy is being distributed among an empirical number of ***s*** equivalent effective modes of the complex selected from the total number of atoms involved in the complex.

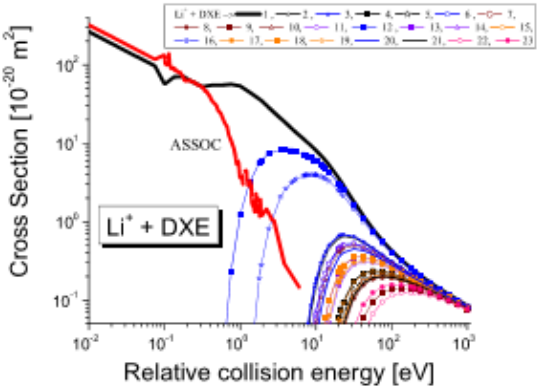

Figure 1. Cross section sets for Li^+in DXE.

Elastic momentum transfer cross section is modified in order to fit approximate mobility peak characteristic for presented systems. Swarm method [5, 6] is exploited to modify the cross section for elastic momentum transfer where for reduced mobility in the peak region (experimental [7] or theoretical values [8]) similarity with ions of equal or similar reduced mass is targeted. Appropriate gas phase enthalpies of formation for the products were used to calculate thermodynamic thresholds [9]. Elastic momentum transfer cross section for elastic collisions of Li^+ with DXE is presented in Figure 1.

3. DISCUSSION AND RESULTS

Swarm parameters as a function of reduced electric field *E/N* in DC electric fields are generally applied to plasma modeling and simulations.

We have used a Monte Carlo code that properly takes into account thermal collisions [10]. The code has passed all the relevant benchmarks and has been tested in our work on several types of charged particles.

Flux and bulk drift velocities for Li^+ in DXE as a function of *E/N* are given in Fig.2. The drift velocities obtained by Monte Carlo simulation

calculated in real space (bulk) and in velocity space (flux) values which are obtained as $\langle v \rangle$ and dx/dt, respectively. The mass of Li^+ is smaller than the mass of K^+, so as a consequence the drift velocity of Li^+ is bigger [9].

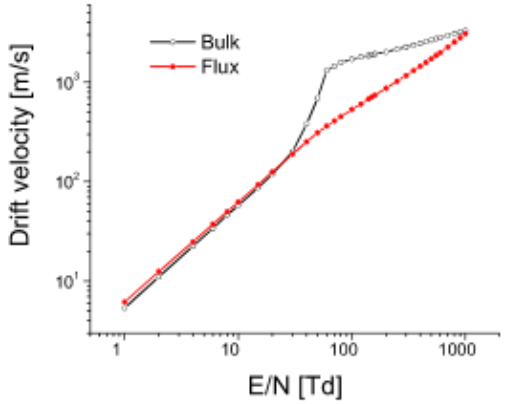

Figure 2. Drift velocity of Li^+ ions in DXE gas as a function of E/N at T = 300 K.

In Figure 3. we show the results of Monte Carlo simulation for reduced mobility as a function of E/N. Due to reactive collisions bulk and flux values of reduced mobility are separated.

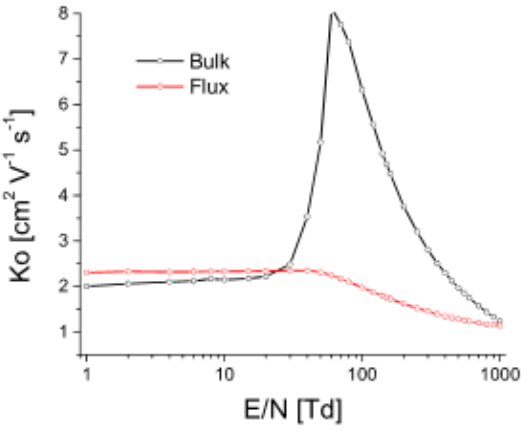

Figure 3. Reduced mobility of Li^+ ions in DXE as a function of E/N at T=300 K.

The mobility K of an ion is the quantity defined as the velocity attained by an ion moving through a gas under the unit electric field. One often exploits the reduced or standard mobility defined as:

$$K_0 = \frac{v_d}{N_0 E} N, \qquad (1)$$

where v_d is the drift velocity of the ion, N is the gas density at elevated temperature T and E is the electric field.

4. CONCLUSION

Calculated cross sections are used to obtain transport coefficients for alkali metal ion Li^+ in DXE gas.

The cross sections and transport data for technologically very important gas DXE have been determined by using simple theory. Peak for flux reduced mobility values is shifted in energy and intensity with respect to peak for bulk values. While it is a good basis for modeling it would be much better to add a data base of measured transport coefficients and then to perform the analysis again.

Acknowledgements

Results obtained in the Institute of Physics University of Belgrade under the auspices of the Ministry of Education, Science and Technology, Projects No. 171037 and 410011.

REFERENCES

[1] Y. Wang, C. Liu, Y. Zhang, Plasma Sci. & Technology 7, No. 3, 2839 (2005).
[2] S. G. Lias, J. E. Bartmess, J. F. Xebman and J. L. Holmes, R. D. Levin and W. G. Mallard, J. Phys. Chem. Ref. Data, Supl. 1 Vol. 17, 1 (1988).
[3] K. Denpoh and K. Nanbu, J. Vac. Sci. Technol. A 16 (3), 1201 (1998).
[4] H. Koizumi, P. B. Armentrout, J. Chem. Phys. 119, 12819 (2003).
[5] V. Stojanović, Z. Raspopović, J. Jovanović, Ž. Nikitović and Z. Lj. Petrović, EPL 101, 45003 (2013).
[6] Ž. Nikitović, Z. Raspopović, V. Stojanović and J. Jovanović, EPL 108, 35004 (2014).
[7] L. A. Viehland and E. A. Mason, At. Data. Nucl. Data Tables 60, 37 (1995).
[8] http://nl.lxcat.net/data/set type.php.
[9] Ž. Nikitović, M. Gilić, Z. Raspopović and V. Stojanović, EPL 116, 15002 (2016).
[10] Z. Ristivojević and Z. Lj. Petrović, Plasma Sources Sci. Technol. 21, 035001 (2012).

13. Рад M33

http://spig2020.ipb.ac.rs/Spig2020-Book-Onine.pdf

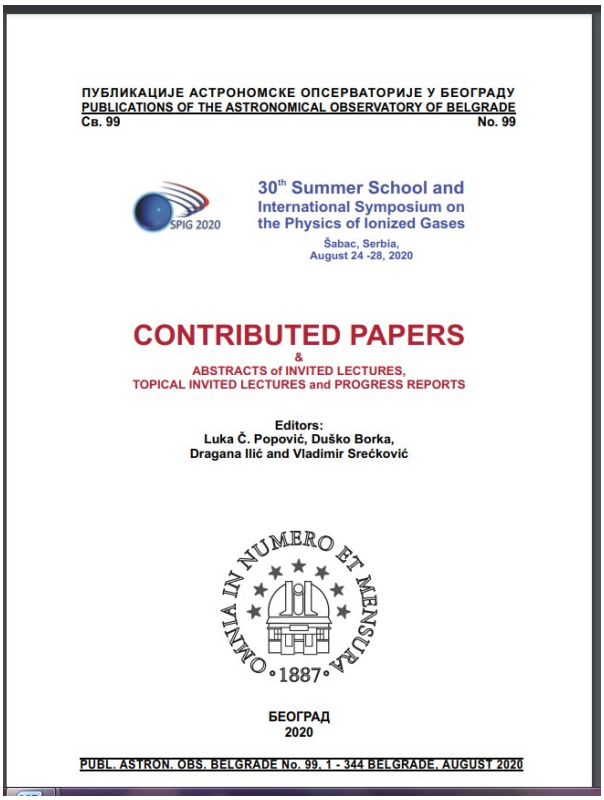

ПУБЛИКАЦИЈЕ АСТРОНОМСКЕ ОПСЕРВАТОРИЈЕ У БЕОГРАДУ
PUBLICATIONS OF THE ASTRONOMICAL OBSERVATORY OF BELGRADE
Св. 99 No. 99

30th Summer School and International Symposium on the Physics of Ionized Gases
Šabac, Serbia, August 24 -28, 2020

CONTRIBUTED PAPERS
&
ABSTRACTS of INVITED LECTURES, TOPICAL INVITED LECTURES and PROGRESS REPORTS

Editors:
Luka Č. Popović, Duško Borka, Dragana Ilić and Vladimir Srećković

БЕОГРАД
2020

PUBL. ASTRON. OBS. BELGRADE No. 99, 1 - 344 BELGRADE, AUGUST 2020

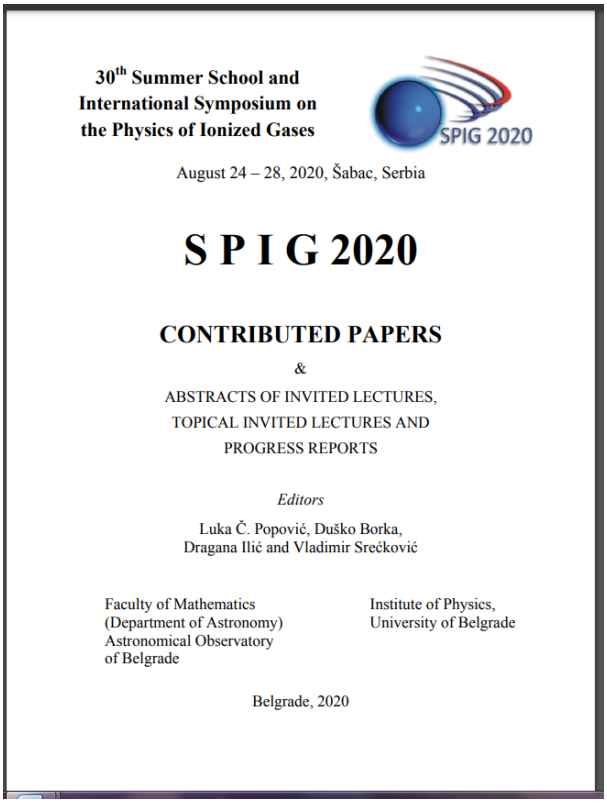

30th Summer School and International Symposium on the Physics of Ionized Gases

August 24 – 28, 2020, Šabac, Serbia

S P I G 2020

CONTRIBUTED PAPERS

&

ABSTRACTS OF INVITED LECTURES,
TOPICAL INVITED LECTURES AND
PROGRESS REPORTS

Editors

Luka Č. Popović, Duško Borka,
Dragana Ilić and Vladimir Srećković

Faculty of Mathematics
(Department of Astronomy)
Astronomical Observatory
of Belgrade

Institute of Physics,
University of Belgrade

Belgrade, 2020

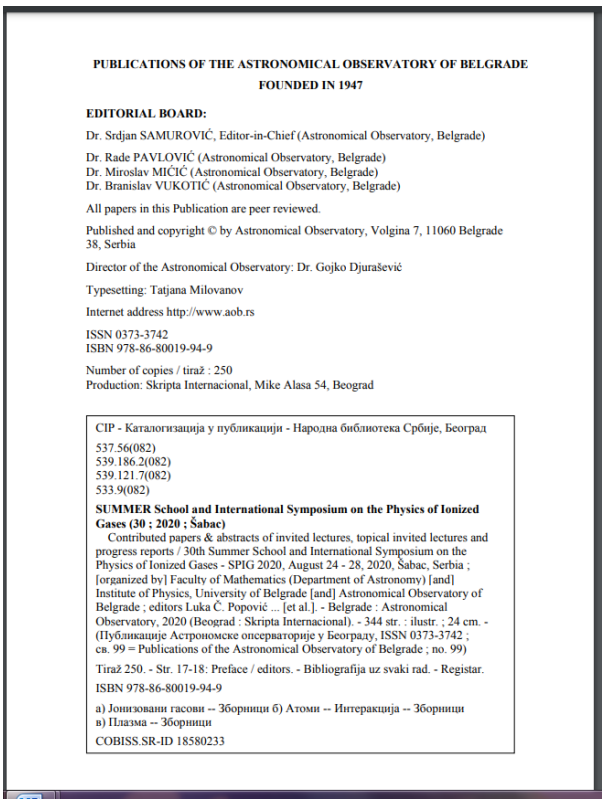

PUBLICATIONS OF THE ASTRONOMICAL OBSERVATORY OF BELGRADE
FOUNDED IN 1947

EDITORIAL BOARD:

Dr. Srdjan SAMUROVIĆ, Editor-in-Chief (Astronomical Observatory, Belgrade)

Dr. Rade PAVLOVIĆ (Astronomical Observatory, Belgrade)
Dr. Miroslav MIĆIĆ (Astronomical Observatory, Belgrade)
Dr. Branislav VUKOTIĆ (Astronomical Observatory, Belgrade)

All papers in this Publication are peer reviewed.

Director of the Astronomical Observatory: Dr. Gojko Djurašević

Typesetting: Tatjana Milovanov

Internet address http://www.aob.rs

ISSN 0373-3742
ISBN 978-86-80019-94-9

Number of copies / tiraž : 250
Production: Skripta Internacional, Mike Alasa 54, Beograd

CIP - Каталогизација у публикацији - Народна библиотека Србије, Београд

537.56(082)
539.186.2(082)
539.121.7(082)
533.9(082)

SUMMER School and International Symposium on the Physics of Ionized Gases (30 ; 2020 ; Šabac)
Contributed papers & abstracts of invited lectures, topical invited lectures and progress reports / 30th Summer School and International Symposium on the Physics of Ionized Gases - SPIG 2020, August 24 - 28, 2020, Šabac, Serbia ; [organized by] Faculty of Mathematics (Department of Astronomy) [and] Institute of Physics, University of Belgrade [and] Astronomical Observatory of Belgrade ; editors Luka Č. Popović ... [et al.]. - Belgrade : Astronomical Observatory, 2020 (Beograd : Skripta Internacional). - 344 str. : ilustr. ; 24 cm. - (Публикације Астрономске опсерваторије у Београду, ISSN 0373-3742 ; св. 99 = Publications of the Astronomical Observatory of Belgrade ; no. 99)

Tiraž 250. - Str. 17-18: Preface / editors. - Bibliografija uz svaki rad. - Registar.

ISBN 978-86-80019-94-9

а) Јонизовани гасови -- Зборници б) Атоми -- Интеракција -- Зборници в) Плазма -- Зборници

COBISS.SR-ID 18580233

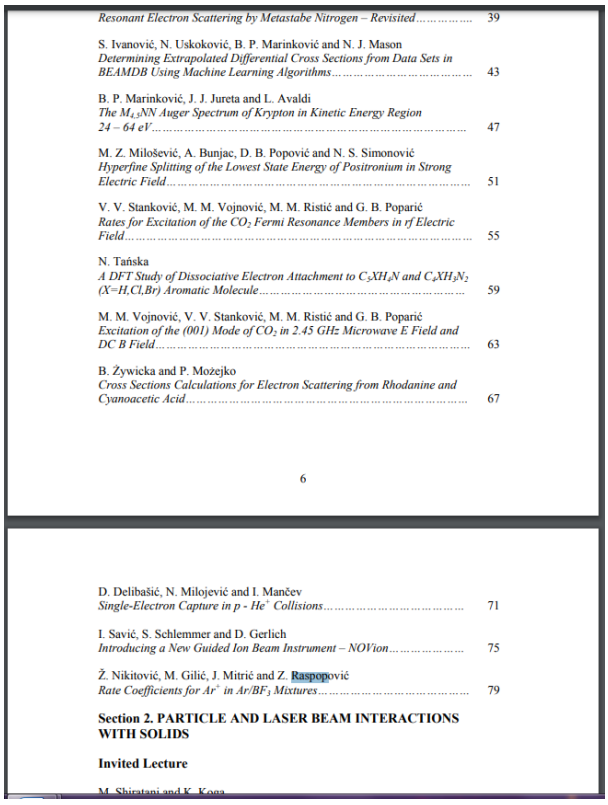

Publ. Astron. Obs. Belgrade No. 99 (2020), 79 – 82 *Contributed Paper*

RATE COEFFICIENTS FOR Ar^+ IN Ar/BF_3 MIXTURES

Ž. NIKITOVIĆ[1], M. GILIĆ[2], J. MITRIĆ[3] and Z. RASPOPOVIĆ[4]

[1,2,3,4]*Institute of Physics, University of Belgrade, Pregrevica 118, 11080 Belgrade, Serbia*

[1]*zeljka@ipb.ac.rs*
[2]*martina@ipb.ac.rs*
[3]*jmitric@ipb.ac.rs*
[4]*zr@ipb.ac.rs*

Abstract. In this paper we present most probable reactions of Ar^+ ion with Ar/BF_3mixtures. Appropriate gas phase enthalpies of formation for the products were used to calculate scattering cross section as a function of kinetic energy. These data are needed for modeling in numerous applications of technologically important BF_3discharges. Results for transport coefficients as a function of *E/N* (*E* -electric field; *N*-gas density), specially rate coefficients were obtained by using the Monte Carlo technique.

1. INTRODUCTION

Cold plasmas are frequently used in new technologies where they open up the possibilities of non-intrusive production or modification of various substances (Makabe et al. 2006.). These plasmas have a high electron temperature and low gas temperature so non-equilibrium behavior of a large number of species becomes important (Robson et al. 2005.). Current computer resources allow studies of complex global models (Murakami et al. 2013.) which describe the behavior of such plasmas by taking into account a very large number of particles. The knowledge of ion-neutral reactions is generally available (see https://nl.lxcat.net/data/set_type.php) although the effects of reactions on transport parameters of particular ions are much less studied due to non-detectability of rapidly vanishing ionic fluxes. This especially holds for ions whose transport is affected by fast reactions (Stojanović et al. 2014. andNikitović et al. 2016.).

In this paper we firstly selected the most probable reactions of Ar^+ with BF_3 gases for thermodynamic threshold energies below about 15 eV.

2. CROSS SECTION SETS

Complete cross section sets for ion transport are scarce in spite of a broad range of specific methods relevant for quantification of particular cross sections. The main problem in heavy particle scattering, easily and precisely selecting the state of the projectile and target before the collision, is still very complicated for a range of conditions, so databases for ion scattering (Murakami et al. 2013. and https://nl.lxcat.net/data/set_type.php) are still devoid of such data. Phelps established the first worldwide accessible database with cross section sets (see https://nl.lxcat.net/cache/5b33772b61cf9/) tested for each particular case either for swarm conditions of spatially resolved measurements of emission or ion mobility values. In order to focus on effects of reactive processes introduced by BF_3 we neglected all but these two components of the $Ar^+ + Ar$ cross section set. Complete cross section sets used in this work are shown in Figure 1.

Appropriate gas phase enthalpies of formation for the products (Table 1) were used to calculate thermodynamic thresholds.

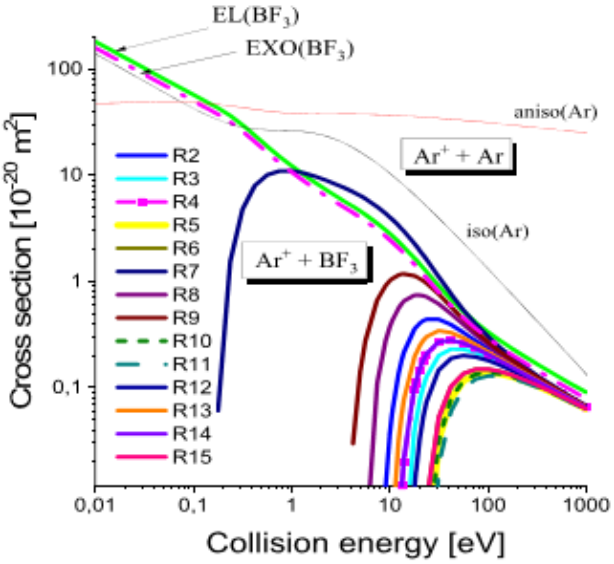

Figure 1: Cross section sets for Ar^+ in BF_3.

Ion/neutral	ΔH_f(ion) kJ/mol (room temperature)	ΔH_f(neutral) kJ/mol (room temperature)
Ar^+/Ar	1520.57	0
Ar_2^+/Ar_2	1398.1	-1.01
B^+/B	1363.3	562.7
BF^+/BF	957	-115.8
BF_2^+/BF_2	314	-589.9
BF_3^+/BF_3	364.3	-1137.0
F^+/F	1760.2	79.4
F_2^+/F_2	1514.5	0

Table 1: Heats of formation $\Delta_f\mathbf{H}^0$ at 298 K (kJ/mol).

3. DISCUSSION AND RESULTS

Monte Carlo Simulations (MCS) have many applications for analysis of the transport of charged particles in plasmas. MCS provide swarm data with the only the uncertainty due to statistical fluctuations and uncertainties in the cross sections. In addition, MCS is the basis of hybrid models of plasmas allowing easy and accurate representation of the end effects and of the non-local high energy groups of particles which are essential in production of plasmas and treatment of surfaces.The MC code used in our analysis is based on the null collisions method.

In Figure 2 we show rate coefficients for reactions of Ar^+ ions with Ar/BF_3 mixtures at T=300K, calculated by Monte Carlo simulations. Rate coefficients are important for applications of the global model to Ar/BF_3 mixtures. We are presenting reaction products and thermodynamic thresholds for Ar^+ + BF_3(Nikitović et al. 2019.)formation a) total attachment and b) attachment for endothermic and exothermic reaction products.

4. CONCLUSION

In addition to presenting the data we show here the effects of non-conservative collisions to ion transport. Data for swarm parameters for ions are needed for hybrid and fluid codes and the current focus on liquids or liquids in the mixtures with rare gases dictates the need to produce data compatible with those models.

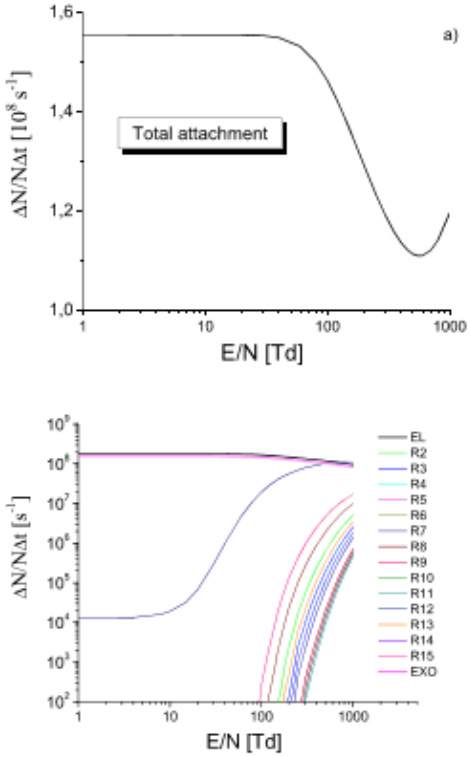

Figure 2: Rate coefficients of Ar^+ in Ar/BF_3 mixtures.

References

Makabe, T., Petrović, Z. : 2006, *Plasma Electronics: Applications in Microelectronic Device Fabrication Taylor and Francis*, New York: CRC Press.

Murakami, T., Niemi, K., Gans, T., O'Connell, D., Graham, W. G. : 2013, *Plasma Sources Sci. Technol.*,**22,** 015003.

Nikitović, Ž.,Gilić, M., Raspopović, Z.,Stojanović, V. : 2016,*EPL*,**116,** 15002.

Nikitović, Ž., Raspopović, Z., Stojanović,V. : 2019, *EPL*, **128**, 15001.

Robson, R. E., White, R. D., Petrović, Z. Lj. : 2005, *Rev. Mod. Phys*., **77,** 1303.

Stojanović, V., Nikitović., Ž., Raspopović, Z., Jovanović, J. : 2014, *Acta Physica Polonica,***A125,** 46.

14. Рад M33

http://sp1ig2022.ipb.ac.rs/Spig2022-Book-Onine.pdf

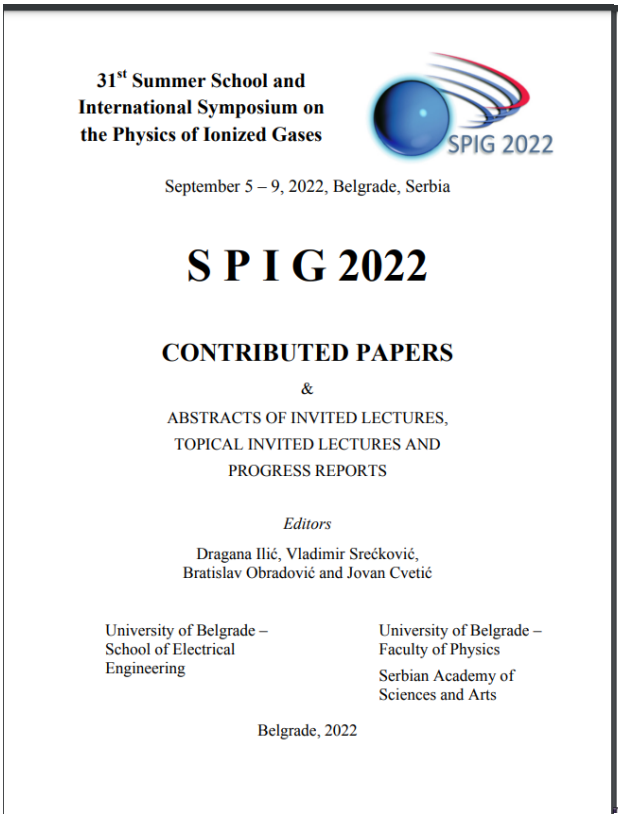

31st Summer School and International Symposium on the Physics of Ionized Gases

SPIG 2022

September 5 – 9, 2022, Belgrade, Serbia

S P I G 2022

CONTRIBUTED PAPERS

&

ABSTRACTS OF INVITED LECTURES,
TOPICAL INVITED LECTURES AND
PROGRESS REPORTS

Editors

Dragana Ilić, Vladimir Srećković,
Bratislav Obradović and Jovan Cvetić

University of Belgrade – School of Electrical Engineering

University of Belgrade – Faculty of Physics

Serbian Academy of Sciences and Arts

Belgrade, 2022

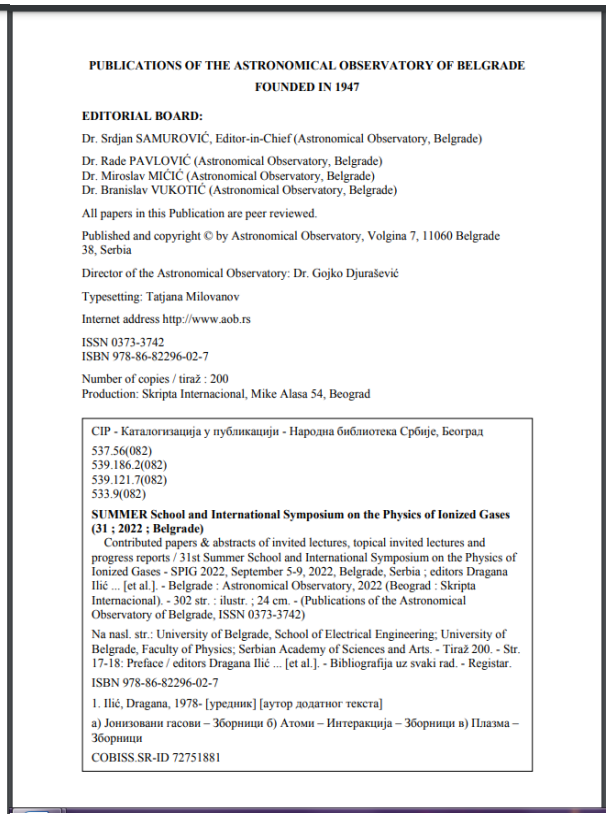

PUBLICATIONS OF THE ASTRONOMICAL OBSERVATORY OF BELGRADE
FOUNDED IN 1947

EDITORIAL BOARD:

Dr. Srdjan SAMUROVIĆ, Editor-in-Chief (Astronomical Observatory, Belgrade)

Dr. Rade PAVLOVIĆ (Astronomical Observatory, Belgrade)
Dr. Miroslav MIČIĆ (Astronomical Observatory, Belgrade)
Dr. Branislav VUKOTIĆ (Astronomical Observatory, Belgrade)

All papers in this Publication are peer reviewed.

Director of the Astronomical Observatory: Dr. Gojko Djurašević

Typesetting: Tatjana Milovanov

Internet address http://www.aob.rs

ISSN 0373-3742
ISBN 978-86-82296-02-7

Number of copies / tiraž : 200
Production: Skripta Internacional, Mike Alasa 54, Beograd

CIP - Каталогизација у публикацији - Народна библиотека Србије, Београд

537.56(082)
539.186.2(082)
539.121.7(082)
533.9(082)

SUMMER School and International Symposium on the Physics of Ionized Gases (31 ; 2022 ; Belgrade)
Contributed papers & abstracts of invited lectures, topical invited lectures and progress reports / 31st Summer School and International Symposium on the Physics of Ionized Gases - SPIG 2022, September 5-9, 2022, Belgrade, Serbia ; editors Dragana Ilić ... [et al.]. - Belgrade : Astronomical Observatory, 2022 (Beograd : Skripta Internacional). - 302 str. : ilustr. ; 24 cm. - (Publications of the Astronomical Observatory of Belgrade, ISSN 0373-3742)

Na nasl. str.: University of Belgrade, School of Electrical Engineering; University of Belgrade, Faculty of Physics; Serbian Academy of Sciences and Arts. - Tiraž 200. - Str. 17-18: Preface / editors Dragana Ilić ... [et al.]. - Bibliografija uz svaki rad. - Registar.

ISBN 978-86-82296-02-7

1. Ilić, Dragana, 1978- [уредник] [аутор додатног текста]

а) Јонизовани гасови – Зборници б) Атоми – Интеракција – Зборници в) Плазма – Зборници

COBISS.SR-ID 72751881

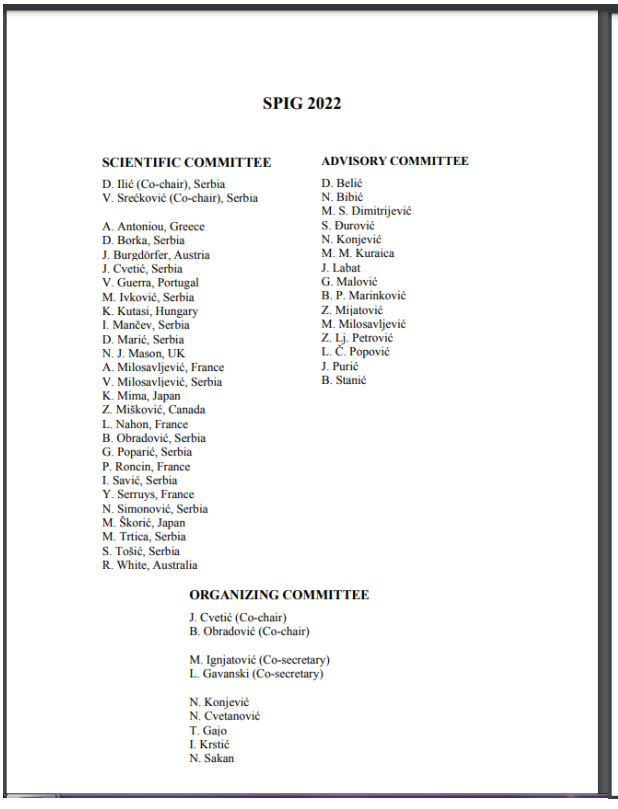

SPIG 2022

SCIENTIFIC COMMITTEE

D. Ilić (Co-chair), Serbia
V. Srećković (Co-chair), Serbia

A. Antoniou, Greece
D. Borka, Serbia
J. Burgdörfer, Austria
J. Cvetić, Serbia
V. Guerra, Portugal
M. Ivković, Serbia
K. Kutasi, Hungary
I. Mančev, Serbia
D. Marić, Serbia
N. J. Mason, UK
A. Milosavljević, France
V. Milosavljević, Serbia
K. Mima, Japan
Z. Mišković, Canada
L. Nahon, France
B. Obradović, Serbia
G. Poparić, Serbia
P. Roncin, France
I. Savić, Serbia
Y. Serruys, France
N. Simonović, Serbia
M. Škorić, Japan
M. Trtica, Serbia
S. Tošić, Serbia
R. White, Australia

ADVISORY COMMITTEE

D. Belić
N. Bibić
M. S. Dimitrijević
S. Đurović
N. Konjević
M. M. Kuraica
J. Labat
G. Malović
B. P. Marinković
Z. Mijatović
M. Milosavljević
Z. Lj. Petrović
L. Č. Popović
J. Purić
B. Stanić

ORGANIZING COMMITTEE

J. Cvetić (Co-chair)
B. Obradović (Co-chair)

M. Ignjatović (Co-secretary)
L. Gavanski (Co-secretary)

N. Konjević
N. Cvetanović
T. Gajo
I. Krstić
N. Sakan

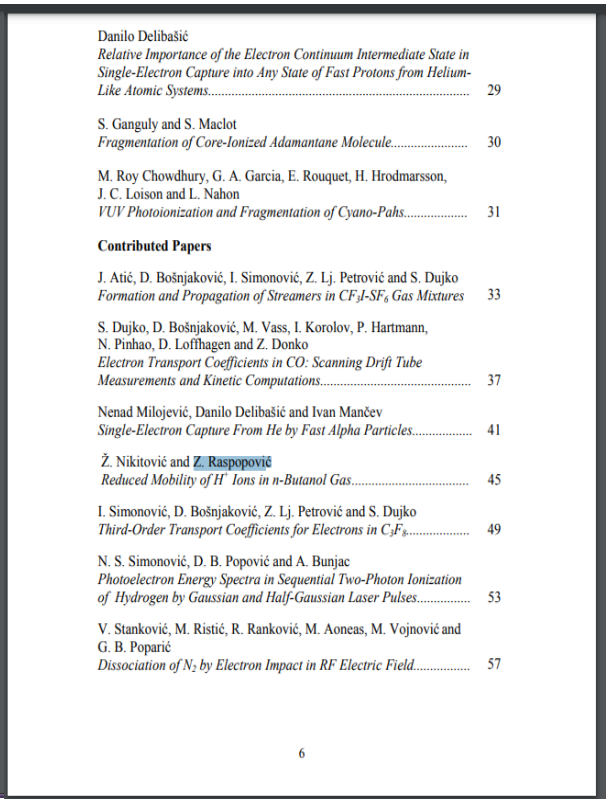

Publ. Astron. Obs. Belgrade No. 102 (2022), 45 - 48 *Contributed Paper*

REDUCED MOBILITY OF H^+ IONS IN n-BUTANOL GAS

Ž. NIKITOVIĆ and Z. RASPOPOVIĆ

Institute of Physics, University of Belgrade, Pregrevica 118, 11080 Belgrade, Serbia

E-mail zeljka@ipb.ac.rs
E-mail zr@ipb.ac.rs

Abstract. In this paper we show predictions for the low energy cross sections and transport properties for the H^+ ions in n-Butanol gas. These data are needed for modelling in numerous applications of technologically importance. Appropriate gas phase enthalpies of formation for the products were used to calculate scattering cross section as a function of kinetic energy. Calculated cross sections can be used to obtain reduced mobility as a function of E/N (E -electric field strength; N-gas density) for H^+ in n-Butanol gas.

1. INTRODUCTION

n-Butanol occurs naturally as a minor product of the fermentation of sugars and other carbohydrates and is present in many foods and beverages as well as in a wide range of consumer products. Although most volatile organic compounds can be detected by fast methods such as ion mobility spectroscopy, precise determination is possible only if reaction of specific ions with targeted compound is well known.

The goal of this work is to calculate transport parameters of fragment ions of n-Butanol. We employ Denpoh-Nanbu's theory (DNT) see Denpoh et al. 1998 to calculate transport cross section sets for H^+ ions scattering on n-Butanol appropriate for low energies of H^+ ions. By using Monte Carlo technique that properly takes into account thermal collisions see Ristivojević et al. 2012 we calculated transport parameters as a function of E/N.

2. CROSS SECTION SETS

The scattering cross sections of H^+ on n-Butanol are calculated by using the DNT see Denpoh et al. 1998. separating elastic from reactive collisions. The induced dipole polarizability of 8.9×10^{-24} cm^3 see Ababneh et al. 2003 is used for the n-Butanol target. In resemblance with our recent work see Stojanović et al. 2013 DNT method is used to separate elastic from reactive endothermic collisions by accounting for the thermodynamic threshold energy and branching ratio according to the Rice-Rampsperger- Kassel (RRK) theory see Rice et al. 1928. Within the RRK theory the internal energy is being distributed among an empirical number of ***s*** equivalent effective modes of the complex selected from the total number of atoms involved in the complex.

Appropriate gas phase enthalpies of formation for the products see Lias et al. 1988 were used to calculate thermodynamic thresholds.

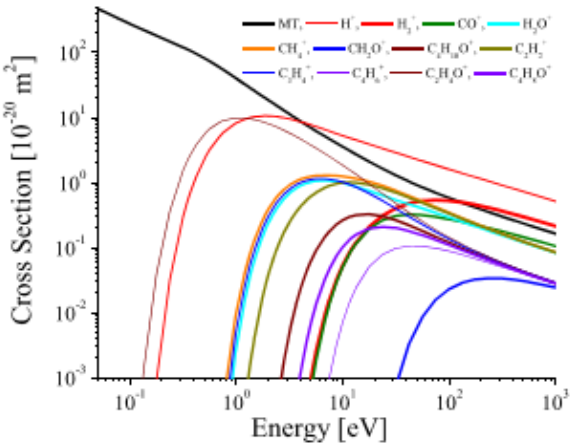

Figure 1: Cross section sets for H^+in n-Butanol gas.

The cross section sets for endothermic and exothermic reactions of H^+ with n-Butanol is presented in Figure 1.

2. RESULTS AND DISCUSSION

The transport properties of species in gas plasma are of great importance for understanding the nature of molecular and ionic interactions in gas mixtures see Todd et al. 2002, Mason et al. 1957. These properties include mean energy, drift velocity, diffusion coefficients, ionization and chemical reaction coefficients, ion chemical reaction coefficients and rarely excitation coefficients, and are very useful in the chemical industry for the design of many types of transport and process equipment. Swarm parameters, which are functions of the reduced electric field *E/N* (E-electric field strength, N-gas density) in direct electric fields are usually used for plasma modeling and simulation.

The flux and bulk drift velocities for H^+ in n-Butanol gas as a function of *E/N* are given in Figure 2. The drift velocities obtained by the Monte Carlo simulation are calculated in real space (bulk) and in velocity space (flux) values which are obtained as $\langle v \rangle$ and $d\langle x \rangle/dt$, respectively. As *E/N* increases, the high-energy ions from the distribution function increasingly have non-conservative collisions in which the H^+ ions disappear, shifting the center of mass of the swarm backward, resulting in a bulk velocity less than the flux.

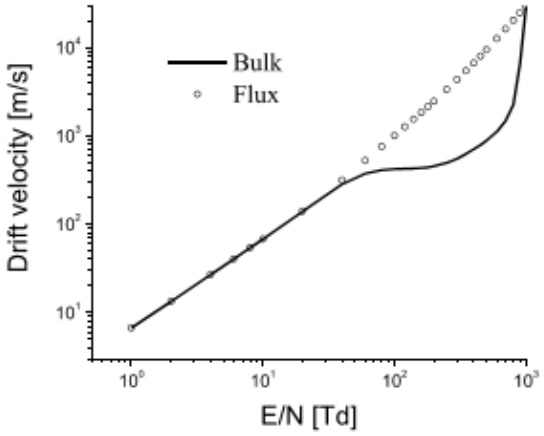

Figure 2: Drift velocity of H^+ ions in n-Butanol gas as a function of *E/N* at $T = 300$ K.

In Figure 3. we show the results of Monte Carlo simulation for reduced mobility as a function of *E/N*. Due to reactive collisions bulk and flux values of reduced mobility are separated.

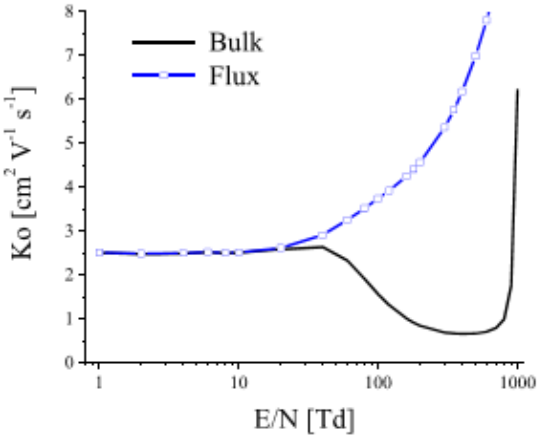

Figure 3: Reduced mobility of H^+ ions in n-Butanol gas as a function of *E/N* at *T*=300 K.

The mobility *K* of an ion is the quantity defined as the velocity attained by an ion moving through a gas under the unit electric field. One often exploits the reduced or standard mobility defined as:

$$K_0 = \frac{v_d}{N_0 E} N \,, \tag{1}$$

where v_d is the drift velocity of the ion, *N* is the gas density at elevated temperature *T* and *E* is the electric field.

Acknowledgements

The authors acknowledge funding provided by the Institute of Physics University Belgrade, through the grant by the Ministry of Education, Science and Technological Development of the Republic of Serbia.

References

A. M. Ababneh, C. C. Large and S. Georghiou: 2003, *Biophysical Journal* **85** 1111.
K. Denpoh and K. Nanbu : 1998, *J. Vac. Sci. Technol.* **A 16 (3)** 1201.
S. Lias, J. Bartmess, J. Liebman, J. Holmes, R. Levin, W. Mallard: 1988, *J Phys Chem Ref Data* **17** 1.
E. Mason: 1957, *J. Chem. Phys.* **27** 782.
O. K. Rice, H. C. Ramsperger: 1928, *J. Am. Chem. Soc.* **50 (3)** 617.
Z. Ristivojević and Z. Lj. Petrović : 2012, *Plasma Sources Sci. Technol.* **21** 035001.
V. Stojanović, Z. Raspopović, J. Jovanović, Ž. Nikitović and Z. Lj. Petrović: 2013, EPL **101** 45003.
B. Todd, J. B. Young: 2002, *J. Power Sources* **110** 186.

15. Рад М34

http://asspectro2022.ipb.ac.rs/book-AsSpectro2022d.pdf

IV Meeting on Astrophysical Spectroscopy -
A&M DATA - Atmosphere

May 30 to June 2, 2022, Fruška Gora, Serbia

BOOK OF ABSTRACTS AND CONTRIBUTED PAPERS

Edited by Vladimir A. Srećković, Milan S. Dimitrijević,
Nikola Veselinović and Nikola Cvetanović

A&M DATA

Belgrade 2022

Text arrangement by computer: Tanja Milovanov

ISBN 978-86-82441-57-1

Financially supported by the Ministry of Education, Science and Technological Development of Serbia

Production: Skripta Internacional, Mike Alasa 54, Beograd in 50 copies

CONTENTS

Rate coefficients of He^+ ions in CF_4 gas

Željka D. Nikitović and Zoran M. Raspopović

Institute of Physics, University of Belgrade, Pregrevica 118, 11080 Belgrade, Serbia
E-mail: zeljka@ipb.ac.rs

This paper is dedicated to the presentation of the set of He^+ ions scattering cross-sections in CF_4 which is estimated using available experimental data for exothermic charge transfer cross-sections producing CF_3^+ and CF_2^+ ions and endothermic charge transfer cross-section producing CF^+, C^+ and F^+ ions. Due to significant particle losses, the experimental transport coefficients were not measured. The transport properties of He^+ ions in CF_4 required to model the discharge containing the mentioned ions were calculated by the Monte Carlo method at a temperature of T = 300 K. In this paper we give the characteristic energy and specially rate coefficients for low and moderately reduced electric fields *E /N* (*E*-electric field, *N*-gas density) and accounting for non-conservative collisions.

He-CF_4 mixtures are used in gas electron multipliers for various imaging purposes (X-rays, charged particles, thermal neutrons and dark matter detection) (Fraga M.M.F.R. et al. 2008). Bursts of electron multiplication affect production of various ions that may affect time distribution of detected particles (Bošnjaković D. 2016).

References

Fraga M.M.F.R., Fraga F.A.F., Fetal S.T.G., Margato L.M.S., Ferreira Marques R., Policarpo A.J.P.L., 2003, Nucl. Instrum. Meth. in Phys. Res. A 504, 88; Kaboth A., Monroe J., Ahlen S., Dujmić D., Henderson S., Kohse G., Lanza R., Lewandowska M., Roccaro A., Sciolla G., Skvorodnev N., Tomita H., Vanderspek R., Wellenstein H., Yamamoto R., Fisher P., 2008, Nucl. Instrum. and Meth.in Phys.Res. A 592, 63.

Bošnjaković D.,2016, Ph Dissertation, Faculty of Electrical Engineering, University of Belgrade, Belgrade, Serbia.

16. Рад M34

http://asspectro2023.ipb.ac.rs/AsSpectro2023_book.pdf

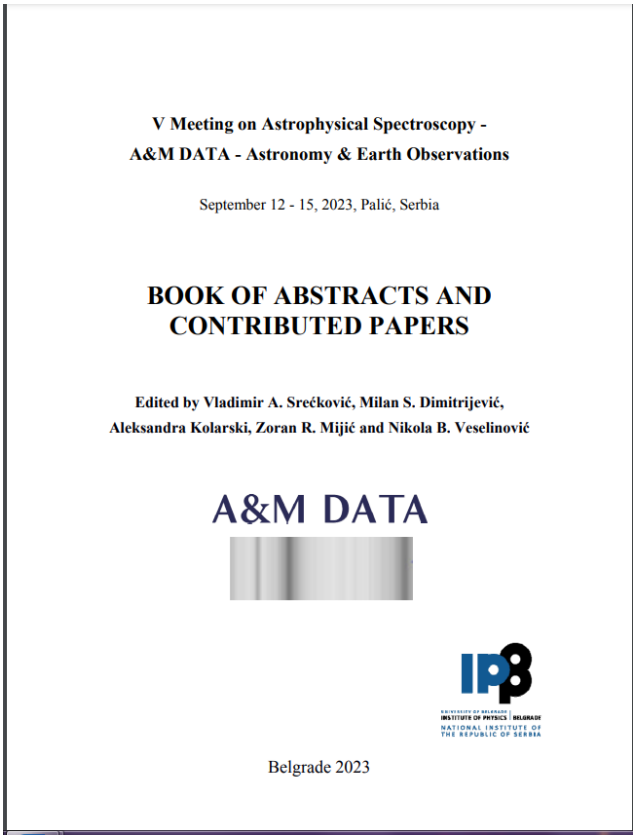

V Meeting on Astrophysical Spectroscopy -
A&M DATA - Astronomy & Earth Observations

September 12 - 15, 2023, Palić, Serbia

BOOK OF ABSTRACTS AND CONTRIBUTED PAPERS

Edited by Vladimir A. Srećković, Milan S. Dimitrijević,
Aleksandra Kolarski, Zoran R. Mijić and Nikola B. Veselinović

A&M DATA

Belgrade 2023

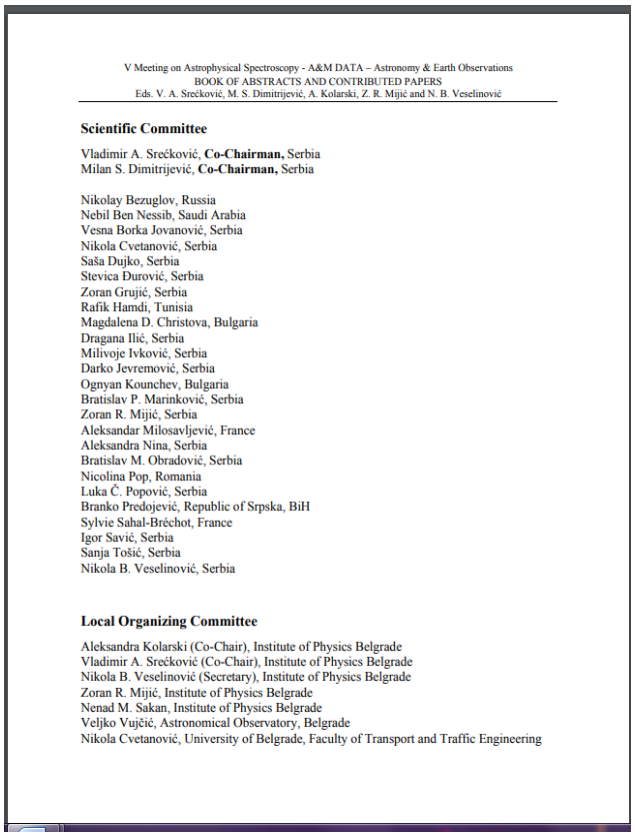

Scientific Committee

Vladimir A. Srećković, **Co-Chairman,** Serbia
Milan S. Dimitrijević, **Co-Chairman,** Serbia

Nikolay Bezuglov, Russia
Nebil Ben Nessib, Saudi Arabia
Vesna Borka Jovanović, Serbia
Nikola Cvetanović, Serbia
Saša Dujko, Serbia
Stevica Đurović, Serbia
Zoran Grujić, Serbia
Rafik Hamdi, Tunisia
Magdalena D. Christova, Bulgaria
Dragana Ilić, Serbia
Milivoje Ivković, Serbia
Darko Jevremović, Serbia
Ognyan Kounchev, Bulgaria
Bratislav P. Marinković, Serbia
Zoran R. Mijić, Serbia
Aleksandar Milosavljević, France
Aleksandra Nina, Serbia
Bratislav M. Obradović, Serbia
Nicolina Pop, Romania
Luka Č. Popović, Serbia
Branko Predojević, Republic of Srpska, BiH
Sylvie Sahal-Bréchot, France
Igor Savić, Serbia
Sanja Tošić, Serbia
Nikola B. Veselinović, Serbia

Local Organizing Committee

Aleksandra Kolarski (Co-Chair), Institute of Physics Belgrade
Vladimir A. Srećković (Co-Chair), Institute of Physics Belgrade
Nikola B. Veselinović (Secretary), Institute of Physics Belgrade
Zoran R. Mijić, Institute of Physics Belgrade
Nenad M. Sakan, Institute of Physics Belgrade
Veljko Vujčić, Astronomical Observatory, Belgrade
Nikola Cvetanović, University of Belgrade, Faculty of Transport and Traffic Engineering

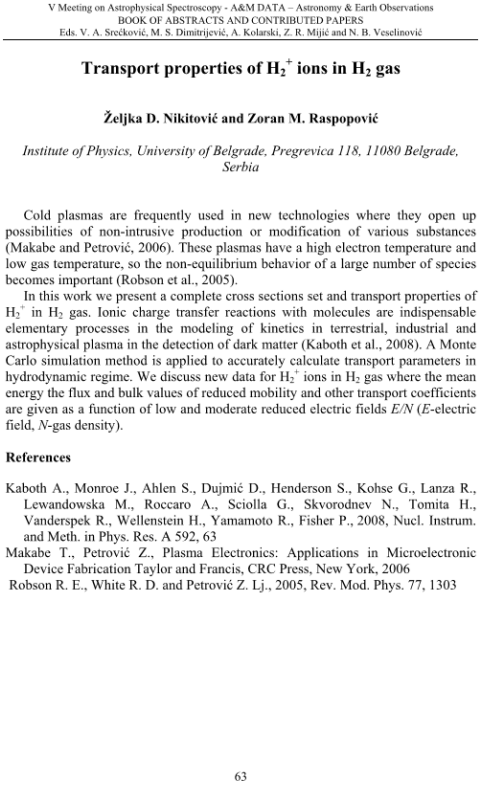

Transport properties of H_2^+ ions in H_2 gas

Željka D. Nikitović and Zoran M. Raspopović

Institute of Physics, University of Belgrade, Pregrevica 118, 11080 Belgrade, Serbia

Cold plasmas are frequently used in new technologies where they open up possibilities of non-intrusive production or modification of various substances (Makabe and Petrović, 2006). These plasmas have a high electron temperature and low gas temperature, so the non-equilibrium behavior of a large number of species becomes important (Robson et al., 2005).

In this work we present a complete cross sections set and transport properties of H_2^+ in H_2 gas. Ionic charge transfer reactions with molecules are indispensable elementary processes in the modeling of kinetics in terrestrial, industrial and astrophysical plasma in the detection of dark matter (Kaboth et al., 2008). A Monte Carlo simulation method is applied to accurately calculate transport parameters in hydrodynamic regime. We discuss new data for H_2^+ ions in H_2 gas where the mean energy the flux and bulk values of reduced mobility and other transport coefficients are given as a function of low and moderate reduced electric fields E/N (E-electric field, N-gas density).

References

Kaboth A., Monroe J., Ahlen S., Dujmić D., Henderson S., Kohse G., Lanza R., Lewandowska M., Roccaro A., Sciolla G., Skvorodnev N., Tomita H., Vanderspek R., Wellenstein H., Yamamoto R., Fisher P., 2008, Nucl. Instrum. and Meth. in Phys. Res. A 592, 63

Makabe T., Petrović Z., Plasma Electronics: Applications in Microelectronic Device Fabrication Taylor and Francis, CRC Press, New York, 2006

Robson R. E., White R. D. and Petrović Z. Lj., 2005, Rev. Mod. Phys. 77, 1303

17. Рад М34

http://www.serbianceramicsociety.rs/doc/aca11-20/aca11/ACA-XI-Program-and-the-book-of-abstracts.pdf

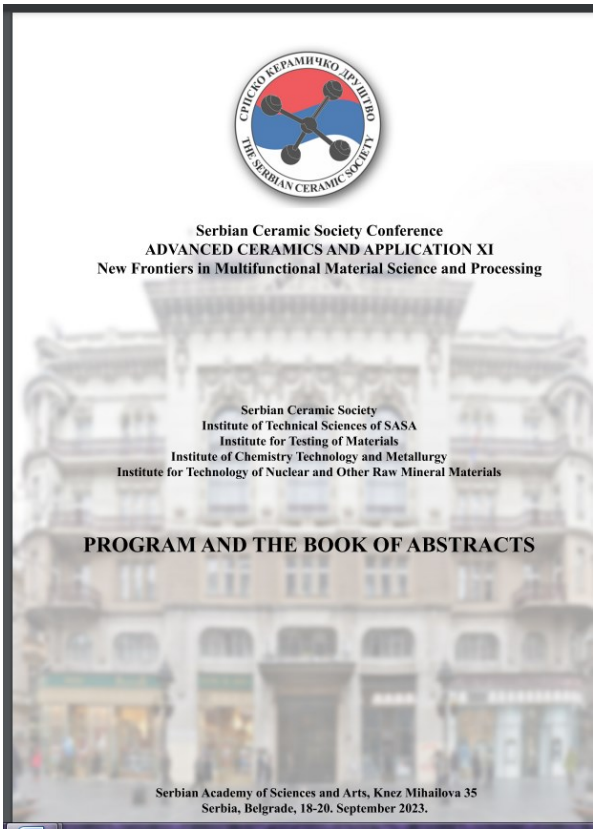

Serbian Ceramic Society Conference
ADVANCED CERAMICS AND APPLICATION XI
New Frontiers in Multifunctional Material Science and Processing

Serbian Ceramic Society
Institute of Technical Sciences of SASA
Institute for Testing of Materials
Institute of Chemistry Technology and Metallurgy
Institute for Technology of Nuclear and Other Raw Mineral Materials

PROGRAM AND THE BOOK OF ABSTRACTS

Serbian Academy of Sciences and Arts, Knez Mihailova 35
Serbia, Belgrade, 18-20. September 2023.

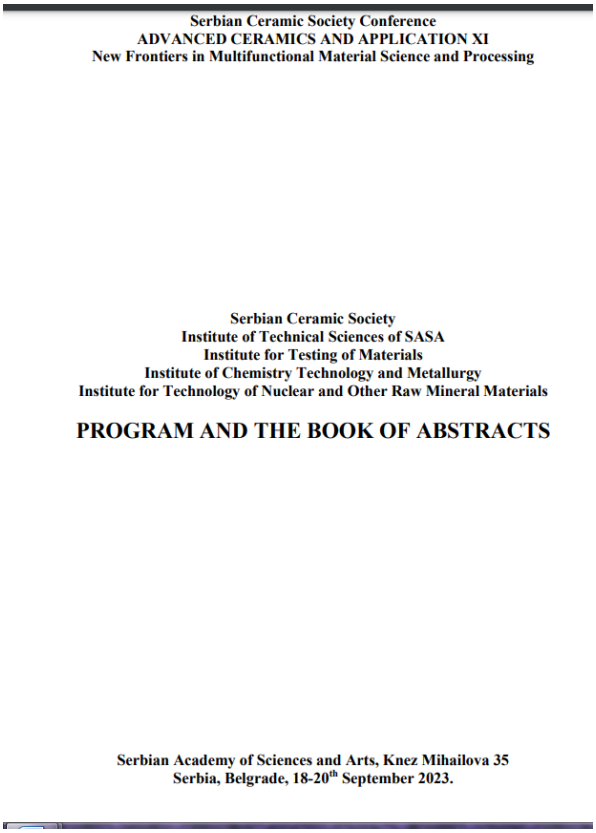

Serbian Ceramic Society Conference
ADVANCED CERAMICS AND APPLICATION XI
New Frontiers in Multifunctional Material Science and Processing

Serbian Ceramic Society
Institute of Technical Sciences of SASA
Institute for Testing of Materials
Institute of Chemistry Technology and Metallurgy
Institute for Technology of Nuclear and Other Raw Mineral Materials

PROGRAM AND THE BOOK OF ABSTRACTS

Serbian Academy of Sciences and Arts, Knez Mihailova 35
Serbia, Belgrade, 18-20th September 2023.

Book title: Serbian Ceramic Society Conference - ADVANCED CERAMICS AND APPLICATION XI Program and the Book of Abstracts

Publisher:
Serbian Ceramic Society

Editors:
Dr. Nina Obradović
Dr. Lidija Mančić

Technical Editors:
Dr. Adriana Peleš Tadić
Dr. Jelena Živojinović

Printing:
Serbian Ceramic Society, Belgrade, 2023.

Edition:
120 copies

CIP - Каталогизација у публикацији
Народна библиотека Србије, Београд

666.3/.7(048)
66.017/.018(048)

SRPSKO keramičko društvo. Conference Advanced Ceramics and Application : New Frontiers in Multifunctional Material Science and Processing (11 ; 2023 ; Beograd)

Program ; and the Book of abstracts / Serbian Ceramic Society Conference Advanced Ceramics and Application XI New Frontiers in Multifunctional Material Science and Processing, Serbian Academy of Sciences and Art Serbia, Belgrade,18-20.September 2023. ; [editors Nina Obradović, Lidija Mančić]. - Belgrade : Serbian Ceramic Society, 2023 (Belgrade : Serbian Ceramic Society). - 90 str. : ilustr. ; 30 cm

Tiraž 120.

ISBN 978-86-905714-0-6

а) Керамика -- Апстракти б) Наука о материјалима -- Апстракти

COBISS.SR-ID 122849545

Acknowledgment: This work was financially supported by the Ministry of Science, technological Development and Innovation of the Republic of Serbia (Grant No. 451-03-47/2023-01/200026).

P27

Modelling of Ar^+ ions in CF_4 gas

Željka Nikitović, Zoran Raspopović

Institute of Physics, University of Belgrade, Pregrevica 118, 11080 Belgrade, Serbia

Understanding plasma distribution, characteristics and phenomena is important for the development and optimization of semiconductor device manufacturing plasma equipment, such as etching and deposition tools. For this reason, plasma simulation is currently being utilized at every stage of equipment design, development and improvement. The cross section sets obtained by applying Denpoh-Nanbu theory to Ar^+ on CF_4 collisions were found to be in general qualitative and in part quantitative agreement with data from the literature. The Monte Carlo technique was applied to perform calculations of transport parameters. Calculated cross sections can be used to obtain transport coefficients, specially mean energy, reduced mobility

and rate coefficients for low and moderate reduced electric fields *E/N* (E-electric field strength; N-gas density) and accounting for the non-conservative collisions.

P28

Co supported chitosan–derived carbon–smectite–catalyst for oxygen evolution reaction in simulated alkaline seawater solution

Gordana Stevanović, Marija Ajduković, Nataša Jović-Jovičić, Sanja Marinović, Biljana Pantić, Predrag Banković, Tihana Mudrinić

University of Belgrade, Institute of Chemistry, Technology and Metallurgy, Department for Catalysis and Chemical Engineering, Njegoševa 12, 11000 Belgrade, Republic of Serbia

Seawater electrolysis has recently been recognized as a new hope for affordable renewable energy storage. However, its practical application is still limited due to the presence of various electroactive ions in seawater. For example, the chloride ions compete with the oxygen evolution reaction (OER) causing low efficiency of the OER, and corrosion of both the anode and the cathode. To overcome these issues, the development of catalysts with high activity and selectivity towards OER is of primary importance.Herein, Co supported

18. Рад М64

https://docs.google.com/viewerng/viewer?url=https://dais.sanu.ac.rs/bitstream/handle/123456789/3621/9788691911133.pdf?sequence%3D1%26amp;isAllowed%3Dy

Title: THE TWENTIETH ANNUAL CONFERENCE
YUCOMAT 2018
Programme and The Book of Abstracts

Publisher: Materials Research Society of Serbia
Knez Mihailova 35/IV, P.O.Box 433, 11000 Belgrade, Serbia
Phone: +381 11 2185-437
http://www.mrs-serbia.org.rs

Editors: Prof. Dr. Dragan P. Uskoković and Prof. Dr. Velimir R. Radmilović

Technical editor: Sava Stoisavljević

Front cover: Modified Photo by Hons084; Wikimedia Commons (https://commons.wikimedia.org/wiki/File:Widoki_z_twierdzy_Forte_Mare_na_Herceg_Novi_03.jpg); CC BY-SA 4.0
Back cover: Modified Photo by Dani Lavi 0007; Wikimedia Commons (https://commons.wikimedia.org/wiki/File:Belgrade_at_night.jpg); CC BY-SA 4.0

Acknowledgments: This conference is celebrating 20 years of YUCOMAT

Printed in: Biro Konto
Sutorina bb, Igalo – Herceg Novi, Montenegro
Phones: +382-31-670123, 670025, E-mail: bkonto@t-com.me
Circulation: 220 copies. The end of printing: August 2018

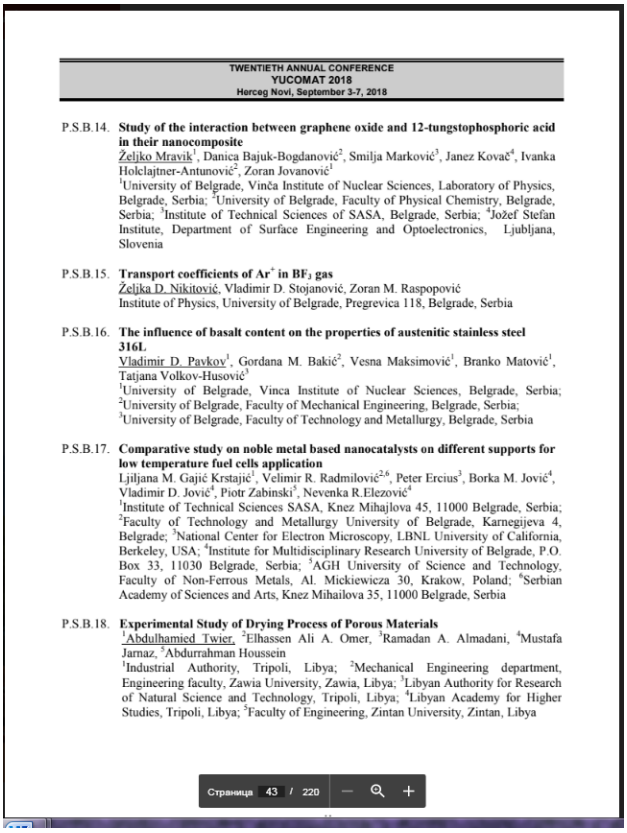

P.S.B.15.

Transport coefficients of Ar^+ in BF_3 gas

Željka D. Nikitović, Vladimir D. Stojanović, Zoran M. Raspopović
Institute of Physics, University of Belgrade, Pregrevica 118, Belgrade, Serbia

Cold plasmas are frequently used in new technologies where they open up possibilities of non-intrusive production or modification of various substances. Transport of Ar^+ plays significant role in various etching and deposition processes [1], in dark matter detection [2] and many more applications. In this work we present a cross section set for Ar^+ in BF_3 gas where existing experimentally obtained data are selected and extrapolated. A Monte Carlo simulation method is applied to accurately calculate transport parameters in hydrodynamic regime. We discuss new data for Ar^+ ions in BF_3 gas where mean energy, flux and bulk values of reduced mobility and other transport coefficients are given as a function of low and moderate reduced electric fields E/N (E-electric field, N-gas density).

[1] Lieberman M. A. and Lichtenberg A. J., Principles of Plasma Discharges and Materials Processing, Wiley, New York (1994).
[2] Kaboth A., Monroe J., Ahlen S., Dujmic D., Henderson S., Kohse G., Lanza R., Lewandowska M., Roccaro A., Sciolla G., Skvorodnev N., Tomita H., Vanderspek R., Wellenstein H., Yamamoto R., Fisher P., Nucl. Instrum. and Meth. in Phys. Res. A 592 (2008) 63.

P.S.B.16.

The influence of basalt content on the properties of austenitic stainless steel 316L

Vladimir D. Pavkov[1], Gordana M. Bakić[2], Vesna M. Maksimović[1], Branko Matović[1], Tatjana Volkov-Husović[3]
[1]University of Belgrade, Vinca Institute of Nuclear Sciences, Belgrade, Serbia;
[2]University of Belgrade, Faculty of Mechanical Engineering, Belgrade, Serbia;
[3]University of Belgrade, Faculty of Technology and Metallurgy, Belgrade, Serbia

The aim of the paper is to examine the influence of basalt content on the properties of austenitic stainless steel as well as the possibility of using this composite material for wider industrial application. In the experiment, powder of commercial austenitic stainless steel (SURFIT TM 316L) of the diameter from 20 to 100 μm was used. The steel powder of the spherical shape obtained by gas atomization was mixed with the basalt from the locality "Vrelo" Kopaonik, Serbia, with particle size below 45 μm in the content of 1, 5 and 10 wt.%. The samples were pressed of about 500 MPa and then sintered into a vacuum furnace at temperatures of 1100 °C and 1200 °C. Characterization of sintered samples was performed using X-ray diffraction (XRD), scanning electron microscope (SEM), Vickers hardness as well as cavitation resistance.

19. рад М64

https://www.mrs-serbia.org.rs/index.php/book-of-abstracts-2023

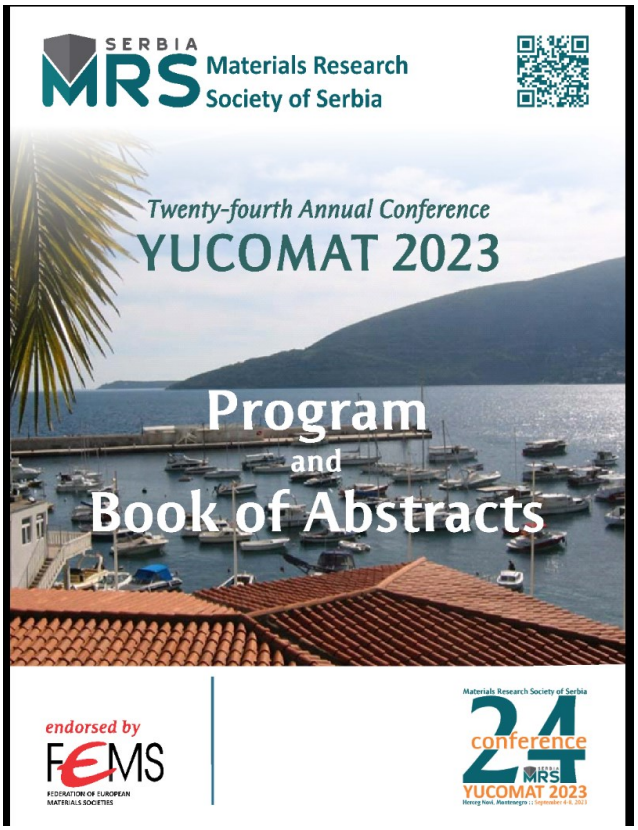

CIP – Каталогизација у публикацији
Народна библиотека Србије, Београд

66.017/.018(048)
621.762.5)(048)

DRUŠTVO za istraživanje materijala Srbije (Beograd). Godišnja konferencija (24 ; 2023 ; Herceg Novi)
Programme ; and The Book of Abstracts / Twenty-fourth Annual Conference YUCOMAT 2023, Herceg Novi, Montenegro, September 4 - 8, 2023 ; organized by Materials Research Society of Serbia ; [editor Dragan P. Uskoković]. – Belgrade : Materials Research Society of Serbia, 2023 (Herceg Novi : Biro Konto) : - XLVII, 183 str. : ilustr. ; 24 cm

Tiraž 220. – Bibliografija uz pojedine apstrakte. - Registar.

ISBN 978-86-919111-8-8

a) Наука о материјалима -- Апстракти b) Технички материјали -- Апстракти
v) Синтеровање -- Апстракти

COBISS.SR-ID 122486537

Title: THE TWENTY-FOURTH ANNUAL CONFERENCE **YUCOMAT 2023** Program and Book of Abstracts

Publisher: Materials Research Society of Serbia
Knez Mihailova 35/IV, P. O. Box 433, 11000 Belgrade, Serbia
Phone: +381 11 2185-437; http://www.mrs-serbia.org.rs

Editor: Prof. Dr. Dragan P. Uskoković

Conference Secretary: Jasmina R. Jevtić

Technical editor: Dr. Ivana Dinić

Typesetting and prepress: Dr. Aleksandar Dekanski

Covers: Front cover photo: property of MRS Serbia
Back cover photo: J. Erskine-Kelli, Attribution-ShareAlike 2.0 Generic (CC BY-SA 2.0)

ISBN 978-86-919111-8-8

MRSS is member of the
Federation of European Materials Societies
FEMS

Printed in: **Biro Konto**, Sutorina bb, Igalo – Herceg Novi, Montenegro
Phones: +382-31-670123, 670025, E-mail: bkonto@t-com.me

Circulation: 220 copies. The end of printing: August 2023

P.S.43
Gas-detonation surface modification for dental implants
Volodymyr Demeka[1,2], Bogdan Drygval[2], Oksana Pogorielova[2], Maksym Pogorielov[1,2], Oleg Mishchenko[2]
[1]University of Latvia, Riga, Latvia, [2]Biomedical Research Centre, Sumy. State University, Sumy, Ukraine, [3]Zaporizhzhia State Medical and Pharmaceutical University, Zaporizhzhia, Ukraine.

P.S.44.
The combined effect of modification and grain refinement in aluminium silicon alloys
Biljana Zlatičanin, Branislav Radonjić
Faculty of Metallurgy and Technology, Podgorica, Montenegro

P.S.45.
Simplified doping-free electroluminescent device reaching 4.6% of external quantum efficiency with the derivative of 1*H*-1,2,3-triazole as emissive layer
Mariia Stanitska[1,2], Nazariy Pokhodylo[2], Roman Lytvyn[2], Ervinas Urbonas[1], Dmytro Volyniuk[1], Khrystyna Ivaniuk[3], Pavlo Stakhira[3], Rasa Keruckiene[1], Mykola Obushak[2], Juozas V. Grazulevicius[1]
[1]Department of Polymer Chemistry and Technology, Kaunas University of Technology, Kaunas, Lithuania, [2]Department of Organic Chemistry, Ivan Franko National University of Lviv, Lviv, Ukraine, [3]Department of electronic Engineering, Lviv Polytechnic University, Lviv, Ukraine

P.S.46.
1,8-Naphthalimide derivatives with room temperature phosphorescence detectable in solid and liquid media
Melika Ghasemi, Naveen Masimukku, Dmytro Volyniuk, Juozas V. Grazulevicius
Department of Polymer Chemistry and Technology, Kaunas University of Technology (KTU), Kaunas, Lithuania

YUCOMAT SYMPOSIUM B:
ADVANCED MATERIALS FOR HIGH-TECHNOLOGY APPLICATION

P.S.47.
Transport properties for Ar+ in CF_4 gas for technological applications
Željka Nikitović, Zoran Raspopović
Institute of Physics University of Belgrade, Pregrevica 118, 11080 Belgrade,Serbia

P.S.48.
Electron structure and peculiarities of the valence state of Ce (Yb) in RM_4Al_8(R=Y, Ce, Yb; M=Cr, Mn, Fe, Cu)
Ivan Shcherba[1], Henrik Noga[2], Viktor Antonov[3], Roman Bilyk[1], Bogdan Jatcyk[4], Vitalij Denys[1]
[1]Physical Department, Ivan Franko National University of Lviv, Ukraine, [2]Institute of Technology, the Pedagogical University of Cracow, Poland, [3]Institute of Physics of Metals, NASU Kyiv, Ukraine, [4]Lviv National University of Veterinary Medicine and Biotechnologies, Ukraine

P.S.47.
Transport properties for Ar^+ in CF_4 gas for technological applications

Željka Nikitović, Zoran Raspopović

Institute of Physics, University of Belgrade, Belgrade, Serbia

Cold plasmas are often exploited in new technologies where they favorably offer non-intrusive production or modification of various substances. The ion-molecule collision model for endothermic reactions created by Denpoh and Nanbu theory (DNT) has been extended to exothermic reactions. Understanding the plasma distribution, characteristics and phenomena is important for the development and optimization of plasma equipment for the production of semiconductor devices, such as etching and deposition tools. For this reason, plasma simulation is currently used in every phase of equipment design, development and improvement.
Monte Carlo simulation method is applied to accurately calculate transport properties in hydro-dynamic regime. These data are needed for modeling in numerous applications of technologically important. We discuss new data for Ar^+ ions in CF_4 gas where mean and characteristic energy, flux and bulk values of reduced mobility are given as a function of reduced electric field E/N (E-electric field, N-gas density).

Acknowledgement: The author acknowledges funding provided by the Institute of Physics University Belgrade, through the grant by the Ministry of Science, Technological Development and Innovation of the Republic of Serbia.